University of Naples "Federico II"

Department of Agricultural Sciences

Ph.D. course in Food Science (XXXIII cycle)

Modelling in vitro digestion as strategy in developing tailored food for specific consumer population

Ph.D. Coordinator

Professor Amalia Barone

Ph.D. Candidate

Veronica Gallo

Ph.D. Supervisor

Professor Paolo Masi

Ph.D. Co-Supervisor

Dr. Annalisa Romano

Academic year 2019-2020

INDEX

List of Figures

Chapter 1

Chapter 2

Chapter 3

Chapter 4

Chapter 5

Chapter 6

Chapter 7

List of Tables

Chapter 3

Chapter 5

Chapter 6

Chapter 7

Thesis overview

Food digestion is a complex sequence of physicochemical and mechanical events, involving food breakdown, the release of nutrients, their uptake or microbial fermentation before their ultimate removal from the body through defecation (Shani-Levi *et al.*, 2017).

Although *in vivo* studies are still considered a "gold standard" for providing the most accurate representation of the complex nature of the human gastro-intestinal tract (GIT), a huge range of *in vitro* digestion models are widely used to study the digestion process, since they have the advantage of being more rapid, less expensive and having less bioethical restrictions than the *in vivo* ones. The majority of the *in vitro* digestion models reported in the literature are static ones. Their results are often different to those found *in vivo* because of the difficulties in accurately simulating the highly complex physicochemical events occurring in human digestive tracts (Hur *et al.*, 2011). Furthermore, they often differ from each other in the digestion conditions applied, such as the number of steps included in the digestion sequence, type and concentration of enzymes, pH, digestion time, and so on. In this context, the INFOGEST network developed a standardized and harmonized static method based on available human data (Minekus *et al.*, 2014; Brodkorb *et al.*, 2019).

On the other hand, several groups have also developed dynamic *in vitro* digestion models which are more complex in their design and fabrication than the static ones but allow for mimic both the physical and chemical conditions encountered in the GIT (Bornhorst & Singh, 2014).

Given the huge gap between these models, the INFOGEST network has developed an intermediate model denominated "semi-dynamic" model which builds upon the harmonised static model (Mulet-Cabero *et al.*, 2020). The semi-dynamic protocol does not require complex laboratory instruments and it is suitable for a wide range of foods. It allows the evaluation of food disintegration modes during digestion, and therefore the assessment of rate and extent of nutrient bioaccessibility. Moreover, it is mainly focused on the gastric digestion, considering the variable composition of the gastric secretions, their flow rate as well as the gastric emptying.

In vitro digestion modelling is a vivid field of research that shows great promise in facilitating the development of foods (Shani-Levi *et al.*, 2017). A survey conducted in 2018 using Scopus as data base for the searches, showed great interest of the scientific community in the *in vitro* digestion of foods. Even if *in vitro* digestion models have been applied to a wide range of foods, the survey also revealed that the most common food tested were vegetables (26%),

dairy foods (23%), bakery foods (17%), meat products (13%), marine foods (12%) and egg foods (7%) (Lucas-González *et al.*, 2018).

Moreover, in recent years there has been an increasing interest of consumers for food with enhanced nutritional characteristics, spurring the industries to look for unconventional raw materials (e.g., dietary fibre and legume flour) for novel food design. However, the use of alternative ingredients may result in interesting modifications in quality as well as nutritional characteristics of the final product.

In this regard, the selection of ingredients is fundamental, since food formulation directly influences its structural features that in turns, may greatly affect the bioaccessibility, digestibility and ultimately the bioavailability of some nutrients (such as starch and proteins). Along with the formulation, food structure can be also extensively impacted during processing. It follows that the investigation of how and to what extend food structure is impacted by process operations is extremely important, since it allows a selection of suitable process conditions that ensure proper food quality.

Considering these recent trends, the primary aims of this PhD research project were:

1. setting up a dynamic *in vitro* digestion apparatus able to mimic both the physical and chemical conditions encountered in the GIT, thereby improving our understanding about the fate of different foods during digestion.
2. using static and semi-dynamic *in vitro* digestion models to understand how food structure can affect nutrients bioaccessibility and digestibility.

   For this purpose, cereal-based products (pasta and bread) were used as model foods and the use of lentil flour as highly nutritious ingredient has been investigated.

SECTION A
State of art

Chapter 1
The human digestive system

1.1. The human digestive system

The human GIT (Fig. 1.1) is a complicated set of bioreactors that are intertwined with the haematological, hormonal, and nervous systems (Remond *et al.*, 2015).

It extends from the mouth to the anus and can be divided into the upper tract, which consists of the oral cavity, esophagus, stomach and small intestine and the lower tract, which comprises the large intestine and the anal canal (Verhoeckx & Cotter, 2015).

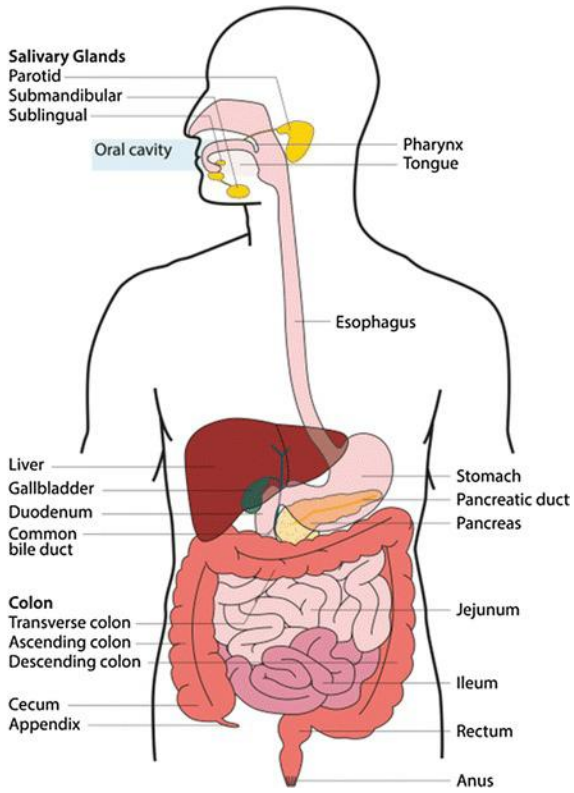

Fig. 1.1. Human Gastrointestinal Tract (GIT).

Human digestion implies both mechanical and enzymatic transformations which occur simultaneously. The mechanical transformation starts in the mouth by chewing and continues into the stomach by the peristaltic and the antral contractions. Instead, the enzymatic transformation, provided by several enzymes, starts in the mouth, and continues until the small intestine (Alminger *et al.*, 2014; Guerra *et al.*, 2012).

Human digestion consists of the following steps: i) oral digestion; ii) esophageal transit; iii) gastric digestion; iv) digestion in the small intestine; v) digestion in the large intestine.

1.1.1. Oral digestion

The digestion process starts in the mouth where food is chewed and mixed with saliva, which contains a wide range of components including water (99.5%), proteins (0.3%) (immunoglobulin A (IgA), α-amylase (ptyalin), lysozyme, lactoferrin, mucins) and electrolytes (sodium, potassium, calcium, magnesium, phosphate, and bicarbonate). Salivary α-amylase is responsible for the hydrolysis of starch into sugars and has a pH-optimum of activity equal to 6.8 (Pedersen *et al.*, 2002). Therefore, it is inactivated by the acid environment and the proteolytic activity in the stomach.

The result of mechanical and enzymatic degradation in the mouth is a lubricated mass known as bolus, which will be swallowed and transported through the oesophagus to the stomach.

The chewing time, the final size of the bolus particles, as well as the amount of saliva secreted, are highly dependent on both physiological variables (gender, personality, teeth condition, degree of hunger) and food properties (hardness, composition, volume) (Minekus *et al.*, 2014). Despite its short duration, mastication has a significant influence on the digestive process, and in particular, on the gastric emptying rate (Guerra *et al.*, 2012).

1.1.2. Esophageal transit

The end product of the oral phase is transported through the esophagus to the stomach both by the force of gravity and the mechanism of peristalsis (Guerra *et al.*, 2012; Bornhorst & Singh, 2014).

1.1.3. Gastric digestion

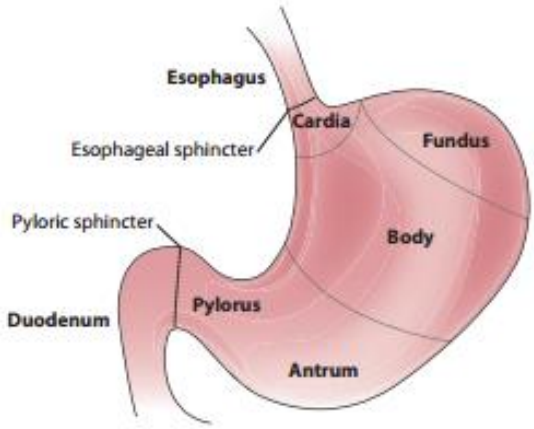

Fig. 1.2. Anatomy of the stomach.

The stomach is the main compartment of the GIT, where both mechanical and enzymatic transformations occur. Functionally, the stomach can be divided into two regions: the proximal stomach which comprises cardia, fundus and the main body and the distal stomach which includes antrum and pylorus (Fig. 1.2) (Bornhorst & Singh, 2014).

The proximal stomach acts as a food reservoir, where the bolus get in touch with the gastric juice which is mostly composed of HCl that leads to a reduction in gastric pH (from 6-5 to 1.5), mucus that protects gastric mucosa from the stomach acidity and enzymes such as pepsin and gastric lipase, responsible for protein and lipid digestion, respectively (Guerra *et al.*, 2012).

Instead, in the distal part of the stomach, the ingested food is crushed and grinded in smaller particles by the antral contraction waves and the peristaltic contractions of the stomach wall.

In fact, stomach contractions, especially the antral ones, play a significant role in the mechanical disintegration of food during digestion.

According to some studies, the contraction forces present in the stomach have values ranging between 0.2 N and 1.89 N depending on the fasting or the fed state (Vassallo *et al.*, 1992; Camillieri & Prather, 1994; Kamba *et al.*, 2000; 2001).

The peristaltic waves originate from tonic contraction on the upper surface of the stomach, travelling toward the pylorus with a frequency of about 3 cycles per minute (Schulze, 2006).

Therefore, they are responsible both for mixing and propelling of the ingested food to the pyloric valve.

On the arrival of the peristaltic waves, the pylorus partially opens, causing a “sieving effect”, allowing liquids and smaller particles (diameter < 1 mm) to reach the duodenum, while the larger particles (diameter > 2 mm) are squirted back and then retained into the stomach to be further processed (Kong & Singh, 2008). After approximately 3-4 hours, also the indigested food is emptied into the duodenum (Schwizer, Steingoetter, & Fox, 2006).

1.1.4. Digestion in the small intestine

At the end of the gastric digestion, chyme is transported to the small intestine, whose main functions are the breakdown of macromolecules and the absorption of nutrients and water (Guerra *et al.*, 2012). Morphologically, the small intestine can be divided into three parts: duodenum, jejunum, and ileum (Fig. 1.3).

When the chyme is delivered to the duodenum, it is neutralized by bicarbonate and mixed with the bile and the pancreatic juice thanks to the segmentation movements and the peristaltic contractions.

The primary function of bile is to emulsify fat promoting the pancreatic lipase activity and to form micelles that solubilize and transport lipophilic components to the gut wall for absorption (Minekus *et al.*, 2014).

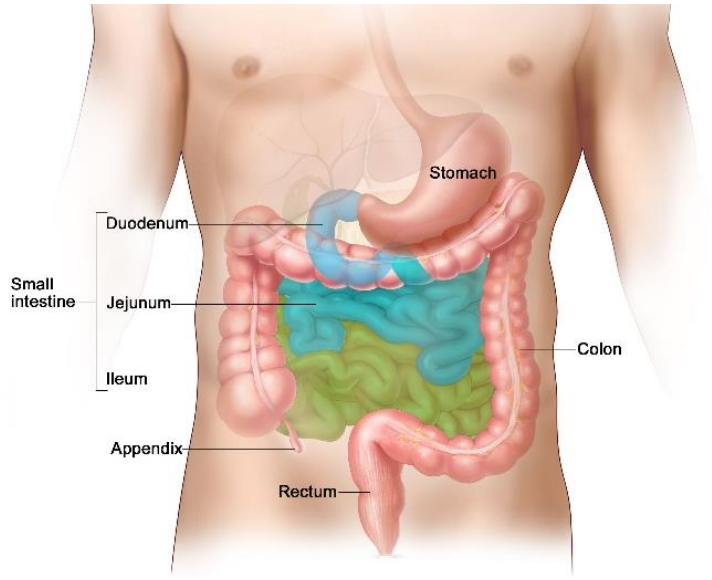

Fig. 1.3. Anatomy of the small intestine.

Instead, the digestive enzymes contained in the pancreatic and in the enteric juices (a complex mixture of proteases, amylases, and lipases) contribute together to the hydrolysis of the food constituents (Guerra *et al.*, 2012). Water and nutrients are mostly absorbed by the enterocytes of the jejunum and to a lesser extent in the ileum (Withney, 2008), while the non-absorbed material is pushed towards the large intestine.

1.1.5. Digestion in the large intestine

The large intestine comprises cecum, colon, rectum, and the anal canal. One of its main functions is the absorption of water and electrolytes. Furthermore, large intestine contains a large microbial population which is responsible for the fermentation of some food components such as proteins and polysaccharides. Finally, in this compartment also occur the formation, the storage, and the elimination of fecal material (Verhoeckx & Cotter, 2015).

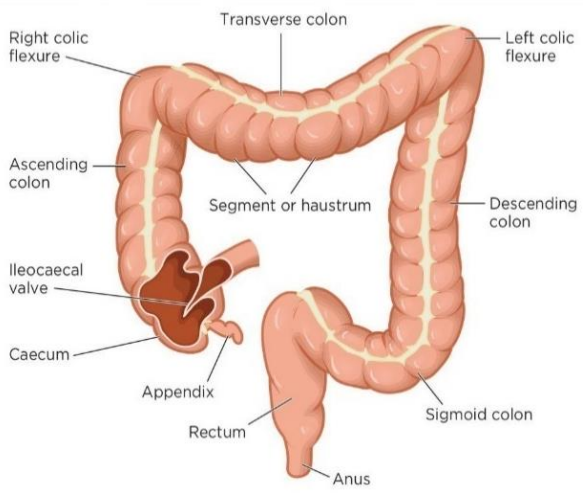

Fig. 1.4. Anatomy of the large intestine.

1.1.6. Control of digestion

The control of the digestion process is carefully maintained by the hormonal and the nervous systems which constantly communicate with the hindbrain sending fast-acting satiation signals. In particular, digestion is controlled throughout the GIT by a wide number of different G-protein coupled receptors, present in different concentration and location, which can detect certain ligands generating cellular responses and secretions of gastrointestinal hormones. So far, about 20 different gastrointestinal hormones with different functions are secreted by endocrine cells (Gouseti *et al.*, 2019). These include:

- **Ghreling:** an acylated 28-amino acid peptide hormone produced by the stomach and to a lesser extent by the small intestine, which causes increased gastric emptying and appetite.
- **Cholecystokinin (CCK):** a gastrointestinal hormone secreted by the I-cells in the proximal small intestine that stimulates the secretions of bile and pancreatic enzymes.
- **Glucagon-like peptide 1 (GLP-1):** secreted by the L-cells (particularly abundant in the colon) that stimulates insulin secretion and inhibits gastrointestinal mobility.
- **Glucose-dependent insulinotropic peptide (GIP)** secreted by the K-cells in the proximal small intestine which stimulates the insulin secretion.

Along with the body's physiological response to food, there is also a psychological component which may have an important role in the control of appetite and satiation (Cummings & Overduin, 2007).

1.2. Changes in the physiology of the human GIT during life

At this point, it is important to emphasise that the physiology of the human GIT undergoes changes during life. Thus, choosing and carefully setting parameters such as nature and concentration of digestive enzymes, flow rates and composition of digestive fluids, pH and temperature, the *in vitro* digestion models can be used to simulate the GIT of a wide range of target populations, like infants, young adults, seniors, and patients with impaired gastrointestinal conditions (Shani-Levi *et al.*, 2017).

1.2.1. Infants

Human GIT functionality develops during the first year of life. In fact, there are differences between the digestive system of infants and adults. Firstly, the digestive process of infants skips the oral phase because of the diet based on liquid foods, which transit very quickly through the oral cavity (Shani-Levi *et al.*, 2017). Regarding the gastric digestion, infants have a smaller stomach storage capacity (10-20 ml) (Abrahamse *et al.*, 2012; Bourlieu *et al.*, 2014) and a lower fasting gastric pH than adults (respectively 4-5 vs. 2) (Henderson *et al.*, 1998). This, in conjunction with the reduced pepsin secretion in new-borns, have a great impact on the gastric proteolysis (Bourlieu *et al.*, 2014; Dupont *et al.*, 2010a; 2010b). Gastric lipase activity, on the contrary, is like that of adults (Armand *et al.*, 1996; Sarles, Moreau, & Verger, 1992).

As regard the intestinal digestion, infants have a similar pH and trypsin concentration as those in the intestine of adults (Edginton & Fotaki, 2010). On the other hand, they have a lower number of pancreatic lipases, which is compensated by the endogenous lipases contained in the human breast milk (Lebenthal, Lee, & Heitlinger, 1983).

Infants differ from adults also for the composition, abundance, and diversity of gut microbiota, which becomes adult-like around 3 years of age (Matamoros *et al.*, 2013).

To date, several research groups have used static infant *in vitro* digestion models to study various aspects of protein and lipid digestion. However, the discrepancies found between these models, call for future efforts in defining a simple and harmonized infant static *in vitro* digestion model.

1.2.2. Elderly

GIT functionality is significantly altered with the ageing, leading to changes in the secretion of saliva, digestive enzymes and fluids, peristaltic and antral contractions, gastric emptying,

and small intestine transit rates (Salles, 2007). The understanding of the mechanism of GIT alteration with age and the knowledge of foods' digestive fate in the elderly GIT, can be useful to develop foods easily digestible and to improve nutrients bioavailability and bioaccessibility. Nevertheless, there are scant elderly *in vitro* digestion models found in literature (Shani-Levi *et al.*, 2017).

1.2.3. Humans with gastro-intestinal disorders

Human gastro-intestinal disorders are defined as diseases and/or conditions that interfere with the intake, digestion, and/or absorption of nutrients, causing various clinical symptoms (Shani-Levi *et al.*, 2017). Changing parameters like nature and concentration of enzymes, flow rates and composition of digestive fluids, pH and temperature, the *in vitro* digestion models can be used to simulate a wide range of impaired gastrointestinal conditions and therefore for developing new tailored food.

Chapter 2
In vitro digestion models

2.1. The existing *in vitro* digestion models

In vitro digestion models are widely used in field such as nutrition, pharmacology, and food chemistry in order to study the fate of orally ingested substances in the GIT (Guerra *et al.*, (2012); Lucas-González *et al.*, 2018). These models range from single static systems to mono-, bi- or multicompartmental dynamic systems and differ, sometimes strongly, from each other as described below.

2.1.1. Static *in vitro* digestion models

Static models represent the most widespread digestive systems. Most of the tests carried out in static models only consider the oral, gastric, and small intestinal digestion. Normally, in each phase, the food product is incubated with a given amount of simulated digestive fluids, under fixed pH and temperature, for a set period. Until a few years ago, the lack of consensus concerning the physiological conditions applied (e.g., pH, mineral type, ionic strenght, digestion time, etc.) made the comparison of preliminary results among laboratories quite difficult. To minimize this problem, in 2014 the INFOGEST network has proposed a first standardised and practical static digestion method based on physiologically relevant conditions that can be applied for various endpoints (Minekus *et al.*, 2014; Brodkorb *et al.*, 2019).

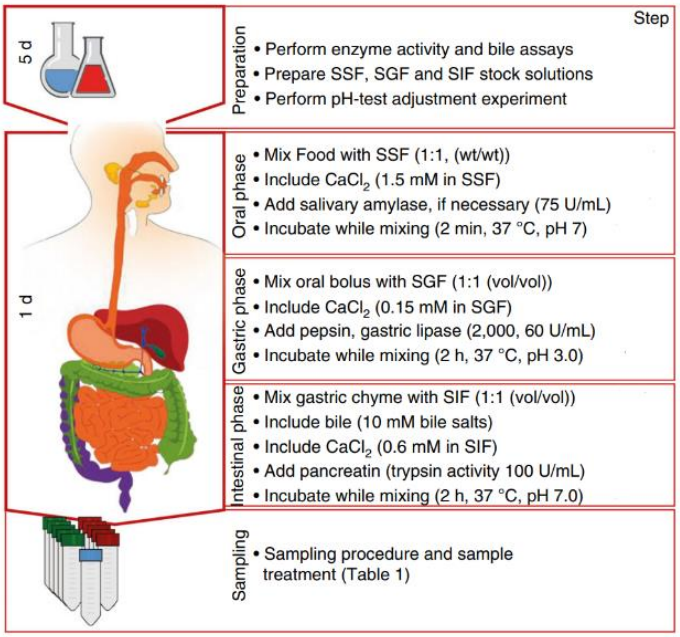

Fig. 2.1. Flow diagram of the INFOGEST 2.0 digestion method.
SGF, simulated gastric fluid; SIF, simulated intestinal fluid; SSF, simulated salivary fluid.

The method proposed by the INFOGEST network provides three digestive phases:

- **Oral:** mastication is simulated by mincing an appropriated amount of solid food using a mincer. For liquid food, the oral phase is optional, but recommended. Then, the sample is mixed with a Simulated Salivary Fluid (SSF) (1:1 wt/wt) to obtain a swallowable bolus with a paste-like consistency, $CaCl_2(H_2O)_2$ (1.5 mM in SSF), human salivary α-amylase (75 U/mL) if needed, and the necessary amount of water to dilute the stock solution of SSF.

  $CaCl2(H2O)_2$ is part of the digestive fluids' composition. However, it needs to be added immediately before the digestion experiment to avoid precipitation during storage.

  It is recommended to place the reaction vessel into a shaking incubator (to ensure a sufficient mixing during the digestion) for 2 minutes at 37°C (it requires a pre-warming of all reagents to 37°C).
- **Gastric:** liquid food or oral bolus is mixed with Simulated Gastric Fluid (SGF) (1:1 v/v), $CaCl_2(H_2O)_2$ (0.15 mM in SGF), porcine pepsin (2000 U/mL), gastric lipase (60 U/mL), water and 1M HCl to reduce the pH to 3.0. The recommended time of incubation is 2 hours at 37°C.
- **Small intestinal:** gastric chyme is mixed with Simulated Intestinal Fluid (SIF) (1:1 v/v), $CaCl_2(H_2O)_2$ (0.6 mM in SIF), bile (10 mM bile salts), pancreatin from porcine pancreas (trypsin activity of 100 U/mL) or individual enzymes, water and 1M NaOH to bring the mixture to pH 7.0. The recommended time of incubation is 2 hours at 37°C.

Despite the numerous advantages of the static *in vitro* digestion models such as the flexibility, accuracy, and reproducibility, they are unable to accurately mimic the physical and the physiological processes occurring *in vivo*.

2.1.2. Semi-dynamic *in vitro* digestion models

As stated earlier, semi-dynamic models represent an interim solution between the static and the dynamic ones. The INFOGEST semi-dynamic model (Mulet-Cabero *et al.*, 2020) does not require complex laboratory instruments and it is mainly focused on the gastric digestion (since the stomach is the main compartment of the GIT where both mechanical and enzymatic

transformations occur). Therefore, among the advantages of this model is the possibility to evaluate food disintegration and nutrients bioaccessibility during digestion.

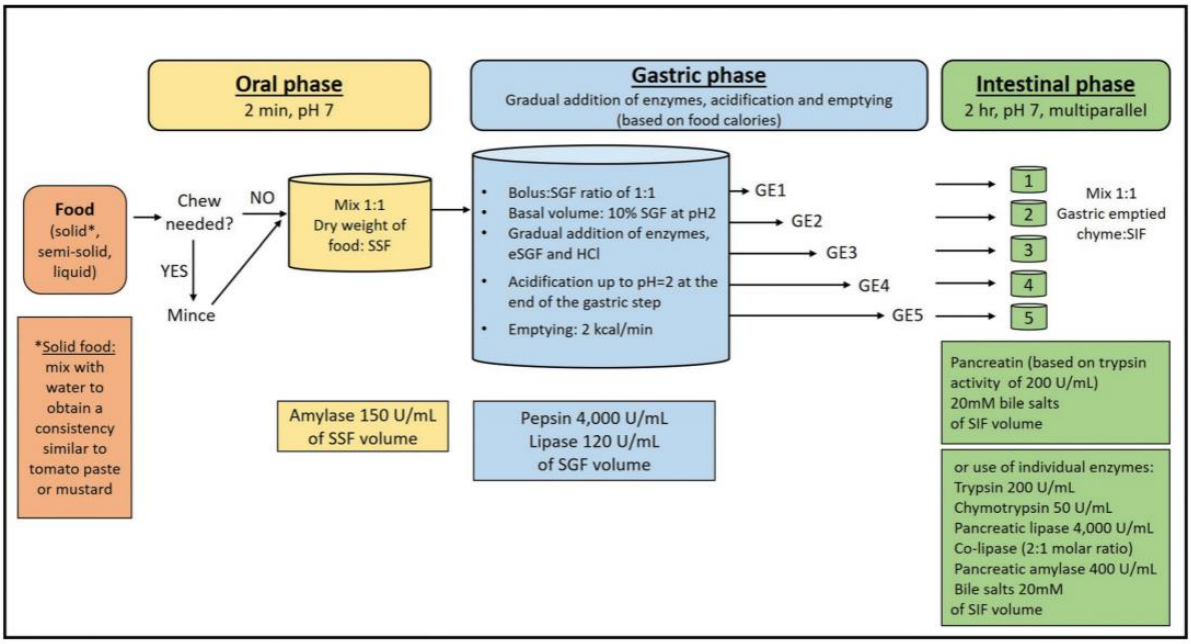

Fig. 2.2. Overview of the simulated semi-dynamic *in vitro* digestion method. Simulated salivary fluid SGF, simulated gastric fluid; SIF, simulated intestinal fluid; SSF, simulated salivary fluid; GE, gastric emptying.

Just like the static method, the semi-dynamic method proposed by the INFOGEST network provides three digestive phases:

- **Oral:** performing this phase is recommended both for liquid and solid foods. In case of solid products, mastication is simulated by mincing an appropriated amount of food using a manual or electric mincer. Then, the sample is mixed with an amount of Simulated Salivary Fluid (SSF) which correspond to the dry weigh of sample (1:1 v/w), $CaCl_2(H_2O)_2$ (1.5 mM in SSF), human salivary α-amylase (150 U/mL in SSF) if required, and the necessary amount of water to achieve the required concentration of SSF. The recommended time of incubation is 2 minutes at 37°C (a pre-warming of all reagents to 37°C is required).
- **Gastric:** gastric phase can be simulated with a generic apparatus composed by an auto-titrator including an attached pH probe and dosing units for the simulated digestive fluids, syringes infusion pump for the gradual addition of enzyme solutions, and a vessel with thermostat jacket connected to a heated circulating bath. Stirring can be achieved with an overhead stirrer (10-15 rpm) including a paddle stirrer blade.

Sample is mixed with Simulated Gastric Fluid (SGF) (1:1 v/v), $CaCl_2(H_2O)_2$ (0.15 mM in SGF), pepsin (2000 U/ml), gastric lipase (120 U/ml), water and 6M HCl to reach pH 2.0 at the end of the gastric digestion.

To simulate the fasted state, a basal volume of SGF (corresponding to the 10% of the total gastric secretion) is placed into the thermostated vessel before adding the bolus.

Unlike the INFOGEST static method, the semi-dynamic one takes into consideration the amount and type of food tested, and specifically its caloric content. In fact, the digestion time is positively related to the energy content of the food. For convenience, in the calculations, the amount of food tested is scaled down from a standard meal volume which needs to be realistic for that specific food (e.g., for milk could be 200 mL). The calculations of the energy emptying rate (kcal/min) and volume emptying rate (mL/min) are based on the delivery of 2 kcal/min of a food volume of 500 mL based on *in vivo* considerations.

Subsequently, gastric halftime (min) and thus total digestion time (min) can be calculated, where the gastric halftime ($t_{1/2}$) represents the time required by the stomach to empty 50% of the ingested meal (Seok, 2011). Gastric emptying can be performed by manually taking selected aliquots (from 3 to 10) from the bottom of the vessel using a plastic pipette with an end diameter of ~ 2-3 mm (to simulate the sieving effect of pylorus).

- **Small intestinal:** each aliquot emptied from the gastric phase is mixed with Simulated Intestinal Fluid (SIF) (1:1 v/v), $CaCl_2(H_2O)_2$ (0.6 mM in SIF), bile salts (20 mM in SIF), pancreatin (trypsin activity of 200 U/mL) or individual enzymes, water and 1M NaOH to bring the mixture to pH 7.0. The recommended time of incubation is 2 hours at 37°C.

Despite its numerous benefits, the semi-dynamic model is simpler and less accurate than the dynamic computerised versions. Specifically, among its disadvantages include:

- The need to fix some parameters (e.g., the amount of food, number of gastric emptying aliquots, mixing speed) to reduce the variability between different laboratories.
- The incapacity to properly simulate the peristaltic contractions of the stomach.
- The difficulty in performing the gastric emptying. Depending on the complexity (in terms of structure and other properties) of the food tested, there could be sample losses through the emptying process.

2.1.3. Dynamic *in vitro* digestion models

Several dynamic *in vitro* digestion models have been developed during the past decades to mimic both the physical and chemical conditions encountered in the GIT (Bornhorst & Singh, 2014). In fact, it is well known that the digestion is a dynamic process during which the physicochemical conditions: pH, ionic strenght, digestive enzyme concentration, among others evolve with the time in each compartment. The dynamic models, unlike the static ones, consider these evolutions as well as the physical forces, such as peristaltic contractions, which are primarily responsible for food mechanical breakdown into the stomach (Dupont & Mackie, 2015).

Such dynamic *in vitro* models include the TIM developed at the TNO Nutrition and Food Research Centre (Zeist, Netherlands), the Dynamic Gastric Model (DGM) drawn up at the Institute of Food Research (Norwich, United Kingdom), the Human Gastric Simulator (HGS) developed at the University of California (Davis, California, USA), the DIDGI® system developed at the French National Institute for Agricultural Research (INRA) and the SIMGI® system located in the Institute of Food Science Research (CIAL) (Madrid, Spain).

2.1.3.1. TNO's *in vitro* gastro-intestinal model (TIM)

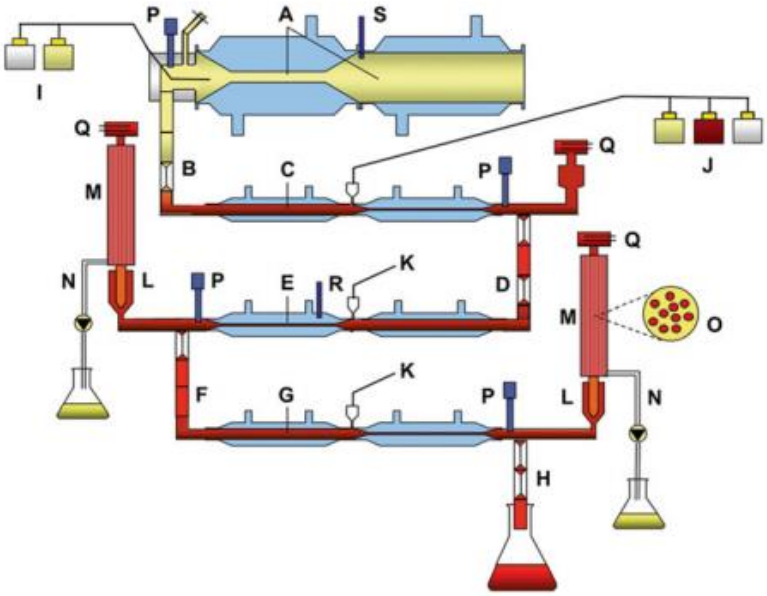

Fig. 2.3. Schematic representation of TIM-1.

The Netherlands Organisation for applied scientific research (TNO) has developed an *in vitro* gastrointestinal model (TIM) that allows to gain insights into the release, solubility and bioaccessibility of nutrients and pharmaceutical compounds within the GIT.

The TIM system can simulate the physiological processes and conditions within the GIT of a wide range of target populations, thanks to the possibility to dynamically monitor and regulate parameters such as temperature, pressure, acidity, and electrolyte concentrations (Minekus, 2015).

Briefly, the model consists of several interconnected glass compartments, with a flexible membrane inside. In between the glass jacket and the membrane there is water at body temperature (37°C for human). By applying pressure on the water at regular intervals and in a certain sequence, the flexible membrane contracts and causes peristaltic waves which mixes the luminal contents and moves it through the system.

TIM has been divided in two systems: TIM-1 and TIM-2.

- **TIM-1** comprises the stomach and the small intestine which is divided into three parts: duodenum, jejunum, and ileum. These compartments are connected by peristaltic valve pumps (PVP) that allow the transfer of controlled amounts of chyme. Prior to introduction into the gastric compartment, the meal is masticated with a food processor and mixed with artificial saliva containing electrolytes and α-amylase. When the bolus reaches the stomach, it is mixed with gastric secretion (containing gastric acid, electrolytes, pepsin, and lipase) and pushed forward and backward due to the simulated mixing movements. Then, in the first part of the small intestine, the duodenum, chyme is mixed with the duodenal secretion consisting of electrolytes, bile and pancreatin. Bicarbonate is added to neutralize the pH value, bile to emulsify fat and pancreatic enzymes to digest fat, carbohydrates, and proteins. Subsequently, the digested and undigested food transit into the jejunum and ileum where dialysis systems remove the released and dissolved compounds (the bio accessible fraction). At the end of the TIM-1 the non-digested and the non-released components can be collected for further analysis or be used as input for TIM-2.
- **TIM-2** simulates the large intestine or the colon (Venema, 2015). This part of the intestine contains many bacterial species (the microbiota), which play an important role in the digestion of the indigested materials from the small intestine. The system is kept at a pH of 5.8 and to ensure an anaerobic environment, it is flushed with gaseous nitrogen. TIM-2 has 10 units available, allowing multiple parameters to be tested in

parallel. The model is incubated by using fecal donations from volunteers. Fecal donations can be obtained from healthy volunteers of different age-classes (baby, adults, elderly), people with diseases or disorders, or from lean vs. obese individuals. These can be used in two ways: (a) a fecal donation from individual 1 can be introduced into one of the TIM-2 units, the donation from individual 2 in a second unit, and so on. In this way the composition and the activity of microbiota from different individuals can then be compared on the same substrate; (b) the fecal donations of several donors are mixed to create a standardized microbiota. This allows comparison of multiple substrates or conditions starting with the same microbiota composition. Upon introduction of the microbiota in the system, an adaptation period of about 16 hours is applied (to allow the microbes to adapt to their new environment). The system is equipped with a dialysis system to prevent the accumulation of microbial metabolites, which would lead to the inhibition or death of the microbes in the model. Since these metabolites are taken up by the epithelial cells of the colon (colonocytes) *in vivo*, the dialysis system is required to mimics better the physiological situation in the large intestine.

In 60% of these experiments, TNO used the TIM system to investigate the influence of drugs on the composition and metabolic activity of the microbiota after single or repeated dose.

Advantages of the TIM systems are:

- They can be used for a variety of purposes both in the pharmaceutical and the nutritional field.
- Samples can be collected from each compartment for further analysis.
- The experimental tests are highly reproducible thanks to the possibility to constantly control all the settings.
- They allow for the evaluation of the bioaccessibility of food compounds.

Limitations of the TIM systems are that:

- There is no feedback on the food energy content on the GI conditions.
- The systems are not provided by an intestinal mucosa; therefore, nutrients absorption should be studied by the combination with intestinal cell lines or tissues.
- The bioavailability including metabolism and excretion is not evaluated.

2.1.3.2. Dynamic Gastric Model (DGM)

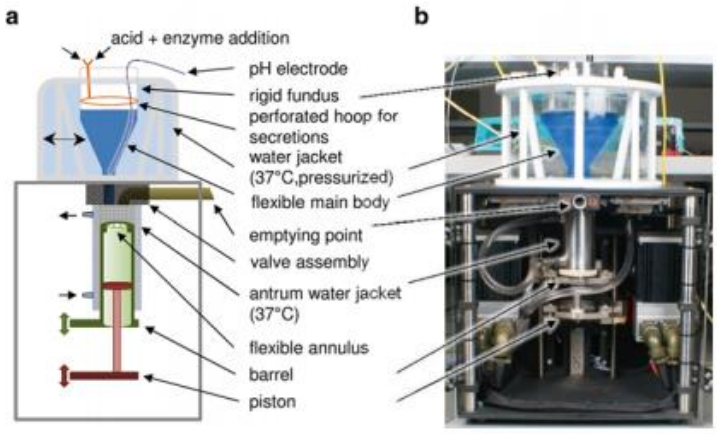

Fig. 2.4. The Dynamic Gastric Model (DGM).

The Dynamic Gastric Model (DGM) has been developed at the Institute of Food Research (Norwich, UK) to meet the need for an *in vitro* model able to simulate both the mechanical and biochemical events that occur during the gastric digestion (Thuenemann *et al.*, 2015). This model has been extensively used for food and pharmaceutical applications, such as to study the structural changes of food matrices during digestion and therefore to investigate the release and the bioaccessibility of nutrient compounds and drugs. As the human stomach, the DGM consists of three distinct zones which differ in the physical forces applied to the bolus: the fundus, the main body, and the antrum.

Before starting gastric digestion, parameters such as the total gastric residence time and the maximum rate of gastric secretion are estimated based on mass, volume energy content, and composition of the test meal.

Firstly, the test meal can be masticated or not. The mastication can be carried out by human chew, or it can be simulated using a food processor with or without addition of artificial or human saliva.

Then, the meal is added to the fundus, where, as well as in the main body, the food bolus is subjected to low physical forces. In detail, it is rhythmically squeezed by cyclical pressurization of the 37°C water jacket surrounding the main body. Here, food bolus is mixed with gastric acid and enzyme solutions, whose rate of addition slows gradually in response to the acidification of meal and the gradual decrease in food bolus volume, respectively.

Subsequently, the test meal is pushed towards the antrum where it is subjected to higher shear force, resulting in greater mixing as well as gradual size reduction of particles.

The DGM antrum consists of a barrel and a piston, which move within a 37°C water jacket. As it happens in the stomach, to allow to the larger and denser particles to stay longer in the antrum and then of being subjected of extended processing, a “death volume” is maintained between the barrel and the piston.

This system has various advantages, including:

- The vessel capacity (800 ml) that allows to analyse large amounts of test meal.
- The possibility to perform tests in real time because the length of each experiment is established considering the estimated gastric residence time of the test meal.
- The possibility to constantly monitor and then control temperature and pH values.

This system also has a few drawbacks, like:

- It is made of not transparent material. Consequently, visual observations are not possible during the antral processing.
- There are no *in vivo* satiety signals controlling rate of digestion.

2.1.3.3. Human Gastric Simulator (HGS)

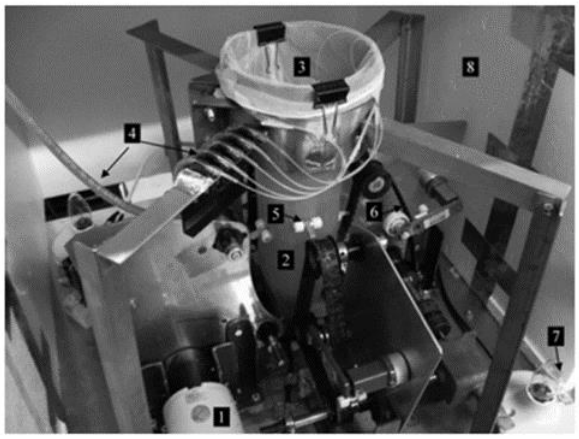

Fig. 2.5. Human Gastric Simulator (HGS).

The HGS has been developed to allow a better understanding of the physical processes driving food disintegration in the stomach as well as mixing of gastric contents during digestion (Ferrua & Singh, 2015).

Considering the central role of the mechanical forces in the food disintegration and consequently in the bioavailability of nutrients, there is a real need for a model able to replicate the actual motility of the gastric wall during digestion.

Briefly, the HGS consists of a cylindrical latex vessel that ends in the form of a conic frustum and four conveyor belts that periodically impinge a series of Teflon rollers upon the latex wall to mimic the antral contraction waves. The model is maintained at constant temperature of 37°C thanks to two 60 W light bulbs and it is also fitted with gastric secretion and emptying systems.

The simulated bolus can be prepared cutting or grinding the food sample which will subsequently be mixed with artificial saliva for 30 s and allowed to stand at 37°C for 2 min. Food bolus can be placed into the vessel through the upper opening.

To simulate the fasting conditions of the stomach, 50–70 mL of simulated gastric juice is first loaded into the HGS, while the gastric juice is released immediately after the bolus is loaded. The simulated gastric juices are delivered at about 10–15 cm from the bottom of the compartment through five polyethylene tubes at a rate of 0.03-8.2 mL/min.

Furthermore, to simulate the sieving effect of the pylorus, a thin polyester mesh bag with net pore size of 1.5 mm, is used to cover the inner surface of the latex vessel. This bag retains the larger particles (diameter > 2 mm) for further breakdowns and releases the smaller particles (diameter < 1 mm) for emptying. At the end of the test, the mesh bag and then the remaining digesta, can be easily taken out from the vessel and analysed. The rate of gastric emptying is of 3 mL/min and depending on the test meal, after 3-5 h the digesta remaining inside the HGS is removed for further analysis.

Several studies have confirmed the ability of the HGS to emulate the mechanical forces that develop *in vivo*. However, further efforts are necessary to automate the adjusting of the secretory and the emptying rates based on the specific composition and volume of the food sample.

2.1.3.4. The DIDGI® system

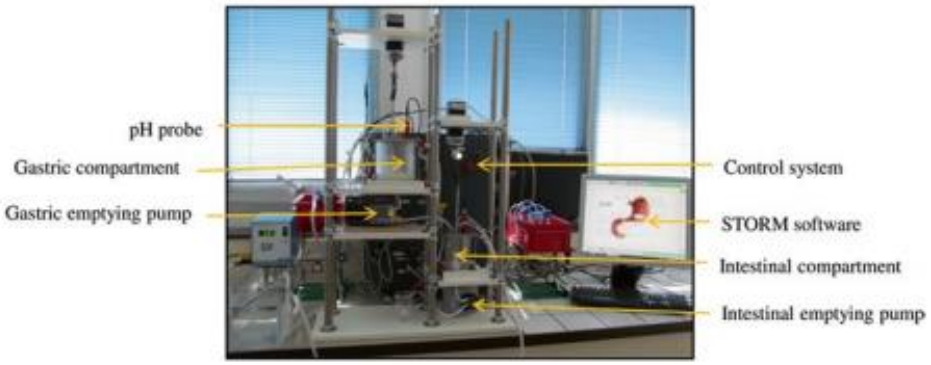

Fig. 2.6. Schematic presentation of the DIDGI® system.

The DIDGI® system has been developed at INRA with the purpose to investigate the mechanism of food disintegration in the GIT, to identify the molecules released during digestion as well as to understand how food structure affects food digestion and the nutrients bioaccessibility and bioavailability (Ménard, Picque, & Dupont, 2015).

It is a simple computer-controlled system consisting in two consecutive compartments simulating the stomach and the small intestine and each of them is surrounded by a glass jacket filled with water at 37°C. The system can be set up using parameters and data obtained from *in vivo* studies such as pH, volumes and flow rates of secretions, nature and quantity of enzymes, amount and duration of the meal.

To simulate the sieving effect of the pylorus, a Teflon membrane with net pore size of 2 mm is placed before the transfer pump between the gastric and the intestinal compartment. The system is also provided with variable speed pumps to control the incoming and outgoing flows.

The DIDGI® System has been used to study the digestion of several food matrices such as dairy products, meat, fruit, vegetables, and emulsions, but most of all infant formulas.

This system has various advantages, among them the following:

- The capacity of the vessel up to 200 ml.
- The possibility to perform tests in real time because the length of each experiment is established taking into account data obtained from *in vivo* studies.
- The possibility to constantly monitor and then control temperature and pH values.
- The system can be easily used to study the digestion of a wide range of drink/food matrix.
- It is made of transparent material. Consequently, visual observations are possible during the digestion process.
- The system has been validated against *in vivo* (porcine) data for the digestion of infant formula.

This method also has a few drawbacks, including:

- There are no *in vivo* satiety signals controlling rate of digestion.
- The bioreactors do not mimic neither the anatomy nor the stomach contractions.
- The system does not provide a simulation of nutrient absorption.

2.1.3.5. The SIMGI® system

Fig. 2.7. SIMGI® system.

The SIMGI® (Dynamic Gastrointestinal Simulator) is a computer-controlled dynamic simulator of the human GIT. As well as the TIM, this system permits to mimic the overall digestive process, from the oral phase to the digestion in the large intestine. It comprises two compartments simulating the stomach and the small intestine, and three-stage culture reactors meant to emulate the microbial conditions of ascending, transverse, and descending colon. Each compartment can work individually, and samples can be collected by each of them to be analysed. Stomach is composed of a reservoir made of flexible silicone walls covered by a methacrylate jacket, where thermostated water (37°C) is pumped allowing the simulation of peristaltic contractions. Gastric emptying into the small intestine can be also mimed. The small intestine and the colon consist of continuously stirred reactors operating under anaerobic conditions (by continuously flushing N_2) and controlled pH. In the small intestine, the product of gastric digestion is mixed with simulated intestinal secretions while colon can host a large population of human fecal microbiota (fecal samples from healthy and non-healthy donors can be used according to the study).

Among the main advantages of this system, it is worth noting:

- The fully automation which allows an accurate control of the chemical-physical parameters used to simulate gastro-intestinal conditions.
- The opportunity to monitor food structural changes during gastro-intestinal digestion and nutrients bioaccessibility.
- The possibility to monitor the effect of foods and food components on intestinal microbiota composition, metabolic activity, nutritional status, and health.

2.1.3.6. The SHIME® system

The Simulator of the Human Intestinal Microbial Ecosystem (SHIME®) from ProDigest is a multicompartmental and computer controlled dynamic simulator that represents an evolution of the simulator of the University of Reading presented by Macfarlane *et al*. (1989) (Van de Wiele *et al.*, 2015). The SHIME® system operates at 37°C and under anaerobic conditions (by daily flushing the headspace of the compartments with N_2 gas or a 90/10 % N_2/CO_2 gas mixture).

It consists of five double-jacketed glass vessels connected by peristaltic pumps which simulate the stomach, the small intestine, the ascending, transverse, and descending colon, respectively. Within each compartment, mixing of the digestive slurry is provided by magnetic stir bars.

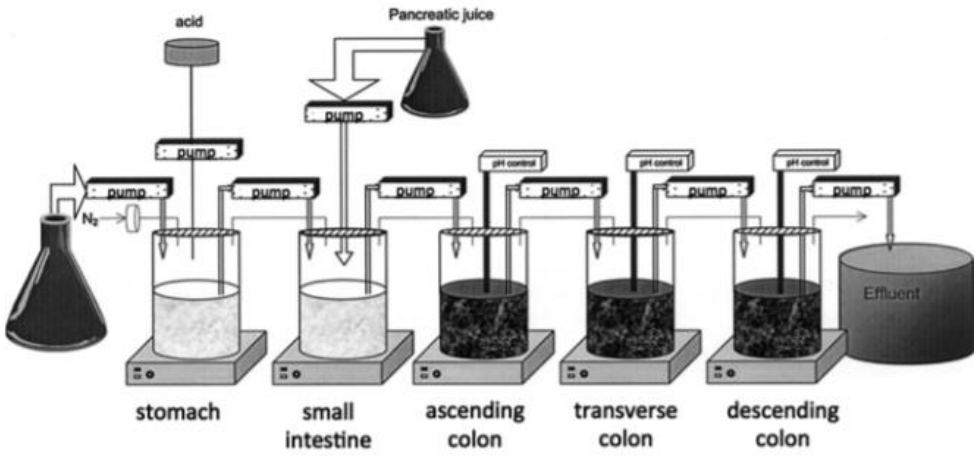

Fig. 2.8. Schematic representation of the SHIME®

The SHIME® software allows the definition of specific pH profiles for each compartment. In detail, the gastric vessel works at acidic conditions while the small intestine at slightly acidic to neutral conditions. Besides, the pH of the colon compartments is set between 5.6 and 5.9 in the ascending, 6.1–6.4 in the transverse and 6.6–6.9 in the descending colon. Three times per day, the gastric compartment is added with a nutritional medium (made of carbohydrate and protein sources, mucins, and mineral and vitamin mix) while the small intestine reactor with pancreatic and bile liquid. Instead, the colon is inoculated with fecal microbiome derived from one individual. Since the fecal microbiome differs greatly from the *in vivo* one (in terms of composition and metabolic activity), the fecal microbiome is inoculated and let it adapt to the conditions of each colon compartments. Generally, the adaptation time is around 5–10 times its residence time which is approximately 48 hours for a male individual.

In the human GIT there is also a fraction of microorganisms that can selectively adhere to the mucus layer that covers the gut wall, forming a barrier against pathogens and therefore playing a key role in human health. To evaluate this bacteria fraction, the SHIME® system has been extended with the M-SHIME® (Mucus-SHIME) a model that integrates a mucosal compartment in the colonic regions.

Compared with other dynamic simulators the SHIME® system shows the following strengths:

- It comprises the entire GIT, from the stomach to the descending colon.
- It permits the gradual emptying of the gastric content into the intestine reactor.
- The definition of specific pH profiles for each compartment by means of the specific software.
- The easy sampling from all the compartments provides detailed information on the digestive fate of specific compounds.
- The possibility to perform long-term experiments using a stable and *in vitro*-adapted microbial community.
- The opportunity to sample high volumes from each colon area allows to perform parallel analyses without impacting the microbial community.

On the other hand, the SHIME® presents two huge lacks:

- The absence of a dialysis system able to remove the bioaccessible fraction and to avoid the accumulation of microbial metabolites.
- The impossibility of simulating the peristalsis since mixing is performed by means of magnetic stir bars.

2.2. Limitations of the existing *in vitro* digestion models

Despite their complexity, the existing gastro-intestinal models are still unable to mimic fully the overall processes occurring *in vivo*, such as peristaltic movements, hormonal and nervous control, feedback mechanism, and mucosal cell activity (Guerra *et al.*, 2012). As regards the latter point, the Caco-2 cell culture model has been widely used in combination with the TIM system to get information about the absorption process of drugs and dietary components through the intestinal epithelium. The Caco-2 cell line is originally derived from a colon carcinoma (Lea, 2015). One of its most advantageous properties is its ability to spontaneously differentiate into a monolayer of cells with many properties typical of absorptive enterocytes with brush border layer as found in the small intestine. For this reason, the Caco-2 cell line has been used for a huge range of applications, such as:

- To study the effects of microbiota, microbiota metabolites, food digesta and bioactive food components on the barrier function of the intestinal epithelium.
- To study the potential toxic effects of drugs or food metabolites in the intestinal mucosa.
- To investigate how food components may influence the transport of bioactive molecules across the intestinal epithelium.
- To study the interactions between bioactive molecules during the transport across the intestinal epithelium.

However, despite its bright prospects, the Caco-2 cell line model has several limitations.
First, it does not consider the presence of the mucus layer and unstirred water layer close to the epithelium which strongly influence the uptake *in vivo*. Secondly, the intestinal epithelium contains not only enterocytes, but different cell type.
Therefore, further efforts will be necessary to simulate the complexity of the human intestinal tract.
Since the stomach is the major compartment for food disintegration in the human body, another important challenge for the scientific community is to simulate as accurately as possible both the realistic shape of the stomach and the continuous peristaltic movement of its walls, with similar amplitude and frequency of contraction forces as reported *in vivo* (Kong & Singh, 2010). Most of the current models seek to reproduce the forces in play during digestion by simply mixing food and gastric fluid using a magnetic stirrer or a shaking bath (Kong & Singh, 2008). On the other hand, some of the more sophisticated dynamic gastrointestinal models such as the DGM and TIM, have been designed in a way to provide a better simulation of gastric digestion, producing continuous peristaltic movement of stomach wall like *in vivo* observations. However, also the types of forces applied on foods in these *in vitro* digestion models are different from the forces that foods receive during the gastric digestion, suggesting that there remains a need for a system able to create realistic gastric environment for food breakdown (Kong & Singh, 2010).
To date, a limitation of the *in vitro* digestion is that none of the developed multicompartmental models include all the stages from the mouth to the large intestine. In fact, most *in vitro* studies lack the oral phase and/or the digestion in the large intestine, which are particularly difficult to simulate but, at the same time, they have a relevant impact on the digestion process. Therefore, a further step could be the development a model integrating all the digestion steps (Guerra *et al.*, 2012).

2.3. Possible applications of the existing *in vitro* digestion models

In vitro digestion models have been widely used in nutrition and health studies. For example, they can be used to understand the existing correlation between the bioaccessibility of a specific compound (like nutrients, drugs, allergens, food pollutants) and its chemical form, as well as the food structure, the interaction with other food components or the type of process applied. Then, of course, the information obtained could be helpful to design functional foods. In this context, the dynamic models should be preferred to the static ones, since they take into account parameters which may influence the bioaccessibility of specific ingested substance, such as the gastrointestinal transit time or the stomach emptying rate (Guerra *et al.*, 2012).

Furthermore, the *in vitro* digestion models can be used to test the ability of microcapsules to protect functional compounds (e.g., probiotics) from the adverse gastric conditions and to release food ingredients at a specific target site.

Chapter 3

Lentil flour: nutritional and technological properties, *in vitro* digestibility and perspectives for use in the food industry

Abstract

The use of lentil flour in bakery (bread, cake, crackers), extruded (pasta, snacks) and other products (dressings, soups, dairy, and meat products) is gaining attention of food technologists and of industry as well as popularity among consumers due to an excellent and balanced nutritional composition. This research interest has extended our knowledge of nutritional and functional properties (solubility, emulsification, gelation, foaming) of lentil flour, which, in turns, has disclosed its technological potential for preparation of high-quality foods (gluten free bakery, yogurt and meat products). However, addition of lentil flour may introduce technological problems and novel allergens. This chapter covers the use of lentil flour in food preparations, with focus on protein and starch digestibility and on the challenges to design lentil-based products with improved quality.

3.1. Introduction

Lentil (*Lens culinaris Medik.*) is a pulse crop belonging to the *Fabaceae* family which is primarily produced in Canada and India (2.09 MT and 1.62 MT in 2018) (FAOSTAT, 2020; URL: http://www.fao.org/faostat/en/#data/QC/visualize), ranking fourth in the global grain legumes production after bean (*Phaseolus vulgaris L.*), pea (*Pisum sativum L.*) and chickpea (*Cicer arietinum L.*) (Kumar & Pandey, 2020). Just like other legumes, lentil is considered a sustainable crop because it can fix atmospheric nitrogen and thus reduces the use of fertilizers for cultivation, enhancing soil quality (Clune, Crossin, & Verghese, 2017). Furthermore, lentil requires less water and can tolerate drought stress better than other crops making them well adapted to water scarce soil (MacWilliam *et al.*, 2018). Lentil cotyledon is lens-shaped and may have a wide range of colors (yellow, orange, red or green) as reported in Figure 3.1, even though the most traded classes are the red and green ones.

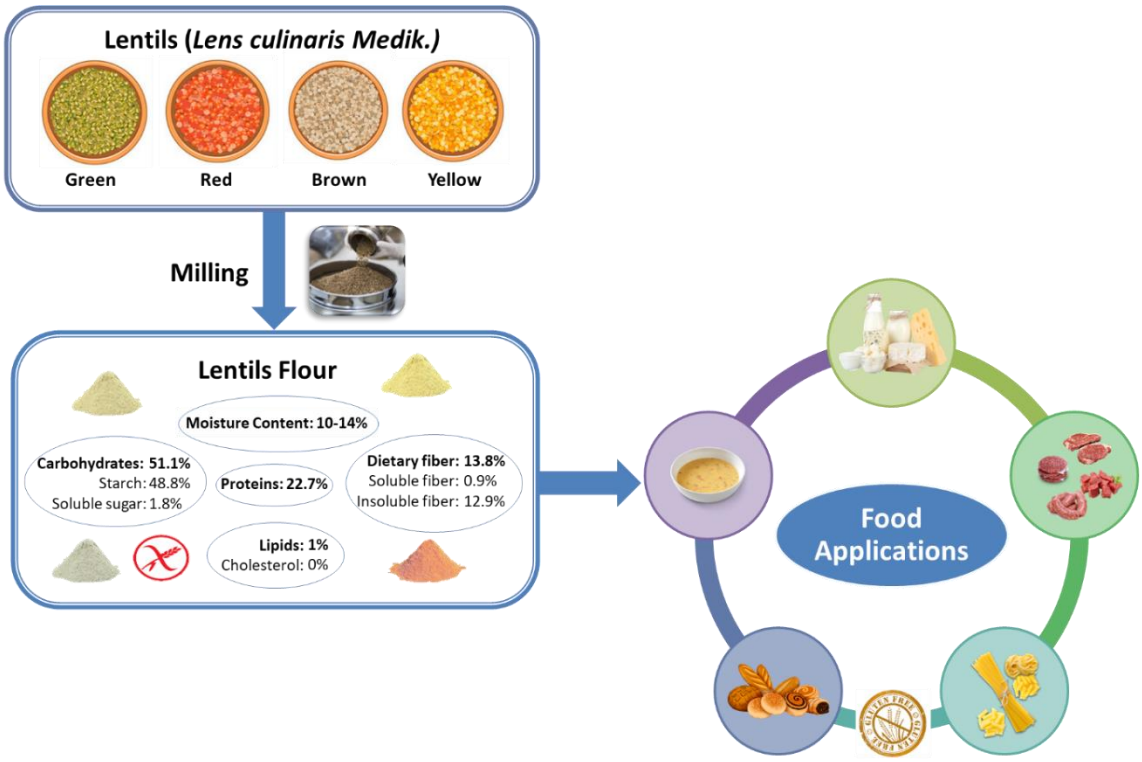

Fig. 3.1. Flour from Lentils (*Lens culinaris Medik.*): composition and food applications.

They have been classified as soft seed-coated pulses and require a short preparation time (Khazaei *et al.*, 2019) (e.g., no soaking required), but a longer cooking time, which limits their usage in European and Western countries (Chelladurai & Erkinbaev, 2020). Lentils can be also classified in two types based on their seeds size: Chilean/large-seeded (> 50 g per

1000 seeds) and Persian/small seeded (≤ 50 g per 1000 seeds), which is a crucial parameter influencing the techno-functional properties of lentil flour (LF) (Liu *et al.*, 2020). Lentils are usually used for human and domestic consumption in the form of cooked whole seeds or split cotyledons or processed into various ingredients (e.g., flour) to be used in different food applications (Figure 3.1). In the last years, an increased trend in lentil consumption has been observed, that is due to a better knowledge of its excellent nutritional composition and potential health-beneficial effects associated with a decreased risk of chronic diseases (e.g., obesity, type-2 diabetes, hypertension, cancer, and cardiovascular diseases), mainly in elderly Mediterranean population (Papandreou *et al.*, 2019). Lentil composition varies significantly with genetic and environmental factors, but overall, it contains a high number of nutritional components and it is gluten free. In details, lentil is known as poor man's' meat, since it is a cheap source of proteins (21–31%) (Saricaoglu, 2020) representing an important food resource for developing countries, low-income people, vegetarian and vegans (Argel *et al.*, 2020). Lentil proteins contain all the essential amino acids (39.3 g of essential amino acids per 100 g of proteins) and are rich in lysine, leucine, arginine, aspartic and glutamic acid. However, they are limited in sulfur-containing amino acids (methionine and cysteine) and tryptophan, and thus the consumption of lentils mixed with other plant protein sources, such as cereal grains, represents an efficient way to obtain an adequately well-balanced amino acid profile (Monnet *et al.*, 2019). The total carbohydrate content in lentil seeds (62–69%) includes primarily starch (35-53%), with low glycemic index (GI) value (21-22%) (Chelladurai & Erkinbaev; Revilla *et al.*, 2019), followed by high concentrations of dietary fibres (5–20%) (Revilla *et al.*, 2019; Graf *et al.*, 2020) and oligosaccharides. Furthermore, lentils are rich in micronutrients such as vitamins (mainly vitamin B9/folate), zinc (4.8 mg/100gr) and iron (7.5 mg/100gr). Lentils also represent an abundant source of phytochemicals, many of which have been identified as potential chemopreventive candidates. Among these, phenolics (760 mg GAE/100g), which are present in much higher concentrations than in other legume species can contribute to their high antioxidant, antidiabetic, anti-obesity, anticancer and anti-inflammatory properties (Faris, Mohammad, & Soliman, 2020). These properties are not only linked to the phytochemicals but also to bioactive peptides (e.g., lectins, defensin), proteins (e.g., trypsin and protease inhibitors) and saponins. Most of these compounds are classically known as anti-nutritional factors (ANFs) which can inhibit the activity of digestive enzymes or sequester nutrients (making them unavailable for digestion), or even give a bitter or unacceptable taste (Nosworthy *et al.*, 2018). The amount of ANFs in lentils is reported to be reduced or inactivated by different

pre-processing and processing methods (e.g., cooking, fermentation, soaking, germination, or mechanical methods such as dehulling and milling) (Faris, Mohammad, & Soliman, 2020), which helps to remove the major obstacles in the consumer's mind about including lentil-based products in their diet. In particular, the greatest part of ANFs (e.g., tannins) can be found in the seed coat and thus it could be reduced in LF by pre-treatment methods such as dehulling (physical removal) and grinding/milling (size reduction) of whole or decorticated seeds (Khazaei *et al.*, 2019). More recently, however, a number of these compounds (e.g., saponins, phytic acid, lectins) are attracting considerable interest in the fields of biochemistry, medicine, pharmacology, and nutrition as a result of their beneficial anticancer, antimicrobial properties in humans (Mattila *et al.*, 2018). For example, lectins have been recognised as potent anticancer compounds, as they have the ability to bind to cancer cell membranes/receptors, causing their apoptosis, cytotoxicity, and autophagy. At the same time, being ANFs, lectins can reduce nutrients bioavailability and solubility in raw lentils seeds, but heat treatments have been shown to hinder their activity significantly.

Protease inhibitors inhibit the activity of trypsin, chymotrypsin, and other intestinal proteases, but once inactivated by cooking, they may have some potential health benefits such as anti-inflammatory activity as well as the ability to suppress cancer cell proliferation.

Moreover, lentils represent one of the greatest sources of saponins (34 mg/100g of lentils) which are responsible for the bitterness of raw lentils seeds. Saponins also have positive nutritional properties which are primarily linked to their molecular structure. In fact, they can bond with cholesterol leading to a reduction of its absorption in the small intestine and inhibiting the growth of cholesterol-rich cancer cells and/or kill them (Foschia *et al.*, 2017; Faris *et al.*, 2020).

Lentil is among the plant foods causing allergic reactions in paediatric patients in the Mediterranean area, especially in Spain, Turkey, and Asia. This may reflect the use of lentil as a weaning food in Spain as well as in the Asian continent. The symptoms of allergic individuals after eating lentil range from relatively mild symptoms. However, approximately 20% of patients allergic to these legumes presents severe and systemic symptoms, although cutaneous reactions are the most common. Lentils contain a variety of allergenic proteins (mainly belonging to the storage protein family) which are often heat-stable and protease resistant. They may be responsible for IgE-mediated hypersensitivity reactions that can hit the cutaneous, cardiovascular, respiratory, and gastrointestinal tracts of consumers causing symptoms such as erythema, urticarial, hypotension, arrhythmia, cardiac arrest, bronchospasm, diarrhea, vomiting and abdominal pain. The major allergenic proteins reported

in lentils are the Len c 1, a 47-kDa vicilin belonging to the cupin superfamily and the allergen Len c 2 which is a 66 kDa seed-specific biotinylated protein (Shaheen *et al.*, 2019). The potential health risk for allergic consumers due to these allergens, also in consideration of the demonstrated cross reactivity with the homologous allergens from other legumes (e.g., peanut and soybean), have to be carefully considered when LF is proposed as ingredient for novel food preparations. Very recently, the Len c 3 allergen, a non-specific lipid transfer protein cross-reacting with the homologous peach allergen, has been isolated and characterized (Sackesen *et al.*, 2020). The allergenic capacity of Len c 3 and the effects of different lipid ligands on the protein stability and IgE-binding capacity upon technological treatments and to simulated gastrointestinal digestion have been investigated (Finkina *et al.*, 2020). These studies are opening new perspective for the production of hypoallergenic LF-based foods. One major way in which lentils are used as ingredient in the food industry is in the form of flour, which is commonly used as a thickener, binder, gelling agent and/or stabilizer (Saricaoglu, 2020) in a broader range of food products (Table 3.1).

Table 3.1. Summary of functional properties of lentil flour (LF) in foods.

Functional Properties	Food Products	Addition range (%)	Action mechanism	Attributes
Water Absorption Capacity (WAC)	• baked goods • meat products • dairy products (yogurt)	• < 30% in baked goods • 4-15% in meat products • 1-4% in yogurt	lentil starch, fibre and proteins containing polar amino acids create hydrophilic interactions and hydrogen bonds with the molecules of water.	- enhancement in viscosity - providing resistance to dough expansion - better cooking quality - shelf-life extension
Oil Absorption Capacity (OAC)	• baked goods • meat products	• < 30% in baked goods • 4-15% in meat products	lentil proteins containing nonpolar amino acids interact with oil and hold it.	- improvement in texture - better cooking quality - enhancement in consumers sensory acceptability - shelf-life extension
Solubility	• baked goods • pasta	• < 30% in baked goods • Until 100% in pasta	interaction between the hydrophilic groups of proteins, sugars, some vitamins and phytochemicals with water.	- enhancement of emulsification - promotion of foaming properties - promotion of gelling properties
Emulsification	• baked goods • meat products • salad dressing	• < 30% in baked goods • 4-15% in meat products • 3-11% salad dressing	lentil proteins act as emulsifiers by forming a film around oil droplets dispersed in an aqueous medium, therefore lowering interfacial tension.	control of: - creaming - coalescence - flocculation - sedimentation
Gelation	• cereal-based products	• Until 100% in cereal-based	formation of gels from proteins or starch	- improvement in texture

	• meat products • dairy products (yogurt)	products • 4-15% in meat products • 1-4% in yogurt	granules. Gel formation can be induced by physical and chemical agents.	- enhancement in consumers sensory acceptability
Foaming properties	• baked goods	• < 30%	lentil proteins act as foaming agents migrating to the air-water interface and forming a cohesive layer around the air bubbles.	a better crumb structure and loaf volume

In fact, like other pulses flour, LF possess good functional properties (e.g., solubility, emulsification, gelation, foaming properties, water, and oil absorption capacities), which may enhance and control the attributes of foods through different action mechanisms (Table 3.1). On the other hand, lentil has a high lipoxygenase activity, which may result in the reduction of shelf-life and in the production of off-flavours during processing or storage of either seeds or the derived flour for industrial use. All these factors have a deep impact on nutritional characteristics, digestibility, sensory and acceptability attributes of lentil-based products, and present industrial challenges that need to be dealt with modern technological approaches. In this chapter, key aspects related to presence of LF in the novel food formulations are discussed, with special reference to protein and starch digestibility and to the presence of allergens, as well as to the technological challenges faced by food industry to design lentil-based products with improved sensory and nutritional quality.

3.2. Lentil Flour: production process and protein and starch digestibility

LF production involves grinding/milling of whole or decorticated seeds. Moreover, LF can be subjected to a wide range of processing methods, more or less intensive, which however may positively or negatively affect the proteins and starch properties (e.g., starch gelatinization and protein denaturation) and hence their digestibility, resulting in ingredients with improved or impaired characteristics (Drulyte & Orlien, 2019). Interestingly, recent studies showed that the degree of milling (Marchini *et al.*, 2021; Boukid *et al.*, 2019) is positively associated with nutrients bioaccessibility since a very thorough milling process involves an extended cell rupture (Marchini *et al.*, 2021) increasing nutrients accessibility, thereby promoting their hydrolysis by the digestive enzymes (Boukid *et al.*, 2019). The lower digestion rate of raw flours with larger particle sizes is usually attributed to the slower action of enzymes due to hindrance by larger protein bodies or cell wall fragments. Instead, the impact of heat treatments on the *in vitro* digestibility of LF has not yet been well elucidated, as depending on

the type of the process applied (Table 3.2) and the food matrix examined. In particular, improvement of protein digestibility is dependent on the hydrolysis of the indigestible proteins, deactivation of protease inhibitors (ANFs), and improvement of protein solubility. Food processes such as extrusion, cooking and baking may induce changes in proteins secondary structure in LF, allowing the digestive enzymes to easily access the peptide bonds, thus leading to a rapid protein hydrolysis (Nosworthy *et al.*, 2018). Consequently, it can be reasonably assumed that a high β-sheet content in raw LF proteins is inversely associated with the protein digestibility. Furthermore, cooking may also inactivate and/or reduce the content of ANFs such as protease inhibitors which are known to decrease protein digestibility.

Conflicting and partial results are reported in the literature (Nosworthy *et al.*, 2018; Drulyte & Orlien, 2019; Chávez-Murillo *et al.*, 2018; Berrazaga *et al.*, 2020) about the impact of cooking on the *in vitro* protein digestibility in LF (Table 3.2).

Table 3.2. Recent studies about the effect of process type on *in vitro* protein and starch digestibility of lentil flour (LF) (2018-2020). ↑ indicates increased digestibility, ↓ indicates decreased digestibility. Empty cell denotes that information was not provided.

Process	Market class of Lentil Flour (LF)	Process conditions (T; t)	Protein digestibility	Starch digestibility*	References
COOKING					
	Red LF	Lentils were soaked in water (1/1 – 1.5); t=12-16 h, then boiling (T= 100 °C; t= 25 –35 min), freeze drying and milling (hammer mill)	No effect		Drulyt & Orlien, 2019
	Green LF	Lentils were soaked in water (1/1 – 1.5); t=12-16 h, then boiling (T= 100 °C; t= 25 –35 min), freeze drying and milling (hammer mill)	No effect		Drulyt & Orlien, 2019
	Red LF	Lentils were soaked in water (1/4); t=16 h, then boiling (T= 100 °C; t= 25 –35 min), freeze drying and milling (hammer mill)	↑ effect		Nosworthy *et al.*, 2018
	Green LF	Lentils were soaked in water (1/4); t=16 h, then boiling (T= 100 °C; t= 25 –35 min), freeze drying and milling (hammer mill)	↑ effect		Nosworthy *et al.*, 2018
	Red LF	LF and water (100/2) were mixed for t= 1 min, then boiling (T= 100 °C; t= 20 min)		↑ RDS ↓ SDS ↓ RS	Lu *et al.*, 2018
	Green LF	LF and water (100/2) were mixed for t= 1 min, then boiling (T= 100 °C; t= 20 min)		↑ RDS ↓ SDS ↓ RS	Lu *et al.*, 2018
BAKING					
	Red LF	T= 198.3°C; t= 35 min T= 165.6°C; t= 35 min	↑ effect		Nosworthy *et al.*, 2018
	Green LF	T= 198.3°C; t= 35 min T= 165.6°C; t= 35 min	↑ effect		Nosworthy *et al.*, 2018

	Red LF	T= 198.3°C; t= 35 min T= 165.6°C; t= 35 min	No effect		Drulyt & Orlien, 2019
	Green LF	T= 198.3°C; t= 35 min T= 165.6°C; t= 35 min	No effect		Drulyt & Orlien, 2019
EXTRUSION					
	Red LF	T= 30−50°C, T= 70−90°C T= 100−120°C	No effect		Drulyt & Orlien, 2019
	Green LF	T= 30–50°C, T= 70–90°C T= 100–120°C	No effect		Drulyt & Orlien, 2019
	Red LF	T= 30–50°C, T= 70–90°C T= 100–120°C	↑ effect		Nosworthy *et al.*, 2018
	Green LF	T= 30–50°C, T= 70–90°C T= 100–120°C	↑ effect		Nosworthy *et al.*, 2018
AUTOCLAVING					
	LF	T= 121°C; t= 7 min	↑↓: variety dependent		Drulyt & Orlien, 2019
HYDROTHERMAL TREATMENTS					
ANNEALING	Whole LF	T= 65°; t= 24 h	↓ effect	↓ RDS ↑SDS ↑ RS ↑ pGI	Chávez-Murillo *et al.*, 2018
HEAT MOISTURE TREATMENT	Whole LF	T= 65°; t= 24 h	↓ effect	↓ RDS ↑ SDS ↑ RS ↑ pGI	Chávez-Murillo *et al.*, 2018

*RDS: rapidly digestible starch; SDS: slowly digestible starch; RS: resistant starch, pGI: predicted glycemic index.

Specifically, Nosworthy *et al.* (2018) investigated the effect of extrusion, cooking and baking on the *in vitro* protein quality of LF from red and green lentils measured by the Protein Digestibility Corrected Amino Acid Score (PDCAAS) and reported that extruded flour both of red and green lentils had the highest PDCAAS followed by the cooked and baked samples. Besides red LF after all types of processing exhibited higher PDCAAS than the green ones. On the contrary, a decrease in protein digestibility can be observed when LF is subject to hydrothermal treatment such as annealing (ANN) and heat moisture treatment (HMT) (Table 3.2), probably because of their structural rearrangements as well as the reorganization of the other flour components (Chávez-Murillo *et al.*, 2018). Moreover, according to Drulyte & Orlien (2019), cooking (100°C, 25–35 min), baking (165.6°C and 198.3°C, 35 min) and extrusion (30−50°C, 70−90°C and 100−120°C) do not affect the *in vitro* protein digestibility in LF. Only autoclaving (121°C, 7 min) causes a significant increase/decrease in protein digestibility depending on the lentil's variety (Table 3.2). Berrazaga *et al.*, (2020) also reported the negative impact of LF addition in wheat pasta on the *in vitro* protein digestibility. In particular, the enrichment of wheat pasta with LF led to significant changes in the protein network structure, thus negatively affecting the protein digestibility. This could be attributed to the higher covalently reticulated protein network of lentil pasta compared to the conventional one, which was due to the higher cysteine content and thus to the higher number of S-S bridges.

Concerning the *in vitro* starch digestibility, lentil starch has a lower GI than legumes and cereal starches (Chelladurai & Erkinbaev, 2020), supporting the use of LF as an excellent alternative to conventional cereal starches. LF is also a rich food source of prebiotic carbohydrates (low-digestible carbohydrates) which are not digested in the small intestine of humans, but instead fermented by microorganisms in the large intestine into short chain fatty acids essential for colon health (Siva *et al.*, 2018). Food processing can positively or negatively affect starch granule's structure, leading to a redistribution of the different starch fractions: Rapidly Digestible Starch (RDS), Slowly Digestible Starch (SDS) and Resistant Starch (RS).

First of all, dehulling and splitting of lentils significantly decreases RS concentrations compared to the whole seeds. This is clearly due to the mechanical removal of the hull which is richer in RS and fibre (Siva *et al.*, 2018). Furthermore, a positive association has been demonstrated between the use of coarse LF (rich in intact cells) and the reduced glucose release upon simulated gastrointestinal digestion (Kathirvel *et al.*, 2019). Regarding instead the effect of cooking on the LF starch digestibility, conflicting results are reported in the literature probably because of the different process conditions used in the various studies. Generally, it has been found an increase in the RDS content and a significant decrease in the

SDS and RS content after cooking in a boiling water bath for 20 min (Lu *et al.*, 2018). On the other hand, when whole LF is subjected to hydrothermal treatments such as ANN and HMT, a significant reduction in the amount of RDS together with a rise in the SDS and RS fractions can be observed. Since RDS is the starch fraction that is rapidly and totally digested in the gastrointestinal tract and it is associated with fast elevation of postprandial plasma glucose, a decrease in the RDS content can be positively related to a reduction in the expected Glycemic Index (eGI) (Chávez-Murillo *et al.*, 2018). Comparing flour from different lentil varieties such as red and green, it appears that after cooking red LF samples has significantly lower RDS content and higher RS content than the cooked green LF due to the higher total flavanol index of red lentils compared with the green ones. In fact, phenolic compounds, and, in particular, the flavanols, are known to be the major contributors to the α-glucosidase inhibitory activity which implies reduced starch digestibility.

3.3. Application of lentil flour as novel ingredient in the food industry

The uses of LF as food ingredient (Table 3.3) are based on its techno-functional and nutritional properties (Argel *et al.*, 2020; Bouhlal *et al.*, 2019; Turco *et al.*, 2019). Generally, these properties are closely related to the flour composition (protein, complex carbohydrates, and fibre content) as well as to the flour particle size (Marchini *et al.*, 2021). In particular, LF proteins functionality is mainly linked to their amino acid composition and sequence, net charge, hydrophobicity (Khazaei *et al.*, 2019) while starch functionality is associated to the amylose and amylopectin ratio together with their physical organization within the granule (. Villas-Boas *et al.*, 2019). It is therefore clear that the LF proteins and starch functionality is largely dictated by their structural and physicochemical properties as well as by the physicochemical changes induced by food processing (Liu *et al.*, 2020) or chemical-physical interactions with other food constituents (Monnet *et al.*, 2019). Regarding flour granulometry, a fine particle size is generally associated to greater starch damage, lower water absorption capacity (WAC), and higher peak and final viscosities compared to coarser fractions (Bourré *et al.*, 2019). Whatever the milling technique (hammer, pin, roller, or stone milling) or its extent (fine or coarse flour), the health properties attributed to lentils are usually kept in LF, representing a promising functional ingredient for numerous food applications (Figure 3.1 and Table 3.3).

As reported in Table 3.3, a number of food applications have been performed using several market classes of LF. Based on these ingredients, the technological, nutritional, and sensorial properties of the final product differ.

Thanks to its dense nutritional composition, food enrichment with LF usually leads to an improvement of the nutritional properties, resulting in an increase of protein, dietary fibre, total polyphenol, ash, mineral, and vitamin content (Bouhlal *et al*., 2019). Currently, the application of LF in bakery (bread, cake, crackers) (Chelladurai & Erkinbaev, 2020; Turfani *et al*., 2017; Polat *et al*., 2020; Portman *et al*., 2018; Hernandez-Aguilar *et al*., 2020; Carcea *et al*., 2019) extruded (pasta, snacks) (Berrazaga *et al*., 2020; Luo *et al*., 2020; Teterycz *et al*., 2020; Turco *et al*., 2019; Trevisan, Pasini, & Simonato, 2019) and other products (dressings, soups, dairy, and meat products) (Chelladurai & Erkinbaev, 2020; Argel *et al*., 2020; ul Haq *et al*., 2019; Baugreet *et al*., 2018, 2019; Göncü & Çelik, 2020) has gained in popularity among researcher and consumers worldwide. Because of their balanced fat and protein content, LF also represents an excellent choice for the development of novel GF products, more performing and healthier than the conventional ones, that have in general low protein and high fat content (Carcea, 2020; Ciudad-Mulero *et al*., 2020; Di Cairano *et al*., 2020). Due to their large consumption all over the world, baked goods and pasta represent excellent bases for the enrichment with highly nutritious raw materials such as LF. Overall, the replacement of wheat flour (WF) with LF causes an improvement in the nutritional profile of the final product (Marchini *et al*., 2021), with a reduction in total carbohydrates content and a significant increase in protein, total polyphenol, flavonoid, iron and zinc content and antioxidant activity (Bouhlal *et al*., 2019). Moreover, the addition of LF in wheat products such as pasta has been found to reduce its GI (Trevisan *et al*., 2019). This is probably due to two important factors: i) the reduction in total starch content as well as the increase in resistant starch content; ii) the action of ANFs which can inhibit α-amylase activity, thereby delaying the starch hydrolysis. In agreement with above, Fujiwara, Hall, & Jenkins (2017) used *in vitro* methods to assess the eGI of five products (pasta, bread, cracker, granola bar, and cookie) after the incorporation of green and red LF (up to 50%). The partial substitution of WF with LF led to a reduction of the eGI although the differences between pulse variants and the controls (containing 100% WF) were not statistically significant ($P > 0.05$). From a technological point of view, the incorporation of LF can have different effects depending on the food system in which it is incorporated (Table 3.1).

Table 3.3. Recent studies about the use of lentil flour (LF) in foods applications (2018-2020). ↑ indicates increased property, ↓ indicates decreased property. Empty cell denotes that information was not provided.

Market class of Lentil Flour (LF)	Foods Applications	PRODUCTS	MAIN RESULTS			References
			Technological and physicochemical	Nutritional	Sensorial	
	Bakery products					
Whole LF		wheat - lentil bread	↓ dough strength ↓ loaf volume at high concentrations (up to 20%) ↓ baking quality at high concentrations (up to 20%)	↑ protein content ↑ ash content		Portman *et al.*, 2018
Germinated LF		wheat - lentil bread	↑ hardness ↓ cohesiveness		↑ sensory descriptors (overall acceptability)	Hernandez-Aguilar *et al.*, 2020
Germinated green LF		crackers		↑ protein content ↑ ash content ↑ total polyphenol content ↑ antioxidant activity	↑ sensory descriptors (overall acceptability) for the 5% enriched samples	Polat *et al.*, 2020
Red LF		wheat - lentil bread		↑ protein content ↑ dietary fibres content ↑ vitamins ↑ minerals ↑ intestinal immune system		Carcea *et al.*, 2019
		puffed snacks	↓ level of expansion during extrusion process ↓ microstructural appearance ↓ product textural appeal	↑ protein content ↑ dietary fibres content		Luo *et al.*, 2020
	Pasta					
Red LF		gluten free pasta		↑ resistant starch content ↑ dietary fibres content ↑ total polyphenol content ↓ starch digestibility		Trevisan, Pasini, & Simonato, 2019; Turco *et al.*, 2019
Green LF		wheat - lentil pasta	↑ firmness		↑ sensory descriptors (colour acceptance)	Berrazaga *et al.*, 2020;
	Dairy products					

Red LF		fermented dairy products (yogurt)	↑ water holding capacity ↑ viscosity ↓ syneresis ↑ pH ↓ acidity	↓ moisture content ↑ protein content ↑ dietary fibres content ↑ total solids ↑ intestinal microflora growth and functionality		ul Haq *et al.*, 2019
Roasted and unroasted LF		fermented dairy products (yogurt)	↑ viscosity ↓ syneresis ↑ pH ↓ acidity		↑ sensory descriptors for yoghurt with unroasted LF	Benmeziane *et al.*, 2021
	Meat products					
LF		pork meat burgers	↑ water holding capacity ↑ hardness ↑ cooking yield ↓ product size reduction during cooking	↑ protein content	↑ sensory descriptors (appearance and taste)	Argel *et al.*, 2020
LF		beef steaks	↑ firmness	↑ protein content ↑ release of free amino acids after the *in vitro* gastrointestinal digestion ↑ free fat content		Baugreet *et al.*; 2018; Baugreet *et al.*, 2019
	Soups					
Whole red, green and yellow LF				↑ protein content ↑ dietary fibres content ↑ fat content ↑ ash content ↑ minerals content ↑ total phenolic content ↑ antioxidant activity ↑ lactic acid bacteria		Göncü & Çelik, 2020

For example, the ratio of LF in the bakery goods formulation may influence dough rheology and consequently, physical, and sensory characteristics of their baked goods. This directly influences consumer acceptability of final products. In particular, the use of LF in dough formulation impair some rheological properties by decreasing dough stability and strength and increasing the water absorption time, development time and degree of softening (Portman *et al.*, 2018) (Table 3.1 and 3.3). On the other hand, the addition of high concentrations of LF to pasta may enhance its firmness while does not affect other quality parameters such as weight increase and cooking loss (Teterycz *et al.*, 2020). Recently, LF has been also used to produce healthy and texturally appealing puffed snacks (Luo *et al.*, 2020). In this specific case, the high protein and fibre content of LF negatively affected technological features such as the level of expansion, microstructure uniformity and the product textural appeal (Luo *et al.*, 2020). Beside the cereal-based products, LF has been used to improve the technological, nutritional, and sensory properties of meat (Argel *et al.*, 2020; Baugreet *et al.*, 2018, 2019) and dairy products (ul Haq *et al.*, 2019; Benmeziane *et al.*, 2021). The partial meat replacement with LF in low-fat burgers, can lead to a stronger water binding capacity which resulted in a rise of hardness and cooking yield as well as in a decrease of the diameter reduction and expressible liquid (liquid extracted by compression). These findings may be linked to the high protein content of LF (175 g/kg) which in turns is responsible for its great water holding capacity (WHC) and emulsifying properties. At the same time, the addition of LF caused a reduction in burger lightness and an increase in a* value due to the high carotenoid content. Moreover, sensory analysis revealed a good consumer acceptability both for appearance and taste (Argel *et al.*, 2020). Flour from lentil and other seeds has been used to increase the protein content in steak samples restructured using transglutaminase. A previous study by Baugreet *et al.* (2018) have already suggested that the inclusion of plant-derived protein ingredients in restructured beef steaks results in improved physico-chemical properties. LF enriched, restructured beef steaks were found to have a more compact structure and LF inclusion led to the presence of more free fat as well as to the release of significant amounts of free amino acids after the *in vitro* gastrointestinal digestion (Baugreet *et al.*, 2019). A very recent and innovative Canadian study compared nutritional and environmental benefits of beef burgers reformulated with LF (Chaudhary & Tremorin, 2020) compared to all-meat burger. Partial replacement of a lean beef burger with cooked lentil

puree increased the nutrient density (measured through the nutrient balance score, that was >20% compared with traditional beef burger), as well as fiber, folate, manganese, and selenium content. The amounts of disqualifying nutrients (fat, trans fat, saturated fat, and cholesterol) in LF reformulated burger were ~17% less than the regular beef burger. Regarding sustainability issues, substitution decreased the life cycle environmental footprint by ~33% and reduced the production cost by 26%. This report highlights how nowadays the research in the food sector has to be carried out with a comprehensive vision embracing technological, nutritional, economic, and environmental issues, and the results achieved underscore the high potential of innovation in the field of lentil-based ingredients to contribute towards global sustainable development goals. LF has been also advantageously used in the manufacture of yogurt (ul Haq *et al.*, 2019; Benmeziane *et al.*, 2021) (Table 3.3). The addition of LF in fortified yogurt leads to good results both in nutritional, technological and sensory terms. In fact, it represents a good source of oligosaccharides (e.g., inulin and raffinose) who promote growth and functionality of the intestinal microflora. Meanwhile, LF provides great amounts of proteins, glycoproteins, and complex carbohydrates, thus enhancing WHC, viscosity and syneresis of the final product. Not least, the high buffering capacity of LF leads to an increase in pH and simultaneously to a reduction in yogurt acidity. This promises a longer shelf life and a better taste than the control (0% LF) which may be particularly appreciated by the consumers. Therefore, LF may represent a functional ingredient in the manufacture of yogurt to develop new probiotic and prebiotic products. Finally, the uses of LF as food additive or adjuvant, or as basis to produce improved materials in food technology are increasing. A potential application of LF in the food industry is as a colouring component (Teterycz *et al.*, 2020). The addition of 5-20% of red LF in durum wheat semolina pasta enhances overall consumer acceptance, in particular color descriptors (Teterycz *et al.*, 2020). In fact, red LF has generally lower luminance (L*) and higher (b*) values than wheat, probably due to the higher bran content which results in greater amounts of pigment (Bouhlal *et al.*, 2019). An innovative technological application has been very recent reported. LF has been employed as a biopolymer material nanofiber at different pH values (Tam *et al.*, 2017), and the latter used to encapsulate gallic acid by electrospinning technology (Aydogdu *et al.*, 2019). This nanomaterial constituted an active packaging matrix that was tested in order to decrease oxidation of walnuts during storage.

The produced nanofibers were characterized in terms of pH stability, loading efficiency, antioxidant activity, thermal and chemical properties. These achievements can potentially open new avenues for production of natural-based, environmentally friendly, innovative food packaging strategies.

SECTION B

Study cases

Chapter 4
The CAISIAL Dynamic Digester (DICA)

4.1. Introduction

The CAISIAL Dynamic Digester (DICA) has been developed at the Academic Centre for Innovation and Development in the Food Industry (CAISIAL) within the project PON03PE_00180_1 "M2Q – Laboratorio Pubblico Privato di R&S in campo Agroindustriale". As stated in the 2nd chapter, right now few dynamic *in vitro* digestion systems have been developed worldwide, each of which presents some advantages but also limitations, thereby making the search for better solutions essential. This apparatus was built with the primary aim to gain insight into the fate of different foods during digestion. Specifically, the expectations are to improve our understanding about: i) the mechanism of food disintegration, ii) the impact of food structure on nutrients bioaccessibility and iii) the kinetics of nutrients hydrolysis during simulated gastrointestinal digestion. Hence, using a reverse engineering approach, we are going to model *in vitro* digestion to develop tailored food for specific target population. A large part of this PhD project has been dedicated to the setting up of this multi-compartmental and computer-controlled system, also playing an important role in the development of the program used for its control.

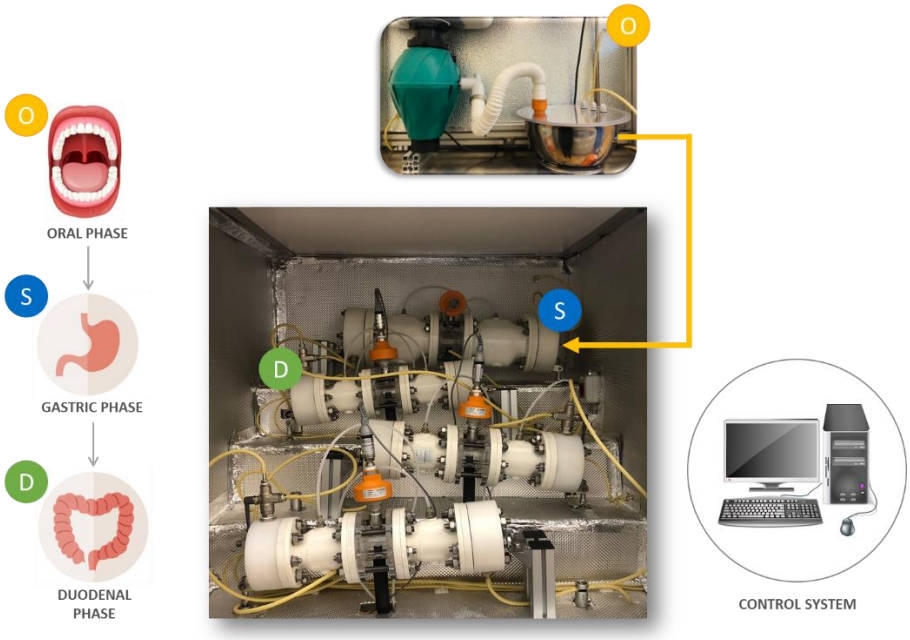

Fig. 4.1. The dynamic digester DICA.

4.2. General description of the model

DICA is a multi-compartmental and computer-controlled (LabVIEW® software) digestion apparatus (Fig. 4.1) kept at body temperature (37°C) through a heating plate (Fig. 4.2) located on the upper wall. Specifically, it comprises four successive reactors. Two of these are used to simulate the stomach (S) and the first part of the small intestine, the duodenum (D). The remaining two compartments in the future will be probably destinated to other purpose (e.g., microbial fermentation in the large intestine). Stomach has a capacity of 1000 mL, while duodenum and the other compartments have a capacity of 500 mL.

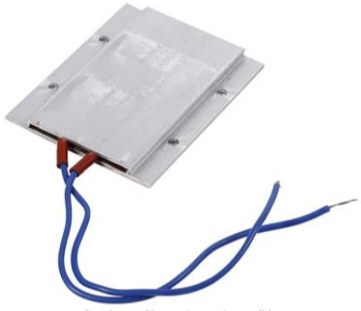

Fig. 4.2. Heating Plate.

As shown in Fig. 4.1 the central part of each reactor is made of transparent material (polymethylmethacrylate) allowing visual observation. Moreover, each compartment is provided with a tap for collecting samples to be analysed, thereby allowing to monitor and study the entire digestion process.

Mastication is simulated with a food processor (GREEN POWER - TDH00500) located upstream the apparatus (Fig. 4.3). Then, the shredded food is tipped into a bowl (Fig. 4.3) and mixed with Simulated Salivary Fluid (SSF) and eventually α-amylase solution by an overhead stirrer (Fig. 4.4) (Witeg Germany – HS-30D).

Fig. 4.3. Collecting bowl and food processor**.**

Fig. 4.4. Overhead stirrer.

Compartments are interconnected by peristaltic pumps (Watson-Marlow Pumps – 621F/RE) (Fig. 4.5) and pipes (with a diameter of 4.5 millimeters) that allow the transfer of content between successive units. Pipes are made of Santoprene which is resistant to a wide variety of solvents and chemicals.

Fig. 4.5. Watson-Marlow Pumps - 621F/RE.

During test, it is possible to dynamically monitor and regulate flow rates of digestive fluids and enzymatic solutions which are kept in thermostatically controlled pans (37 ± 1 °C for the digestive fluids and 4 ± 1 °C for the enzymatic solutions) until use. At the right time, they are taken and transported in the respective compartment by drive pumps (Watson-Marlow Pumps - 114FD) (Fig. 4.6) and pipes (with a diameter of 1.0 millimeters).

Fig. 4.6. Drive pumps.

Downstream of each compartment there is an on-off valve (Sirai - S206) (Fig. 4.7) followed by a proportional valve (Resolution Air - MPPV) (Fig. 4.8). The on-off valves have the main task to isolate each compartment, avoiding material outflows. Proportional valves instead, can be opened gradually thus allowing the release of defined amount of sample. These can be used for

example to simulate the muscular rings cardias and pylorus located upstream and downstream the stomach, respectively.

Fig. 4.7. on/off valve.

Fig. 4.8. Proportional valves

Furthermore, each compartment comprises two air operated pinch valves (Blue Valve S.r.l - type V/VF) (Fig. 9) which opening and closing alternatively, can simulate the peristaltic contraction of stomach and intestinal wall. This also ensure an adequate mixing of food material with the simulated digestive fluids and the enzymatic solutions.

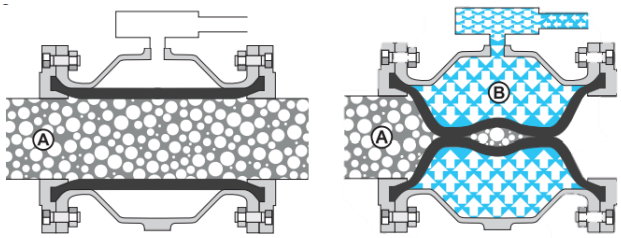

Fig. 4.9. Pinch valve in **a)** open and **b)** close position.

At the end of each phase, the reactor is raised on one side by an air compression piston, promoting material flow along the simulated GIT.

During digestion it is essential to monitor and eventually regulate parameters such as pressure, temperature, pH. For this reason, each compartment is equipped with a pressure sensor (Atlas Scientific IXIAN™ 0-100 PSI) (Fig. 4.10) as well as an industrial pH probe integrated with a PT-1000 Temperature Probe (Atlas Scientific) (Fig. 4.11) which works properly when it is completely immersed into the sample.

Fig. 4.10. Pressure sensor.

Fig. 4.11. pH/temperature probe.

Concerning the temperature-reading, the output signal given by the probe is an electrical resistance whose value changes as a function of temperature. Atlas Scientific EZO™ RTD temperature circuit (Fig. 4.12) connected to the PC via usb, translates the electrical resistance into tension, which in turns is translated into temperature via software. As regard instead the pH probes, the Atlas Scientific EZO™ class pH circuit (Fig. 4.13), converts a current generated by hydrogen ion activity into pH values.

Fig. 4.12. EZO™ RTD temperature circuit.

Fig. 4.13. EZO™ class pH circuit.

To manage and control every single part of the digester, a CompactDAQ Chassis (cDAQ-9179) with 14-Slot (National Instruments, Austin, Texas, U.S.) is connected to the PC via usb (Fig. 4.14).

Fig. 4.14. CompactDAQ Chassis (cDAQ-9179).

It can activate or deactivate the functioning of single components (e.g., valves, pumps) through different control modules connected to it (Fig. 4.15). Specifically, it contains eight Input/Output C Series control modules (National Instruments, Austin, Texas, U.S.) to create a combination of analog and digital I/O measurements.

Fig. 4.15. C Series control modules.

4.3. LabVIEW program

As previously described, DICA system is fully computer-controlled by a program written in the LabVIEW (National Instruments, Austin, Texas, U.S.) programming language. LabVIEW programs contain a wide range of tools for acquiring, analyzing, displaying, and storing data. User can control and monitor process parameters from the user interface, also called front panel, with the aid of controls (e.g., knobs, push buttons, dials) and indicators (such as graphs and LEDs).

When user launches the program, front panel opens (Fig. 4.16). From this it is possible to control parameters such as:

- Opening and closing of proportional valves. Specifically, it is possible to set the number of steps (n) in the opening/closing direction, where the minimum and the maximum number of steps is 0 and 1000, respectively.

- The number of peristalsis (n) and the duration of each peristalsis (s) for the pinch valves. Peristalsis is defined as the paired motion of the pinch valves located in a single reactor: when a pinch valve open, the other one close simultaneously.
- The duration of each digestion phase.

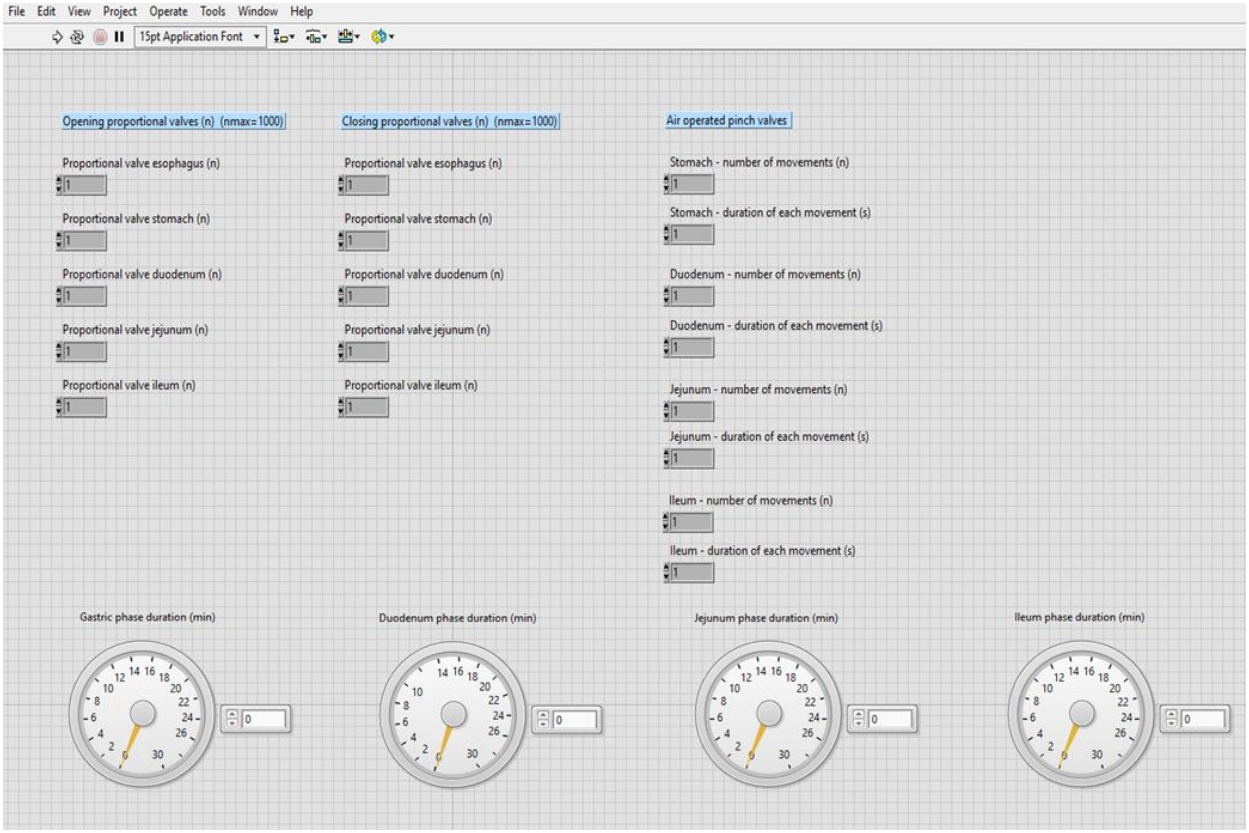

Fig. 4.16. User interface or front panel.

The length of gastric phase can be calculated as suggested by Mulet-Cabero *et al.* (2020) and it is affected by several factors, including volume, consistency and the energy content of the meal (Camilleri, 2006). Gastric halftime ($t_{1/2}$), which represents the time required by the stomach to empty 50% of the ingested meal (Seok, 2011), can be calculated as follow:

$$t_{1/2}\ (\text{min}) = \frac{\text{Gastric volume (mL)}}{\text{Volume emptying rate } \left(\frac{\text{mL}}{\text{min}}\right)} \text{ x } \frac{1}{2} \qquad (1)$$

The calculation of this parameter is based on the delivery of 2 kcal/min of a food volume of 500 mL based on *in vivo* considerations (Hunt, Smith, & Jiang, 1985). As a result, total gastric

digestion time can be estimated by multiplying the gastric halftime by two. Concerning the intestinal phase, some tests before establishing its duration are needed.

Once all these parameters have been set, program can be runned by clicking on the arrow in the top menu (Fig. 4.16). At the beginning, all the proportional valves are totally closed (n = 0) to ensure the same starting point.

Afterwards, a control window appears (Fig. 4.17) displaying numeric controls for the insertion of fluids volume (digestive fluids: Simulated Salivary Fluid (SSF), Simulated Gastric Fluid (SGF) and Simulated Intestinal Fluid (SIF); enzyme solutions: amylase, pepsin, pancreatin; others: bile, 1M NaOH). The simulated digestive fluids (SGF, SIF and SSF) might be prepared as indicated by the INFOGEST methods (Brodkorb *et al.*, 2019; Mulet-Cabero *et al.*, 2020).

Once finished, clicking on Done the simulated gastrointestinal digestion will start.

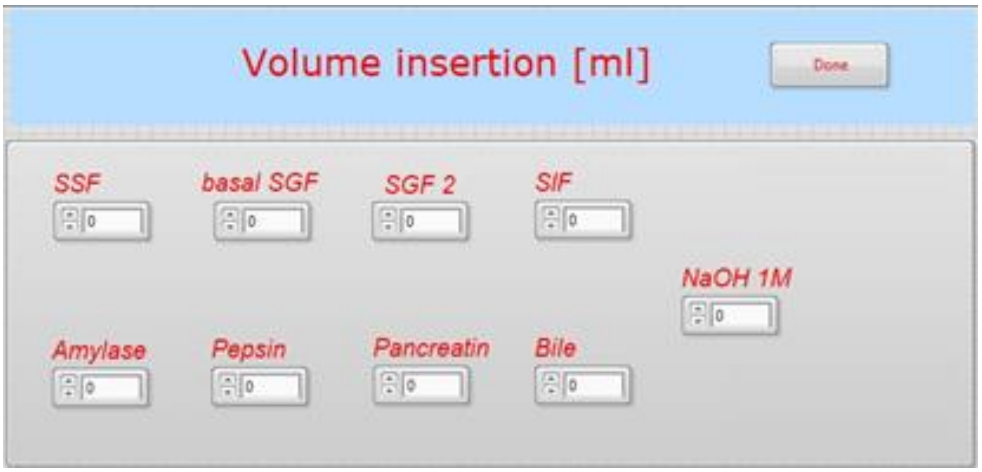

Fig. 4.17. Control window for the insertion of fluids volume.

In Fig. 4.18 is represented the flow diagram of the digestion process as it is performed using the DICA system. As stated above, this digestion system provides the simulation of the oral, gastric and the duodenal phase.

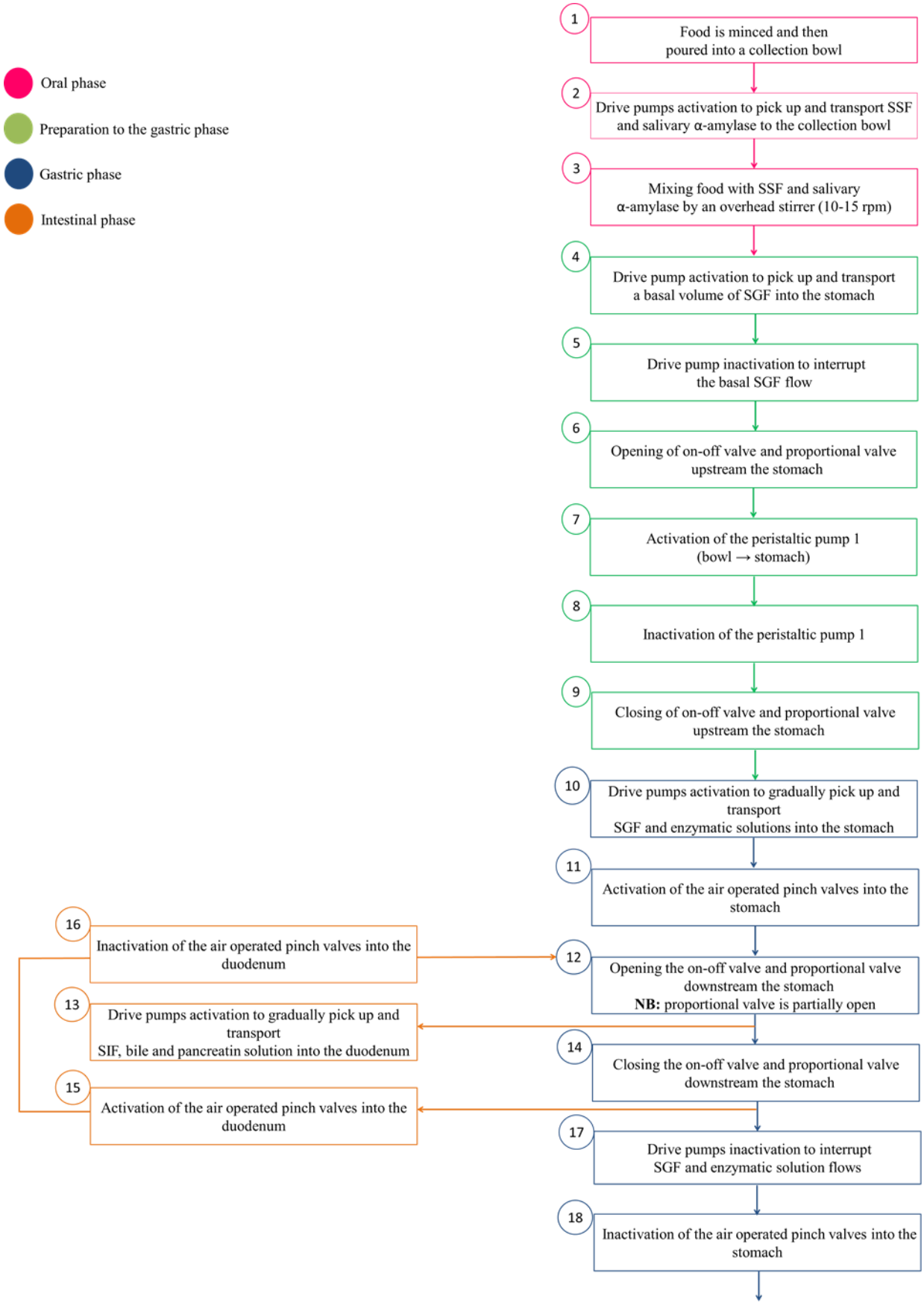
Oral phase
Preparation to the gastric phase
Gastric phase
Intestinal phase
1
Food is minced and then poured into a collection bowl
2
Drive pumps activation to pick up and transport SSF and salivary α-amylase to the collection bowl
3
Mixing food with SSF and salivary α-amylase by an overhead stirrer (10-15 rpm)
4
Drive pump activation to pick up and transport a basal volume of SGF into the stomach
5
Drive pump inactivation to interrupt the basal SGF flow
6
Opening of on-off valve and proportional valve upstream the stomach
7
Activation of the peristaltic pump 1 (bowl → stomach)
8
Inactivation of the peristaltic pump 1
9
Closing of on-off valve and proportional valve upstream the stomach
10
Drive pumps activation to gradually pick up and transport SGF and enzymatic solutions into the stomach
11
Activation of the air operated pinch valves into the stomach
12
Opening the on-off valve and proportional valve downstream the stomach
NB: proportional valve is partially open
13
Drive pumps activation to gradually pick up and transport SIF, bile and pancreatin solution into the duodenum
14
Closing the on-off valve and proportional valve downstream the stomach
15
Activation of the air operated pinch valves into the duodenum
16
Inactivation of the air operated pinch valves into the duodenum
17
Drive pumps inactivation to interrupt SGF and enzymatic solution flows
18
Inactivation of the air operated pinch valves into the stomach

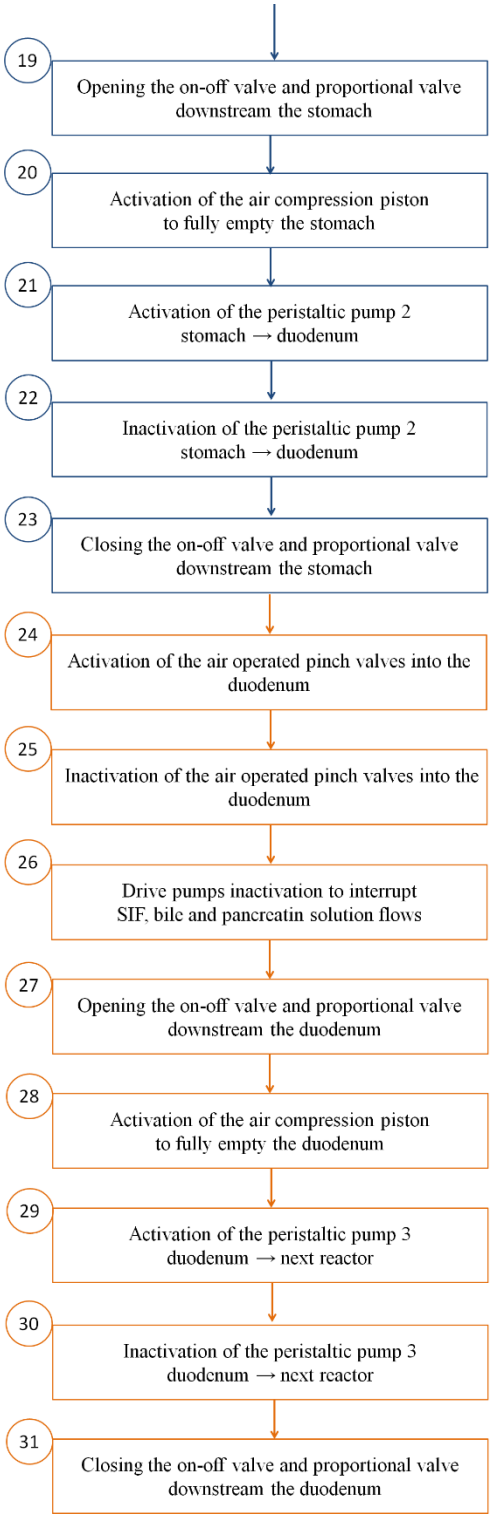

Fig. 4.18. Flow diagram of the digestion process as it is performed using the DICA system.

The program is completely automated, except for the oral phase since food mincing and mixing will be carried out manually and independently.
Each phase illustrated in the flow diagram (Fig. 4.18) is precisely described below.

4.3.1. Protocol for the *in vitro* dynamic digestion using the DICA system

4.3.1.1. Oral phase

1) Firstly, food is "masticated" for few seconds (approx. 30 seconds) using a food processor and then tipped into a collection bowl. Since this phase is not computerized, the program will ask if "mastication" has been completed by clicking on a "Ready" button.

2) SSF and salivary α-amylase (in case of starchy foods) are withdrawn and transported to the collection bowl, by the activation of the relative drive pumps.

3) Lastly, masticated food is mixed with SSF and α-amylase solution by an overhead stirrer with a low speed (10-15 rpm). Bolus particle size must be < 4.5 mm which is the pipe internal diameter. Even this phase is not computerized, hence the program will ask if "mixing" has been completed by clicking on a "Ready" button.

4.3.1.2. Preparation for the gastric phase / esophageal transit

4) To simulate the fasting state, a basal volume of SGF is transported into the stomach (10% of total gastric secretions) before bolus "swallowing". Thus, the corresponding drive pump is activated to transport the SGF basal volume into the stomach.

5) Once all the basal volume of SGF has been collected into the gastric compartment, the relative drive pump is inactivated.

The esophageal transit involves the following steps:

6) Opening the on/off and the proportional valve upstream the stomach.

7) Activating the first peristaltic pump (bowl → stomach) for the time necessary to deliver all the bolus into the stomach.

8) Disactivating the first peristaltic pump (bowl → stomach).

9) Closing the on/off and the proportional valves upstream the stomach to isolate the reactor and avoid backflows.

4.3.1.3. Gastric phase

Gastric phase starts when all the bolus has been collected into the stomach. During this phase, bolus is mixed with SGF and enzymatic solutions (pepsin and/or gastric lipase), gradually reaching a pH around 2. HCl is already contained into the SGF and the proper amount can be previously calculated through a pre-test. As stated above, gastric pH is dynamically and continuously monitored by the pH probe inserted into the reactor. Hence, if necessary, additional amounts of HCl can be added by activating the corresponding drive pump.

Gastric phase includes the following steps:

10) Once all the bolus reaches the stomach, drive pumps are activated to gradually pick up and transport the remaining part of SGF and enzymatic solutions to the stomach.

11) At this point, the air operated pinch valves located into the stomach are activated. As described above, pinch valves open and close alternatively simulating the peristaltic contraction of the stomach wall. This ensures the adequate mixing of bolus with the SGF and the enzymatic solutions as well as an additional reduction in size of food particles. As shown in Figure 4.16, from the front panel users can set the duration of each peristalsis as well as the number of peristalsis (n) during the entire gastric phase (n/min). Preliminary tests demonstrated that a peristalsis duration of 1 second provide a suitable mixing of the gastric content.

12) After the first 15 minutes of gastric digestion, the on-off and the proportional valves downstream the stomach are opened. Experimental trials demonstrated that this time period (15 min) ensures that all stomach content has been adequately mixed. While the on-off valve is totally open, the proportional valve is only partially open with the purpose to simulate the sieving effect of pylorus. In this way liquids and smaller particles (diameter < 1.5 mm) will be emptied first (as occurs in the human body).

13) Right now, the duodenal phase also begins (it will be detailed discussed in the next paragraph), so SIF, bile, and pancreatin solutions start to be gradually delivered into the duodenum.

From now on until the end of the gastric phase, the following steps (12, 14-16) are repeated on a loop:

12) the on-off and the proportional valves downstream the stomach are opened (the proportional valve is only partially open) while the pinch valves push the chyme towards the duodenum.

14) The on-off and the proportional valves downstream the stomach are totally closed to isolate the reactor and avoid backflows from the duodenum.

15) On the contrary, pinch valves located into the duodenum are activated for few seconds to ensure a proper mix of chyme with SIF, bile, and pancreatic solutions.

16) Then, pinch valves located into the duodenum are inactivated.

The repetition of these phases allows for the simultaneous carrying out of the gastric and the intestinal phases. Furthermore, it avoids generation of overpressure inside the reactors as well as backflows from the duodenum to the stomach. At the same time, this process permits the gradual emptying of the gastric content thanks to the propulsive motions created by the air operated pinch valves.

At the end of gastric phase, program come out from the loop and the flow restarts shifting from step 14 to the 17.

17) At the end of gastric digestion drive pumps are disabled, interrupting the progressive addition of SGF and enzymatic solution.

18) Pinch valves placed into the stomach are inactivated.

19) To ensure the outflow of what remains in the reactor, valves downstream the stomach (on/off and proportional) are totally opened.

20) The stomach is raised on one side by the activation of the relative air compression piston.

21) The second peristaltic pump (stomach → duodenum) is activated for the time necessary to deliver what remains in the stomach into the duodenum.

22) When all the chyme has been transported into the duodenum, the second peristaltic pump (stomach → duodenum) is inactivated.

23) The valves downstream the stomach (on/off and proportional) are totally closed to avoid backflows.

4.3.1.4. Duodenal phase

As stated in the previous paragraph, duodenal phase starts when liquids and food particles (< 1.5 mm) begin to be emptied into the duodenum (step 12). During this phase, chyme coming from the stomach is mixed with SIF, bile, and pancreatin solutions reaching a pH approximately equal to 7. pH is dynamically monitored by the pH probe inserted into the reactor. If pH is lower than 7, it can be adjusted by the addition of 1M NaOH. Pinch valves located into the duodenum create turbulent motions ensuring a proper mix of chyme with SIF, bile, and pancreatin solution (step 16).

24) Since duodenal phase is still continuing, pinch valves inside the duodenum are activated again (they will work continually until the end of the duodenal phase).

25) At the end of duodenal digestion, pinch valves are inactivated.

26) Drive pumps are disabled, interrupting the progressive addition of the intestinal fluids.

27) To ensure the outflow of what remains in the reactor, valves downstream the duodenum (on/off and proportional) are totally opened.

28) To promote the outflow of what remains in the reactor, duodenum compartment is raised on one side by the activation of the relative air compression piston.

29) The third peristaltic pump (duodenum → next reactor) is activated for the time necessary to deliver what remains in the duodenum into the successive reactor. Clearly, if you plan to stop at this stage, it is possible to collect the duodenal samples by opening the appropriate tap.

30) When all the duodenal content has been collected or transported into the next reactor, the third peristaltic pump (duodenum → next reactor) is inactivated.

31) Lastly, the on-off and the proportional valves downstream the duodenum are totally closed.

To date, every single part of this multi-compartmental apparatus can be controlled via software offering the possibility to dynamically monitor and regulate relevant physiological parameters such as the duration of each phase, flow rates of digestive fluids and enzymatic solution, pH, temperature, number, and length of each peristalsis. Hence, DICA might be used to recreate the

digestive system of specific groups of the human population (e.g., infants, young adults, seniors, and patients with impaired gastrointestinal conditions). However, it is at a preliminary stage of development and much more work is still required. Therefore, the next step will be the validation of the system using specific nutrients and model food.

Chapter 5

Effects of formulation on the microstructure and *in vitro* starch digestibility of commercial spaghetti

Abstract

Dry pasta is a staple food in many countries of the world, and it is traditionally made of durum wheat semolina. The aim of this study was to evaluate the impact of pasta composition on microstructure, cooking quality, water absorption and mobility during cooking and nutritional properties of three commercial spaghetti made of durum wheat semolina (S), whole durum wheat semolina (WS) and red lentil flour (LS). Scanning Electron Microscopy (SEM) revealed no significant microstructural differences between the uncooked S and WS samples. Besides, the use of lentil flour for pasta formulation resulted in an irregular microstructure marked by the presence of clearly visible starch entrapped within a web-like protein matrix. The presence of fibre altered the integrity of the protein network in the cooked WS. Moreover, in the case of LS samples, the high protein content led to the development of a strong gluten network which limited water absorption and starch gelatinization during cooking.

Pasta formulation also affects its cooking quality. Specifically, the use of lentil flour as raw material for pasta-making greatly influenced the colour, the swelling index and the cooking loss of the final product.

The water absorption during cooking and the water mobility at molecular level were investigated as weight increase and by low-resolution ^{1}H NMR experiments, respectively. The presence of fibre in WS caused a significant increase in the water absorption, while the presence of a strong protein matrix in LS decreased the proton relaxation times ^{1}H T_2 indicating high water-polymers and polymers-polymers interactions.

Lastly, the rate of starch hydrolysis, evaluated by means of *in vitro* methods, increased when whole durum wheat flour was used for pasta formulation, resulting in higher RDS and expected Glycemic Index (eGI) compared to S and LS, respectively. On the other hand, the use of lentil flour for pasta-making caused a significant reduction in the RDS content and eGI probably due to the formation of a highly cross-linked protein network which limited water uptake and starch gelatinization during cooking.

5.1. Introduction

Traditionally, *Triticum turgidum, subsp. durum* is adopted for the production of semolina, the preferred raw material for Italian pasta making (Raiola *et al.*, 2020). Dry pasta is a traditional cereal-based food largely appreciated by consumers for its convenience, palatability, and nutritional quality (Petitot, Abecassis & Micard, 2009). Primarily made up of carbohydrates (70 g/100 g) and proteins (11.5 g/100 g), pasta is considered to be a slowly digestible starchy food with a low or medium Glycemic Index (GI) (Granfeldt & Björck, 1991): a nutritional quality ruled by its structure as well as its composition.

Dry pasta production can be considered a mature technological process, considering markets acceptance and the widespread use of the final product (Sarghini, Romano, & Masi, 2016). Generally, dry pasta is produced by mixing milled durum wheat semolina and water. In fact, durum wheat semolina represents the best raw material for the production of high-quality pasta because of its chemical, sensorial, and rheological properties.

Pasta, being so popular, easy to cook and therefore widely consumed worldwide, is an ideal matrix for the enrichment with a wide range of ingredients, which can lead to important structural and nutritional changes, thereby determining the final pasta characteristics. Both pasta quality and cooking performances are directly related to the interactions between the main pasta components (starch and proteins) (Witczak & Gałkowska, 2021) and their physico-chemical modifications (protein denaturation, starch swelling and gelatinization), occurring in a different extent during pasta production. Thus, the choice of suitable ingredients for partial or complete replacement of semolina is essential for producing high quality dry pasta, with uniform amber colour, high cooking quality (“al dente” characteristics) and high nutritional properties.

In modern industry, the use of functional ingredients is becoming a strategy to develop novel product categories as well as to attract new classes of consumers (Nilusha *et al.*, 2019).

Two main drive forces can be identified within such recent trend:

1. To increase the nutritional value of wheat pasta, by partial substitution of semolina with highly nutritious and unconventional raw materials.
2. To prevent allergenicity/intolerance, in particular to gluten, by the complete replacement of semolina with gluten-free (GF) raw materials such as rice, corn and legume flour into dry pasta formulation.

There are some ingredients such as, for instance whole durum wheat and legumes flour, which can be used both to improve nutritional value and to reduce adverse reactions to pasta.

Pasta made with whole durum wheat semolina contains larger amount of vitamins, minerals, and fibre than durum wheat pasta, since these substances are mainly contained in the bran and germ which are mostly removed during milling (Vignola, Bustos, & Pérez, 2018). In addition, increasing the fibre content in food products represents an effective approach to overcome health problems such as hypertension, diabetes, colon cancer and coronary hearth diseases (Brand-Miller *et al.*, 2009; Wen *et al.*, 2017) and it is considered a valuable way to reduce the GI of high digestible products.

The use of legume flour to enrich or make GF pasta products is based, respectively, on the high protein content/lysine abundance (limited in cereals) and on the contemporary absence of gluten (Teterycz *et al.*, 2020). Among legumes flour, the one from lentil is gaining attention of food industries as well as among consumers due to its excellent and balanced nutritional composition. In fact, lentil flour represents a great source of nutritional components essential for good human health (e.g., high-quality proteins, fibre, vitamins, minerals, and antioxidant compounds) and thus it is increasingly used in bakery (bread, cake, crackers), extruded (pasta, snacks) and other products (dressings, soups, dairy, and meat products) (Romano *et al.*, 2021).

However, the introduction of fibre and non-gluten proteins can affect the structure of pasta matrix, e.g., compromising the formation of a cohesive gluten network, water absorption (Foschia *et al.*, 2013) and starch granules accessibility.

During cooking, pasta undergoes to multiple heat- and water-mediated transitions (including starch gelatinization and gluten denaturation) resulting in rheological and microstructural modifications of the pasta matrix, which affect its quality and consumer acceptance (Carini *et al.*, 2014).

A thorough understanding of water status (moisture content and water absorption) and water dynamics (molecular mobility) is a key factor for a proper comprehension of the final pasta quality.

Scanning Electron Microscopy (SEM) and proton Nuclear Magnetic Resonance (^{1}H NMR) are analytical techniques used to investigate, respectively, microstructural and protons' molecular dynamics. In particular, ^{1}H NMR technique is able to describe the mobility of molecules (such as water) in pasta matrixes (Carini *et al.*, 2013, 2014) and has been scarcely used to study pasta.

In recent years, low-resolution ^{1}H NMR turned out to be a very useful tool to understand and study how water–polymers interactions change in food matrices as function of composition and process parameters as well. In fact, spin – spin / transverse (^{1}H T_2) relaxation times of protons, are good indicators of the water status (bound, immobilized and free) (Gonçalves & Cardarelli, 2019) in food structures, decreasing when water is highly immobilized and increasing when water is more mobile.

The present work aims to investigate the impact of pasta formulation with a multi-scale analysis, in terms of physico-chemical, macroscopic (moisture content and water absorption), microscopic (microstructure) and molecular (^{1}H mobility) features of three kinds of commercial spaghetti (Barilla n.5) made of durum wheat semolina (S), whole durum wheat semolina (WS) and red lentil flour (LS).

Moreover, we studied the influence of pasta formulation on the *in vitro* starch digestibility of the samples under consideration. This knowledge could provide new insights and competitive advantage to pasta manufacturers, which can offer products with additional nutritional information to customers. In fact, nutritional labelling has emerged as an important aspect of consumers' food purchase decisions.

5.2. Materials and methods

5.2.1. Materials

All the experimental tests have been performed using three types of commercial spaghetti Barilla n.5 (Parma, Italy): durum wheat spaghetti (S), whole durum wheat spaghetti (WS) and red lentil spaghetti (LS).

The three samples had a comparable length of 25.6 ± 0.13 cm, but different diameters: 1.80 ± 0.02 mm for S, 1.66 ± 0.02 mm for WS and 1.62 ± 0.03 mm for LS.

The nutritional composition (% w/w) of spaghetti samples can be reassumed as follows: S – carbohydrates 70.2, proteins 13.5, fat 2.0, fibre 3.0, salt 0.013; WS – carbohydrates 65.7, proteins 13.0, fat 2.5, fibre 6.5, salt 0.013; LS - carbohydrates 47.4, proteins 25.0, fat 2.4, fibre 12.0, salt 0.003.

5.2.2. Sample preparation

S, WS and LS samples were cooked in boiling distilled water (1:10 w/v) for 1, 3, 5, 7, 8, 9 and 10 min. The Optimal Cooking Time (OCT, min) indicated by the producers was 9 min for S and 8 min for WS and LS. The uncooked samples (cooking time = 0 min) were used as control. After boiling, pasta samples were immersed in cold distilled water (T = 4°C) for a few second to prevent overcooking. Samples were collected and stored in polyethylene bags at 4°C until used for analysis.

5.2.3. Microstructural analysis: Scanning Electron microscopy (SEM) analysis and physical characterization

Scanning Electron Microscopy (SEM, LEO EVO 40, Zeiss, Germany) was used to examine the microstructure of transverse cross-sections of S, WS and LS samples. Raw and cooked samples were observed by SEM with a 20 kV acceleration voltage and a x 70 and x 1500 magnification according to Romano *et al.* (2018). The cross-section area (mm^2) of samples was quantified using a method based on image analysis protocol of SEM micrographs. Three micrographs were selected and processed per sample by Image Pro Plus 6.1 for Windows® (Media Cybernetics Inc.).

5.2.4. Water absorption

Water absorption tests were performed by fully immersing single strands of spaghetti (25 ± 2 mm in length) in glass tubes (diameter = 16 mm; h = 125 mm) containing 10 mL of boiling water (1:10 w/v) according to Steglich *et al.* (2014). At each cooking time samples were removed from the tube, cooled down, blotted, and weighed. The water absorption index (WA) was determined as:

$$\text{WA (\%)} = \frac{\text{weight of cooked pasta} - \text{weight of uncooked pasta}}{\text{weight of uncooked pasta}} \text{ x } 100 \qquad (2)$$

For each sample, three replicates have been performed at each cooking time.

5.2.5. Cooking quality at the OCT

All samples (S, WS and LS) were analyzed for colorimetric parameters, moisture content, water absorption, swelling index and cooking loss after cooking at the OCT.

Colorimetric parameters (L*, a*, b* and ΔE) of spaghetti samples before and after cooking at the OCT were determined by an Electronic Visual Analyzer IRIS (Alpha MOS).

The moisture content of each sample was determined before and after cooking at the OCT by the AACC method (number 44−15.02, AACC International Approved Methods of Analysis, 1999). 2.5 g of sample were dried for 24 h at 105°C. Samples were removed from the oven and immediately placed in a desiccator prior to weighting after cooling and within 30 min. The dried samples weight was subtracted to the respective initial weight. The results were calculated as percentage of water per sample weight (%).

The WA at the OCT was determined as described in the previous paragraph (5.2.4.).

The Swelling Index (SI) refers to the weight of water absorbed during cooking at the OCT per weight of dry pasta. It was determined by drying to constant weight the cooked pasta and calculated according to the following formula:

$$SI\ (g/g) = \frac{weight\ of\ cooked\ pasta - weight\ after\ drying}{weight\ after\ drying} \times 100 \qquad (3)$$

The Cooking Loss (CL) represents the number of solids that diffuse from pasta structure to the water during cooking. It was calculated as percentage of solids remaining after evaporation of the cooking water per weight of dry spaghetti:

$$CL\ (\%) = \frac{weight\ of\ cooking\ water\ after\ drying}{weight\ of\ uncooked\ pasta} \times 100 \qquad (4)$$

Each experiment was carried out in triplicate.

5.2.6. Molecular water mobility by low field NMR

A low resolution (20 MHz) ^{1}H NMR spectrometer (Minispec mq-20, Bruker, Milano, Italy) operating at 25.0 ± 0.1°C was used to study proton transverse (^{1}H T_2) relaxation times of all samples (S, WS and LS) at each cooking time (0, 1, 3, 5, 7, 8, 9 and 10 min).

Approximately 4 g of sample cutted in pieces of about 3 cm height were placed into a 10 mm external diameter NMR tube. NMR tubes were immediately sealed with Parafilm® to prevent moisture loss during the NMR experiment. ^{1}H T_2 relaxation times were measured with a CPMG

(Carr, Purcell, Meiboom and Gill) pulse sequence using a recycle delay of 0.4 s and an interpulse spacing of 0.04 ms while the number of data points acquired was 1500.

The raw Carr-Purcell Meiboom-Gill (CPMG) decay curves were provided directly by the minispec and the raw data were analyzed by a multivariate analysis.

Three NMR tubes (from three different trays) were analyzed for each sample at each cooking time.

5.2.7. *In vitro* starch digestibility

Measurement of non-resistant starch (solubilised, Non-RS) were performed using an enzymatic assay kit (Resistant Starch Assay Kit, Megazyme International Ireland) by AACC method (number 32–40.01, AACC International Approved Methods of Analysis, 2009) with minor modifications according to Romano *et al.* (2016). Rapidly digestible starch (RDS) and slowly digestible starch (SDS) were measured after 30 and 120 min of incubation in a shaking water bath (200 strokes/min, horizontal agitation) at 37°C respectively. The digestion kinetics were described by means of a non-linear model following the equation suggested by Goñi, Garcia-Alonso, & Saura-Calixto (1997):

$$C = C\infty\ (1\text{-}e^{-kt}) \quad (5)$$

where C was the hydrolysis degree at each time, C∞ was the maximum hydrolysis extent and k was the kinetic constant. The hydrolysis index (HI) given as percentage was calculated by comparing the area under the hydrolysis curve (0–180 min) of each sample and that of white bread used as reference food. From HI the expected Glycemic Index (eGI) was calculated using the equation proposed by Goñi *et al.* (1997):

$$eGI = 39.71 + 0.549HI \quad (6)$$

5.2.8. Statistical analysis

All experimental results are reported as means and standard deviation of at least three independent experiments. Statistical analysis was performed using SPSS version 19.0 (SPSS Inc., Chicago, IL, USA). One way ANOVA with Duncan's multiple comparison test at the 95% confidence level ($P < 0.05$) were performed in order to evaluate the effect of cooking time on parameters of each spaghetti type (S, WS and LS). Furthermore, statistical differences between samples were

evaluated at each cooking time ($P < 0.05$). Correlations between WA and ^1H T_2 values for each spaghetti sample during cooking were carried out by correlation matrix using the Pearson product moment correlation distribution to significant $P < 0.05$.

5.3. Results and discussion

5.3.1. Microstructural characteristics

SEM was used to examine the impact of pasta formulation on the microstructure of spaghetti samples (S, WS and LS) before and after cooking. Fig. 5.1 shows the transverse cross-section of the uncooked (t = 0 min) samples.

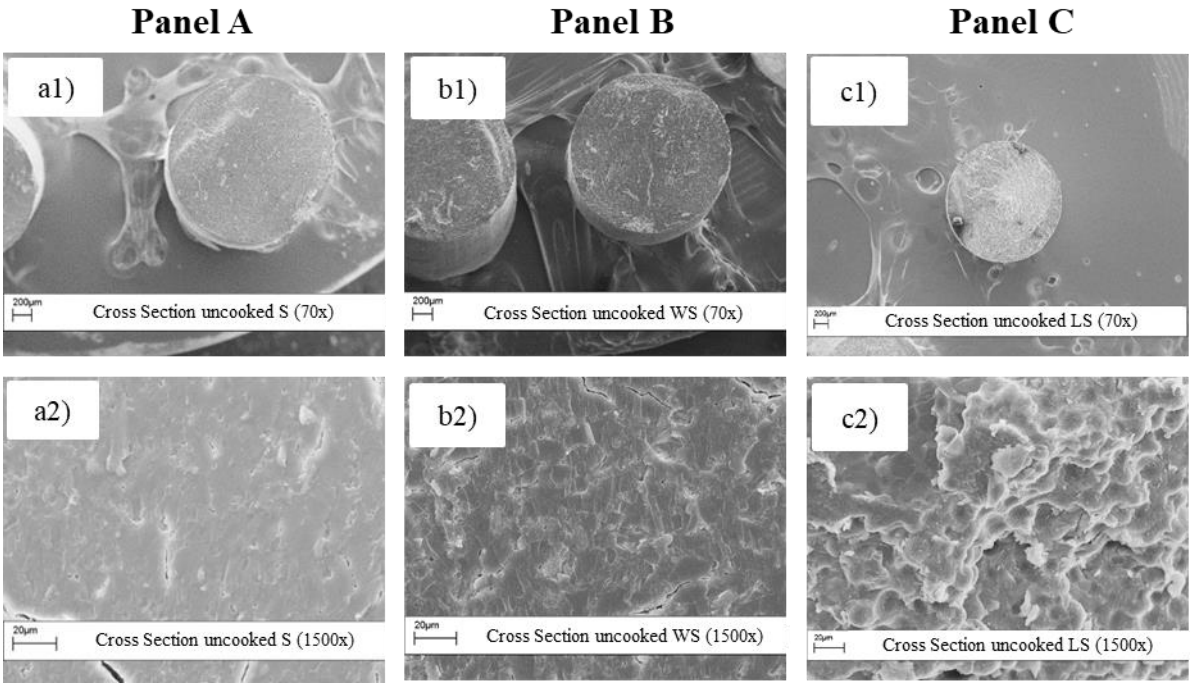

Fig. 5.1. Scanning electron micrographs of the uncooked spaghetti. **Panel A:** durum wheat spaghetti (S) a1) cross section (70x); a2) cross section (1500x). **Panel B:** whole durum wheat spaghetti (WS) b1) cross section (70x); b2) cross section (1500x). **Panel C:** red lentil spaghetti (LS) c1) cross section (70x); c2) cross section (1500x).

The cross-section of S (Fig. 5.1 a_1 - a_2) and WS (Fig. 5.1 b_1 - b_2) appeared as a homogeneous structure where not gelatinized starch granules were deeply incorporated in a protein matrix. Therefore, the presence of fibre in WS samples did not promote significant microstructural

differences between the uncooked S and WS samples whose structure is mainly due to the high pressure applied to the pasta dough during the extrusion process.

Regarding instead the microstructural properties of LS, appreciable differences compared to the other samples could observed, especially at x 1500 magnification (Fig. 5.1c_2). In fact, LS samples exhibited a corrugated surface and starch granules incorporated in a web-like protein matrix were clearly visible. Similar findings have been reported by Wojtowicz & Moscicki (2014) after adding lentil flour to semolina spaghetti (40g/100g).

However, after cooking at the OCT, structural differences between the three spaghetti samples emerged.

In Fig. 5.2 are reported the SEM micrographs of the transverse cross section of the three samples cooked until their OCT (OCT = 9 for S and 8 min for WS and LS).

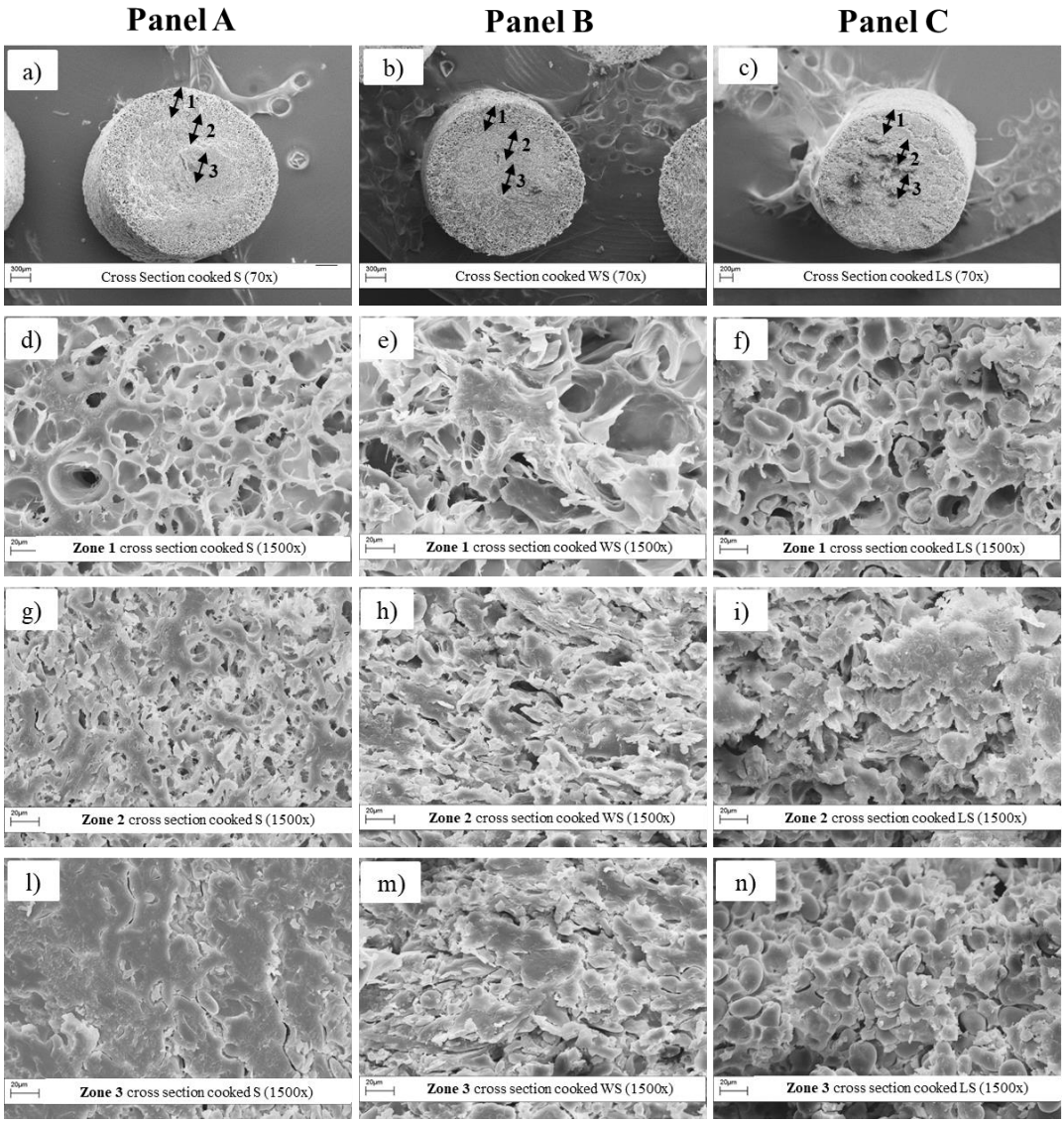

Fig. 5.2. Representative SEM micrographs of spaghetti cooked until the optimal cooking time (OCT). **Panel A:** durum wheat spaghetti (S) a) cross section; d) zone 1 - outer layer; g) zone 2 - intermediate layer; l) zone 3 - central layer. **Panel B:** whole durum wheat spaghetti (WS) b) cross section; e) zone 1 - outer layer);
h) zone 2 - intermediate layer; m) zone 3 - central layer. **Panel C:** red lentil spaghetti (LS) c) cross section; f) zone 1 - outer layer); i) zone 2 - intermediate layer; n) zone 3 - central layer.

As shown in Fig. 5.2a, at the OCT, one can observe three different zones: 1) outer zone; 2) intermediate zone; 3) central zone, which were characterized by various degrees of starch gelatinization and protein coagulation.

Overall, LS samples showed the most heterogeneous microstructure probably because of a non-homogeneous water distribution among the three zones.

In the outer zone of S and WS spaghetti samples (Fig. 5.2 d, e), starch granules and protein matrix were practically indistinguishable because of the high degree of protein coagulation and starch gelatinization, in agreement with the strong impact of the cooking process on the outer pasta surface reported by Diantom *et al.* (2019).

SEM micrographs of LF spaghetti suggested a prevalence of proteins hydration on starch swelling and consequently the predominance of protein network formation on starch gelatinization. In addition, the protein network was more evident and thicker than those of wheat pasta, in accordance with the higher protein content of LS samples.

Between the outer and the central zone, there was an intermediate zone characterized by swollen starch granules embedded in a coagulated but dense protein network (Fig. 5.2 g - i).

The central zone (core) of the S samples (Fig. 5.2l) showed a homogeneous structure in which the protein network was still continuous and dense, and the degree of starch gelatinization was limited since the reduced water absorption in this region allowed starch granules to preserve their structure (Cunin *et al.*, 1995). On the other hand, the central zone of WS samples (Fig. 5.2m) had a more irregular structure in which there were a small number of still intact and therefore non-gelatinized starch granules compared to the durum wheat spaghetti (Fig. 5.2 l). As reported by Manthey & Schorno (2002), in whole-wheat pasta fibre may interfere with a proper gluten development. This results in a highly porous structure in which starch granules are more accessible to water molecules.

Lastly, several intact starch granules could be clearly visible in the central zone of LS (Fig. 5.2n). This might be lineked to a slower water penetration during cooking which hindered starch swelling and gelatinization.

As shown in Fig. 5.2a, b, c all samples underwent a significant ($P < 0.05$) increase in cross-section area during cooking. The image analysis of the SEM micrographs revealed that the cross-section area of sample S varied from 2.55 ± 0.05 mm^2 (t = 0 min) to 5.97 ± 0.16 mm^2 (t = 9 min), from 2.11 ± 0.01 mm^2 (t = 0 min) to 4.91 ± 0.02 mm^2 (t = 8 min) for WS and that of sample LS from 2.07 ± 0.14 mm^2 to 4.18 ± 0.04 mm^2 (t = 8 min).

5.3.2. Effect of pasta formulation on the water absorption

During cooking, starch gelatinization and protein coagulation are the main factors responsible for the changes in pasta structure. These phenomena occur at the same range of temperature and

humidity conditions, and therefore are competitive and antagonist (Fuad & Prabhasankar, 2010). Clearly, the presence of fibre might interfere in this competition (Bock, Connelly, & Damodaran, 2013). The prevalence of starch gelatinization or protein matrix formation establish the final pasta cooking quality (Bustos, Perez, & Leon, 2015). If gluten polymerization dominates, pasta structure appears as a consolidated and non-discontinuous protein network in which starch granules were deeply incorporated. In this kind of structure, water penetrates slowly, starch gelatinises gradually, and cooking loss is limited, resulting in good quality pasta (de Noni & Pagani, 2010). On the contrary, if starch gelatinization prevails, the gluten network weakens, and the final cooking quality of pasta results be impaired (e.g., increase in the amylose leaching in the cooking water) (Resmini & Pagani, 1983). From all this it becomes clear that the inclusion of ingredients different from wheat into pasta formulation can lead to a worsening of its technological properties.

Fig. 5.3 showed the WA kinetics of S, WS and LS within the first 10 min of cooking.

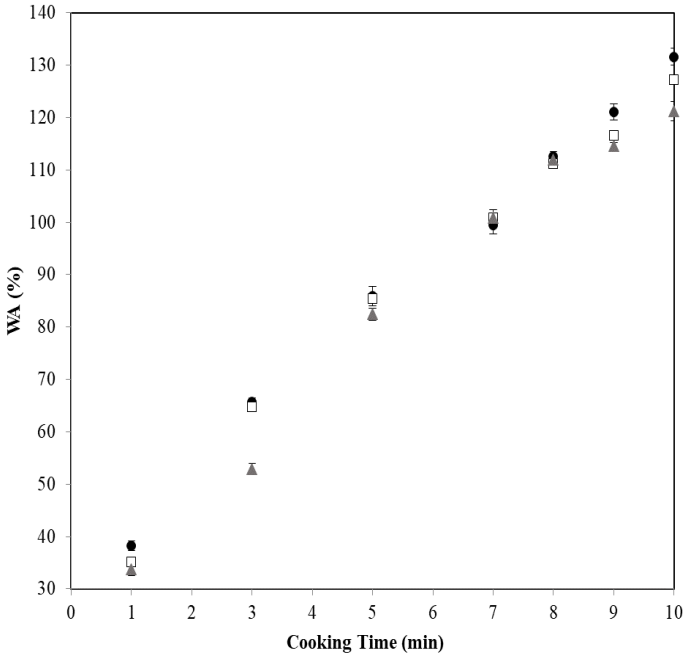

Fig. 5.3. Water absorption (%) kinetics of durum wheat spaghetti (□), whole durum wheat spaghetti (●) and red lentil spaghetti (▲) within the first 10 min of cooking.

Spaghetti samples showed similar trends of WA even with statistically significant variations ($P < 0.05$) at 1, 3, 5, 9 and 10 min of cooking. In particular, WS samples had the highest ($P < 0.05$) WA at 9 and 10 min while LS had the lowest. Throughout the entire cooking process, LS displayed lower WA values than the other samples, even if there were no significant differences ($P > 0.05$) with WS samples at 7 and 8 min of cooking.

Our results are consistent with Aravind *et al.*, (2012) that claimed that presence of fibre in whole-grain pasta may cause the disruption of the protein–starch matrix, promoting the formation of cracks and thus a faster water uptake during cooking and with Sozer & Kaya (2008) who found a lower WA with increasing protein content.

Water penetration during cooking is highly dependent on the degree of protein reticulation (Bonomi *et al.*, 2012). Thus, the lower WA observed for LS could be reasonably attributed to the presence of a highly cross-linked protein network which may limit water uptake during cooking. Our findings agree with Teterycz *et al.*, (2020) which noted a reduction in WA when semolina pasta was enriched with red lentil flour (5-20%) and with Berrazaga *et al.* (2020) which stated that the enrichment of wheat pasta with lentil flour causes the formation of a highly reticulated protein network.

Furthermore, Bernin *et al.*, (2014) found that an increase in protein content may lead to a more heterogeneous water distribution in pasta microstructure as well as to a strong protein network which may hinder starch swelling.

Lastly, our results partially agree with those of Cafieri *et al.*, (2010), which noted an interesting correlation between spaghetti diameter in the dry state and WA during cooking. Specifically, as water uptake depends on contact area, they concluded that the larger the diameter the faster the water uptake. Our outcomes suggest that S samples had a higher diameter (1.80 ± 0.02 mm) in the dry state compared to WS (1.66 ± 0.02 mm) but a lower WA. On the other hand, LS samples showed the lowest diameter in the dry state (1.62 ± 0.03 mm) and the lowest WA as well. This suggested that the pasta formulation can be a major factor in determining the WA during cooking than the pasta shape.

5.3.3. Cooking properties

Colour parameters and cooking quality indices of durum wheat (S), whole durum wheat (WS) and LS spaghetti are listed in Table 5.1. Pasta colour represents an important aspect of pasta

quality, able to influence consumer acceptance (Petitot *et al.*, 2010). Figure 5.4 shows representative pictures of spaghetti samples under examination before and after cooking at the OCT.

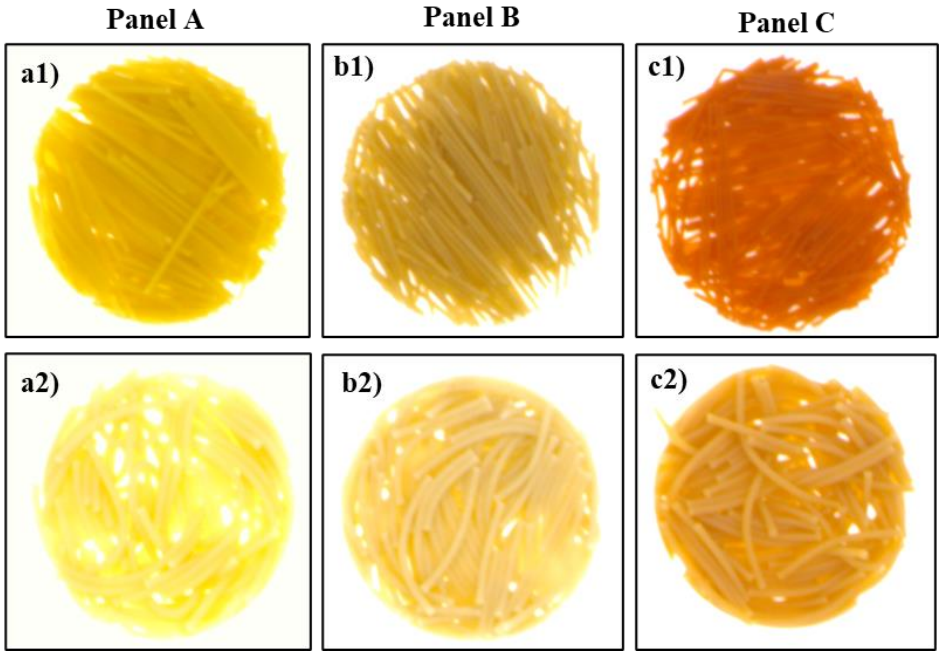

Fig. 5.4. Representative pictures of durum wheat spaghetti (S), whole durum spaghetti (WS) and red lentil spaghetti (LS). **Panel A:** durum wheat spaghetti (S) a1) uncooked; a2) cooked at the OCT. **Panel B:** whole durum wheat spaghetti (WS) b1) uncooked; b2) cooked at the OCT. **Panel C:** red lentil spaghetti (LS) c1) uncooked; c2) cooked at the OCT.

As shown in Table 5.1, colour parameters (L*, a*, b* and ΔE) of raw and pasta cooked at the OCT changed significantly depending on the raw material used. Concerning the raw pasta samples, lightness (L* value) was significantly lower ($P < 0.05$) for LS, followed by WS and S, respectively. The darker colour of red lentil spaghetti may be attributed to the specific colour of lentil flour, which often is also marked by high ash content (Petitot *et al.*, 2010). As expected, the parameter a* (green–red) was significantly higher ($P < 0.05$) for the uncooked LS samples suggesting a reddish colour, and lower ($P < 0.05$) for WS, indicating a greenish shade. Regarding instead the parameter b* (yellow-blue), it was significantly lower ($P < 0.05$) for LS which had a tendency to a yellow hue and higher ($P < 0.05$) for WS. Cooking had a bleaching effect on all the samples, resulting in increased ($P < 0.05$) brightness (L* value). Moreover, it caused a significant decrease ($P < 0.05$) in redness (a*) together with an increase ($P < 0.05$) in yellowness (b*).

The moisture content of the uncooked spaghetti was 10.68 ± 0.14% for S, 8.89 ± 0.07% for WS and 10.19 ± 0.10% for LS (data are not shown). This parameter increased almost fivefold (60.08 ± 0.19%) for S, sevenfold for the sample WS (60.79 ± 0.34%) and sixfold (63.69 ± 0.16%) for LS after cooking at the OCT.

Significant differences ($P < 0.05$) in water absorption, swelling index and cooking loss have been found between samples under investigation (Table 5.1). This variability was strictly related to compositional factors such as the protein, starch, and dietary fibre content.

Table 5.1. Effect of cooking at the OCT on colour parameters and cooking properties (WA - Water Absorption; SI – Swelling Index; CL – Cooking Loss) of durum wheat spaghetti (S), whole durum wheat spaghetti (WS) and red lentil spaghetti (LS), expressed as means ± S.D.

Sample	**L***	**a***	**b***	**ΔE**
uncooked S	$77.05 \pm 0.9_{d}$	$32.44 \pm 1.1_{d}$	$-21.84 \pm 3.0_{b}$	$45.37 \pm 2.7_{a}$
uncooked WS	$68.92 \pm 1.1_{b}$	$16.21 \pm 2.4_{c}$	$46.79 \pm 6.8_{d}$	$58.61 \pm 5.2_{c}$
uncooked LS	$58.93 \pm 0.9_{a}$	$65.26 \pm 0.8_{e}$	$-47.95 \pm 2.6_{a}$	$90.81 \pm 2.2_{d}$
cooked S (9 min)	$94.47 \pm 0.7_{f}$	$-10.04 \pm 0.7_{a}$	$62.66 \pm 2.2_{e}$	$63.71 \pm 2.1_{c}$
cooked WS (8 min)	$85.35 \pm 1.2_{e}$	$4.60 \pm 1.5_{b}$	$59.38 \pm 1.4_{e}$	$61.36 \pm 1.0_{c}$
cooked LS (8 min)	$71.97 \pm 0.9_{c}$	$29.34 \pm 3.2_{d}$	$32.03 \pm 10.7_{c}$	$52.37 \pm 4.5_{b}$
Sample	**Moisture content (%)**	**WA (%)**	**SI (g/g)**	**CL (%)**
cooked S (9 min)	$60.79 \pm 0.3_{d}$	$116.54 \pm 0.3_{b}$	$1.55 \pm 0.02_{b}$	$5.12 \pm 0.2_{b}$
cooked WS (8 min)	$60.08 \pm 0.2_{b}$	$112.53 \pm 0.4_{a}$	$1.51 \pm 0.01_{a}$	$4.45 \pm 0.3_{a}$
cooked LS (8 min)	$63.69 \pm 0.9_{a}$	$111.79 \pm 0.85_{a}$	$1.75 \pm 0.01_{c}$	$5.85 \pm 0.3_{c}$

[a-f] Means within the same column with different letters are significantly different ($P < 0.05$; Duncan test).

As explained previously, at the OCT, WA values were significantly higher ($P < 0.05$) for S samples than the others, shifting from 116.54 ± 0.3% (S) to 111.79 ± 0.85% (LS).

The SI of pasta represents an index of the water absorbed by proteins and/or starch during cooking which is used for proteins hydration and/or starch gelatinization. This parameter ranged from 1.51 g/g (WS) to 1.75 g/g (LS). As suggested by the microstructural findings (paragraph 5.3.1.), the highest ($P < 0.05$) SI values of LS samples may be primarly linked to the protein matrix hydration since starch swelling and gelatinization seemed to be quite limited.

CL is recognized as an important factor for consumer acceptance since it is related to the leaching of dry matter into cooking water and therefore to alterations of food texture. Pasta of good quality should not lose more than 8% d.m. (Teterycz *et al.*, 2020). The highest ($P < 0.05$) cooking loss was observed for LS pasta, but this parameter did not exceed 8% (5.85 ± 0.3%) suggesting satisfactory cooking quality. Moreover, WS samples had the lowest cooking loss ($P < 0.05$) while S samples showed intermediate values. This outcome was quite unexpected since usually, increasing the amount of dietary fibre negatively affects the development of the gluten network, leading to a more open pasta structure, thereby enhancing solid losses.

5.3.4. Effect of composition on molecular water mobility of spaghetti

The effect of pasta composition on water mobility at a molecular level has been investigated by low-resolution NMR experiments. In particular, spin – spin / transverse (^1H T^2) relaxation times have been determined (Table 5.2.), being good indicators of the molecular water mobility (Gonçalves & Cardarelli, 2019). In Fig. 5.5 are reported the TD NMR raw decays of all the spaghetti samples (S, WS and LS) identified by the same colour for each cooking time (0, 3, 5, 7, 8, 9 and 10 min) to stress the impact of the cooking time on proton mobility rather than the raw material used.

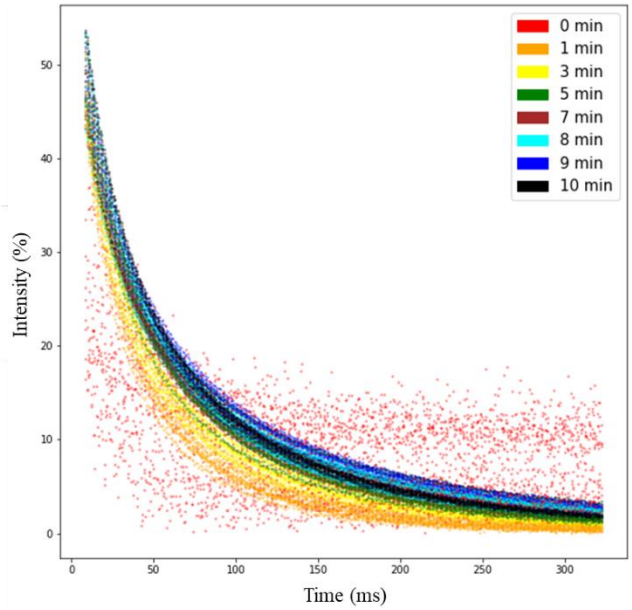

Fig. 5.5. Carr-Purcell Meiboom-Gill (CPMG) decay curves of all spaghetti the samples (S, WS and LS) cooked for 0 (■), 1 (■), 3 (■), 5 (■), 7 (■), 8 (■), 9 (■) and 10 (■) min.

The CPMG relaxation curves could be clustered in two groups marked by different trends. In particular, the dry spaghetti samples clearly differed from the cooked ones since they were characterized by a highly randomized distribution of the signal intensity along the time axis, suggesting unique structural characteristics. In fact, as listed in Table 5.2, the ^1H T_2 values of the uncooked S, WS and LS samples were significantly lower ($P < 0.05$) compared to that of the cooked ones, suggesting a very low water mobility in the dry pasta. This may be reasonably attributed to the predominant presence of rigid non exchanging CH protons present in the amorphous starch and in the gluten chains which establish strong interaction with each other (Bosmans *et al.*, 2012).

On the other hand, all the cooked samples showed decay curves with a similar trend (Fig. 5.5). The signal intensity had a more homogeneus distribution, assuming greater values with rising the cooking time.

Table 5.2. Effect of the cooking time (min) on ^1H T_2 (ms) of durum wheat (S), whole durum wheat (WS) and LS spaghetti, expressed as means ± S.D.

Cooking time (min)	**S T_2 (ms)**	**WS T_2 (ms)**	**LS T_2 (ms)**
0	$27.00 \pm 1.0_{a,y}$	$30.40 \pm 0.6_{a,z}$	$12.33 \pm 2.1_{a,x}$
1	$41.50 \pm 3.5_{b,y}$	$38.70 \pm 1.9_{b,y}$	$32.70 \pm 1.9_{b,x}$
3	$54.20 \pm 0.8_{c,z}$	$49.67 \pm 1.3_{c,y}$	$44.00 \pm 2.8_{c,x}$
5	$61.77 \pm 0.5_{d,z}$	$59.07 \pm 1.6_{d,y}$	$49.70 \pm 1.3_{d,x}$
7	$69.00 \pm 0.8_{e,y}$	$67.50 \pm 0.7_{e,y}$	$52.83 \pm 1.0_{e,x}$
8	$70.60 \pm 0.4_{e,y}$	$69.73 \pm 0.5_{f,y}$	$55.07 \pm 0.5_{e,x}$
9	$73.63 \pm 0.6_{f,z}$	$71.40 \pm 0.8_{f,g,y}$	$58.43 \pm 0.4_{f,x}$
10	$76.17 \pm 1.5_{f,z}$	$72.07 \pm 0.9_{g,y}$	$60.44 \pm 0.7_{f,x}$

$^{a–h}$ For each sample, means followed by a different letter within a column are significantly different ($P < 0.05$).
$^{x-z}$ For each cooking time, means followed by a different letter within the same row are significantly different ($P < 0.05$).

The ^1H T_2 values also increased ($P < 0.05$) with the progress of cooking (Table 5.2) shifting from 27.0 ± 0.1 ms (t = 0 min) to 76.2 ± 1.5 ms (t = 10 min) in the case of S, from 30.4 ± 0.6 ms to 72.1 ± 0.9 ms for WS and from 52.8 ± 1.0 to 60.4 ± 0.7 for LS samples. ^1H T_2 is a measure of the

time required by protons to return to their equilibrium conditions thanks to mutual energy exchange (spin-spin interaction, in the x – y plane) and a raise in this parameter indicates a system that became more mobile during cooking. Thus, the significant increase ($P < 0.05$) of ^{1}H T_2 with increasing cooking time, suggested that molecular water mobility within the pasta structure increased as protein coagulation and starch gelatinization proceed. According to Bosmans *et al*. (2012), this behavior can be explained in term of three phenomena: i) water uptake within the pasta structure; ii) starch gelatinization with the subsequent destruction of the original structure; iii) gluten polymerization accompanied by water expulsion from the gluten network.

Fig. 5.6 shows the CPMG relaxation curves of each cooked spaghetti type (S, WS and LS) to highlight the effect of food formulation on proton mobility.

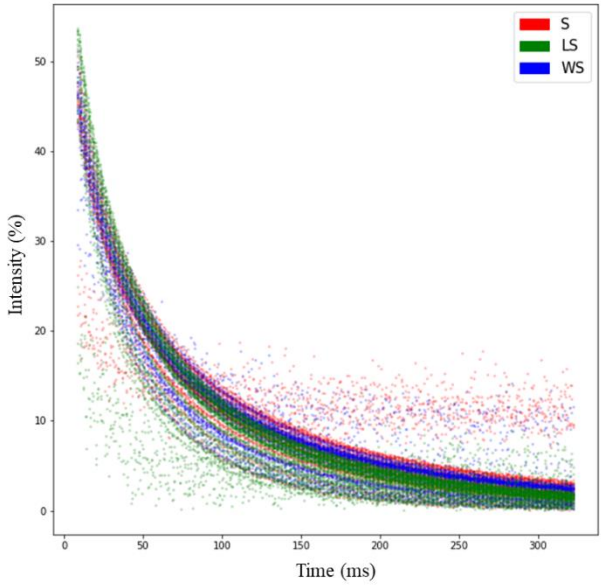

Fig. 5.6. Carr-Purcell Meiboom-Gill (CPMG) decay curves of S (■), WS (■) and LS (■) cooked for 0, 1, 3, 5, 7, 8, 9, and 10 min.

Overall, both for the uncooked and the cooked samples, the CPMG relaxation curves exhibited higher signal intensity in the case of S samples, followed by WS and LS. This trend was also supported by the transversal relaxation times values listed in Table 5.2. In fact, by comparing the behavior of the three samples during the cooking process, one observes that S samples had the highest ^{1}H T_2 values ($P < 0.05$) at 3, 5, 9 and 10 min of cooking compared to the other samples.

LS samples showed the lowest ^{1}H T_2 values ($P < 0.05$) at each cooking time while WS samples had intermediate values except at 1, 7 and 8 min of cooking where no differences ($P > 0.05$) were found with S samples. This suggests that the water mobility was affected by the presence of fibre (in the case of WS) and even more by the presence of high amount of fibre and proteins (in the case of LS). In detail, as suggested by Serial *et al.* (2016), fibre can keep a substantial excess of water during the cooking process, resulting in a reduction of molecular water mobility.

These outcomes were in perfect accord with the microstructural and water absorption results. Regarding the latter, a high correlation between the WA and the corresponding ^{1}H T_2 values has been found for all samples, with a R^2 of 0.985 for S and WS and a R^2 of 0.968 for LS samples.

On the other hand, the higher number of proteins of LS samples may lead to the formation of a highly reticulated protein matrix (Berrazaga *et al.*, 2020) which can negatively affect water penetration, distribution, and mobility during cooking (Bonomi *et al.*, 2012).

These findings are very promising and suggest that the choice to resort a raw data multivariate analysis instead of a multiexponential fitting analysis, represents a useful tool to study the change in molecular water mobility of pasta. This prevents possibly erroneous assumption made from some multiexponential fitting approaches such as: i) the presence of a multiexponential trend; ii) the hypothesis that there is no interaction among the various proton populations; iii) the idea that these populations continuously evolute (e.g., with increasing cooking time), while it can happen that at one point, some populations disappear, or new ones originate.

5.3.5. *In vitro* starch digestibility and expected Glycemic Index

Fig. 5.7 shows the results regarding *in vitro* starch digestibility of spaghetti samples.

The *in vitro* starch digestibility was investigated by measuring the released glucose content during starch digestion using an enzymatic method with minor modifications (Romano *et al.*, 2016) and the hydrolysis curves of uncooked and cooked spaghetti samples were compared with those performed by white bread used as control (reference food). S, WS and LS spaghetti showed a different hydrolysis kinetics either in the dry state (uncooked) and at their OCT. After cooking at the OCT, WS was characterized by a rapid increase of starch hydrolysis within the first 30 min, and then the percentage of digested starch increased gradually for the additional 150 min. By contrast, the slowest starch hydrolysis kinetics was observed for LS followed by S samples.

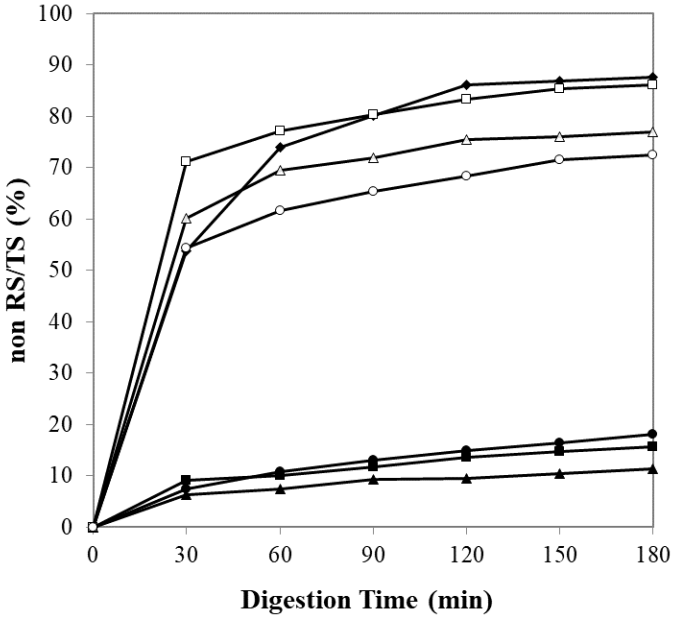

Fig. 5.7. Starch digestibility profiles of white bread (♦) and: uncooked S (▲), uncooked WS (■), uncooked LS (●), S cooked until the optimal cooking time (Δ), WS cooked until the optimal cooking time (□) and LS cooked until the optimal cooking time (○).

The average values of rapidly digestible starch (RDS), slowly digestible starch (SDS) ad expected Glycemic Index are reported in Table 5.3.

RDS is the starch fraction that is rapidly and totally digested in the gastrointestinal tract and it is associated with fast elevation of postprandial plasma glucose, whereas SDS is the starch fraction which is more slowly digested in the gastrointestinal tract (Jenkins *et al.*, 1981; Romano *et al.*, 2019). As expected, The RDS and SDS fractions were significantly lower ($P < 0.05$) in the uncooked samples than the cooked ones. Table 5.3 reports, also, the eGI values. In the case of the uncooked samples, the lower eGI of S (46.17 ± 0.03%) compared with WS (48.51 ± 0.03%) and LS (49.21 ± 0.24%), may be explained in terms of the different firmness of the gluten network (Fig. 5.1) of the three kind of pasta which reflects on the starch granules accessibility to the amylolythic enzymes.

As can be seen from Table 5.3, cooking at the OCT led to significant changes in RDS, SDS and eGI and thus in the *in vitro* starch digestibility. In particular, RDS and eGI reached the highest values ($P < 0.05$) in WS samples and the lowest in LS (Table 5.3). S samples had intermediate RDS and eGI values and the lowest SDS content (11.24 ± 0.6%). The different compactness of pasta structure after cooking at the OCT (Fig. 5.2) can also explain the different accessibility of the enzyme to the starch granules. An additional evidence is the fact that at the OCT, sample S

(Fig. 5.2l) and even more LS samples (Fig. 5.2m) were characterized by a central core in which proteins were not coagulated and starch granules were not gelatinized. The same was not true for sample WS that at the OCT appeared to be completely cooked and no microstructural differences between the intermediate and the central zones could be observed (Fig. 5.2h, m).

Our findings are in good agreement with the achievements of Vignola *et al.* (2018), who demonstrated that the use of whole durum wheat semolina in pasta formulation led to the presence of a weaker gluten network which promoted the starch amylolysis and thus increased the amount of RDS.

Table 5.3. Effect of pasta formulation on starch nutritional fractions: RDS (rapidly digestible starch), SDS (slowly digestible starch) and eGI (expected Glycemic Index) of durum wheat spaghetti (S), whole durum wheat spaghetti (WS) and red lentil spaghetti (LS) spaghetti. Each value is expressed as means ± S.D.

Sample	**RDS (%)**	**SDS (%)**	**eIG (%)**
uncooked S	$4.66 \pm 0.1_{b}$	$2.37 \pm 0.1_{a}$	$46.17 \pm 0.03_{a}$
uncooked WS	$5.87 \pm 0.4_{c}$	$2.90 \pm 0.6_{b}$	$48.51 \pm 0.03_{b}$
uncooked LS	$3.78 \pm 0.19_{a}$	$3.84 \pm 0.02_{c}$	$49.21 \pm 0.24_{c}$
cooked S (9 min)	$44.26 \pm 0.3_{e}$	$11.24 \pm 0.6_{e}$	$89.18 \pm 3.59_{e}$
cooked WS (8 min)	$46.61 \pm 0.5_{f}$	$7.96 \pm 0.2_{d}$	$98.23 \pm 0.26_{f}$
cooked LS (8 min)	$29.15 \pm 0.2_{d}$	$7.58 \pm 0.3_{d}$	$87.24 \pm 0.05_{d}$

[a-f] Means within the same column with different letters are significantly different ($P < 0.05$).

The lower RDS content (29.15 ± 0.2%) of the cooked LS samples than the cooked S (44.26 ± 0.3%) and WS (46.61 ± 0.5%) may be due both to a different microstructure and to the high total flavanol index of red lentils as reported in the literature. In fact, as stated by Lu *et al*. (2018) phenolic compounds, and, in particular, the flavanols, are known to be the major contributors to the α-glucosidase inhibitory activity which implies reduced starch digestibility.

Chapter 6

Properties of bread with flour from typical green lentils during simulated gastrointestinal digestion

Abstract

The effects of replacing wheat flour with lentil flour (LF) (10% and 20%) on some physico-chemical, structural, and nutritional properties of bread have been evaluated. The addition of LF in bread formulation led to a darker appearance and poor-quality attributes, such as a more compact structure (e.g., higher density and lower gas bubble area fraction). Concerning the investigation of bread nutritional properties, starch and protein digestibility have been examined by the combination of different digestion models. Each type of bread was subjected to an *in vivo* oral phase followed by a semi-dynamic *in vitro* gastrointestinal digestion. During the oral and gastric phases, bread with the greatest LF content (20%) exhibited higher starch digestibility and lower protein digestibility compared to the other samples. On the contrary, control bread (0% LF) showed stronger starch digestibility during the intestinal phase than LF bread. This was attributed to the higher content of slowly digestible starch. Furthermore, each sample showed an extensive gluten hydrolysis and thus an increase in low molecular weight peptides during the intestinal phase. These achievements were also supported by structural findings.

The whole study demonstrated that LF plays a critical role in determining the overall bread quality. In addition, the combination of different digestion models proved to be a successful strategy to investigate the effect of LF incorporation on starch and protein *in vitro* digestibility.

6.1. Introduction

Green Altamura Lentil (*Lens culinaris Medik.*), produced in Altamura (Bari, Apulia, Southern Italy) was recently authorized by the Commission of the European Community to receive the Protected Geographical Indication (P.G.I.) (European Union, 2017). As reported by producers on the nutrition label, Altamura lentil is quite rich in components essential for good human health such as carbohydrates (50%), proteins (26%), dietary fibres (8.4%), minerals, vitamins (mainly vitamin B3/niacin) and phenolic compounds. In addition, lentils are gluten-free, have a reduced fat (2%) and caloric content (340 kcal/100g) as well as a low glycemic index (GI) (Di Stefano *et al.*, 2021). Various studies have shown that frequent legumes consumption, including lentils, can be associated with a reduced risk of cardiovascular diseases (CVDs), type 2 diabetes, some types of cancer, overweight and obesity (Chelladurai & Erkinbaev, 2020). Thus, the use of lentils (especially in the form of flour) in the food industry has been increasing rapidly with an explosion of novel products (Romano *et al*., 2021), mostly baked goods (Joshi, Timilsena, & Adhikari, 2017; Bourré *et al.*, 2019; Marchini *et al.*, 2021). The successful performances of lentil flour (LF) as a food ingredient are closely related to its mild taste, protein functionality (Joshi *et al.*, 2017) and improved nutritional properties (Marchini *et al.*, 2021). Lentils are known as poor man's' meat, since they are a cheaper source of high-quality proteins (21–31%) containing all the essential amino acids (Romano *et al.*, 2021; Saricaoglu, 2020). In addition, the amino acid profile of LF complements that of wheat flour (WF), since lysine, leucine, aspartic acid, glutamic acid, and arginine are quite high in LF whereas sulphur amino acids are abundant in WF. This implies that the combined consumption of lentils and cereals represents an efficient way to provide well-balanced essential amino acid profiles (Monnet *et al.*, 2019). The addition of LF to wheat-based products may also lead to a reduction in the GI (Fujiwara, Hall, & Jenkins, 2017). This outcome can be related to the peculiar chemical composition of LF such a lower starch content, a higher amylose/amylopectin ratio and a greater soluble fibres content than WF (Turco *et al.*, 2019). Moreover, lentils represent a great source of polyphenols which are known to strongly inhibit α-glucosidase *in vitro* (Di Stefano *et al.*, 2021). In spite of its nutritional benefits, the addition of LF in bread making may also have a detrimental effect on finished products' quality, which may depend on the inclusion level in product formulation. For this reason, WF substitution should be limited to about 30% (Ragaee *et al.*, 2011). In addition, different formulations can produce a huge variety of food structures which may positively or negatively affect nutrients

bioaccessibility and digestibility (Bhattarai, Dhital, & Gidley, 2016). Hence, in the last year there has been a growing interest in developing *in vitro* digestion models able to address differences between food matrices such as, for bread, compact structure, presence of dietary fiber, physical state of starch, or even firmness of the gluten network (if any).

In vitro digestion models mostly fall into two categories: static and dynamic. Between these models, there are "intermediate solutions" also known as semi-dynamic models. These, are cheaper and less complex than the dynamic models, offering, at the same time, certain advantages compared to the static ones. With respect to the latter, semi-dynamic models consider crucial kinetic aspects associated with the gastric phase of digestion, including progressive medium acidification, gradual release of fluids and enzyme solutions and emptying. Besides, they allow for a better simulation of food breakdown during gastric digestion (Mulet-Cabero *et al.*, 2020) stressing the important role of food structure in nutrients bioaccessibility and digestibility.

The present study investigated some physico-chemical, structural, and nutritional properties of bread samples made with 0% (used as control), 10% (10LF) and 20% (20LF) of lentil flour (LF).

Concerning the evaluation of bread digestibility, the combination of different digestion models has been experimented. In fact, each type of bread was subjected to: i) an *in vivo* oral phase; ii) a semi-dynamic *in vitro* gastrointestinal digestion. Then, products of the oral, gastric, and intestinal digestion were subjected to microstructural analysis, evaluation of the total starch residue and free glucose content through enzymatic methods as well as of the protein profile by means of SDS-PAGE.

The combination of these models turned out to be a powerful means to investigate the digestive performances of the bread samples under examination. However, human digestion is a complex multistage process, technically difficult and costly to study. Therefore, there still remain uncertainties about the effects of food structure on the mechanisms of solid food disintegration and nutrients bioaccessibility during digestion.

6.2. Materials and methods

6.2.1. Materials

Commercial wheat flour type "0" (WF), was purchased from a local market in Madrid, Spain.

Lentil (*Lens culinaris Medik.*) flour (LF) was obtained directly from producers (Terre di Altamura, Bari, Apulia, Italy). LF was achieved by grinding the whole green seeds (not decorticated) and then sifted to obtain a particle size < 300 μm.

Nutritional composition (% w/w) of flour samples can be reassumed as follows: WF – carbohydrates 75.0, proteins 9.0, fat 1.2, salt 0.03; LF – carbohydrates 54.0, proteins 25.2, fat 1.9, fibre 5.0, salt < 0.01.

Digestive enzymes: thermostable α-amylase and amyloglucosidase were purchased from Megazyme (Megazyme International, Ireland), pepsin from porcine gastric mucosa, pancreatin from porcine pancreas and bile extract were all obtained from Sigma Aldrich (St Louis, MO, USA). The chemicals used in this study were of analytical grade.

6.2.2. Bread preparation

Trials have been conducted on three kinds of bread: white bread (control) and bread containing 10% (10LF) and 20% (20LF) of green LF, respectively. Bread dough was prepared in 500 g batches and each dough contained the following ingredients: flour (300 g), water (200 mL), fresh compressed yeast (4.2 g), salt (5.2 g) and white sugar (6.0 g). Bread making was carried out with a bread machine (Benco International, Belgium) using the following program: mixing step (30 min at room temperature); resting and leavening (1 hour and 30 min at 35°C); baking (60 min at 180°C). Bread samples were cooled to room temperature prior to analysis.

6.2.3. Loaf physico-chemical and structural properties

Colorimetric indices (L*, a*, b*, ΔE and Chroma) of crumb were measured in controlled conditions with an electronic visual analyzer (IRIS visual analyzer, Alpha MOS, Toulouse, France). Results were the average of three determinations.

The moisture content of crumb was determined by the AACC method (number 44-15.02, 1999). Results were calculated as percentage (%) of water per sample weight (g/100g). Each result is the average of three different bread production runs.

The apparent bread density was obtained from the weight (W) and volume of samples. W was measured using an electronic balance (Mark 3000, EiB, Italy), while bread volume was determined using a modification of the AACC Method 10–05 (AACC, 2010) rapeseed

replacement method using pearled millet instead of rapeseeds. Three replicates were analysed for each sample.

Bread crumb was studied using digital image analysis as previously reported (Raiola *et al.*, 2020). Briefly, samples were cut into 20 mm thick slices using an electric knife. Approximately four slices were taken from the middle of the loaf. 2D loaf slice images were captured with an Olympus® mod. C-7070Wide ZOOM camera (Olympus, Milan, Italy) and then processed by Image tool software: Image Pro Plus 6.1 for Windows® (Media Cybernetics Inc.).

Structural computed parameters were the following:

• number of bubbles counted (n);

• area of the loaf section (A_d);

• bubble area. Samples are characterized and classified by statistical parameters (arithmetic mean and maximum value) of area (avg bubble area and bubble $area_{max}$).

• bubble wall roundness. Roundness calculates circularity of an object and it is equal to 1 when a bubble is a perfect circle (Romano *et al.*, 2013).

• gas bubble area fractions (VF). This parameter was calculated using the following formula:

$$VF\ (\%) = \frac{\sum_i^n A_i}{Ad} \tag{7}$$

Each result is the average of two different bread production runs.

6.2.4. Loaf nutritional characterization

Protein content (%) was determined by elemental analysis using nitrogen to protein conversion 5.4 (Mariotti, Tomé, & Mirand, 2008).

Total starch (TS), free glucose (FG), rapidly digested starch (RDS), slowly digested starch (SDS) and expected Glycemic Index (eGI) were determined by different enzymatic methods. Each measurement was carried out on bread sample after being frozen, freeze-dried, minced by a blender, and sieved to obtain a particle size ≤ 500 μm.

TS was determined using an enzymatic assay kit (Total Starch Assay Kit, Megazyme International Ireland) by AOAC (Official Method 996.11) and AACC (Method 76.13) and determined using the following formula:

$$TS\ (\%) = \frac{\Delta A \text{ x } F \text{ x } Vt \text{ x } 0.9}{Wt} \text{ x } 100 \tag{8}$$

where:

ΔA: absorbance of test solutions, F: factor to convert absorbance values to mg of D-glucose, Vt: total volume of test solutions, 0.9: adjustment from free D-glucose to anhydro D-glucose (as occurs in starch), Wt: sample weight in mg.

FG was measured according to Englyst, Kingman, & Cummings (1992) using an assay kit GOPOD-format K-GLUC (Megazyme International Ireland) and calculated as:

$$FG\ (\%) = \frac{At \times Vt \times C \times D}{As \times Wt} \times 100 \quad (9)$$

where:

At: absorbance of test solutions, Vt: total volume of test solutions, C: concentration (C = 1 mg glucose/mL) of standard, D: dilution factor 18, As: absorbance of standard, Wt: sample weight in mg.

RDS and SDS contents as well as the eGI were determined using an enzymatic assay kit (Resistant Starch Assay Kit, Megazyme International Ireland) by AACC method (number 32–40.01, AACC International Approved Methods of Analysis, 2009) with minor modifications reported by Romano *et al.*, (2016). RDS was the percentage of total starch hydrolyzed within 30 min of incubation in a shaking water bath (200 strokes/min, horizontal agitation) at 37°C (Romano *et al.*, 2016). SDS was the percentage of total starch hydrolyzed within 30 and 120 min of incubation under the same condition. The *in vitro* digestion kinetics were calculated in accordance with the procedure established by Goñi, Garcia-Alonso, & Saura-Calixto (1997). The digestion kinetics were described by means of a non-linear model following the equation 4 (paragraph 5.2.7) while expected eGI was calculated using the equation no. 5 (paragraph 5.2.7).

6.2.5. Simulated gastrointestinal digestion

Simulated digestion tests consisted of two stages: i) an *in vivo* oral phase; ii) a semi dynamic *in vitro* gastrointestinal digestion (Mulet-Cabero *et al.*, 2020). The choice to resort to an *in vivo* mastication and a semi dynamic *in vitro* gastric digestion, results from the evidence that, during digestion, mouth and stomach represent the main sites for food disintegration. In addition, the extent of food breakdown has a great influence not only on nutrients bioaccessibility, but also on the rate of chyme delivery to the small intestine. A schematic representation of the simulated gastrointestinal digestion is shown in Figure 6.1.

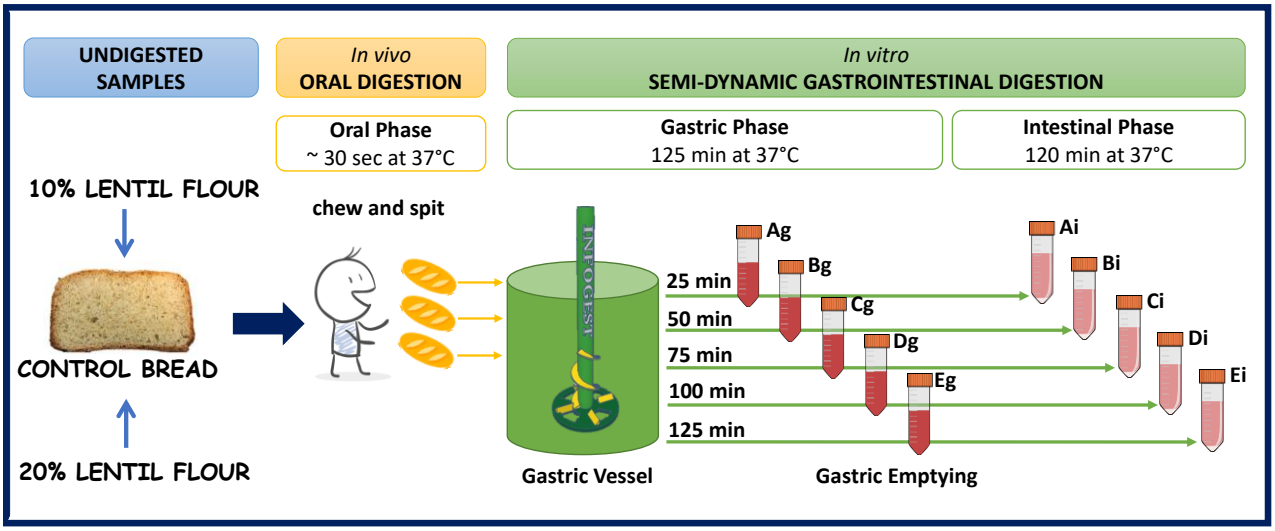

Fig. 6.1. Schematic representation of the simulated gastrointestinal digestion.

6.2.5.1. Oral phase

Mastication was simulated *in vivo*. Briefly, bread samples of approximately 25 g were subjected to "chew and spit" method performed by one volunteer. Food was chewed until the urge to swallow was reached but was expectorated instead and reweighed again (Woolnough *et al.*, 2010). Wickham, Faulks, & Mills (2009) argued that for solid foods, a "chew and spit" method can be more accurate in simulating the oral phase compared to the food grinding. Each sample was placed on ice until use.

6.2.5.2. *In vitro* gastrointestinal digestion

Gastric phase was simulated following the INFOGEST semi-dynamic method (Mulet-Cabero *et al.*, 2020) using a system composed by: a titrator (TritaLab, Radiometer Analytical, Lyon, France) including an attached pH probe and a dosing unit for Simulated Gastric Fluid (SGF), a vessel with thermostat jacket (Metrohm, Spain) connected to a heated circulating bath (JULABO CORIO CD, Italia) and a syringe infusion pump (Cole-Parmer, Vernon Hills, Illinois) for the gradual addition of pepsin solution. Stirring was achieved with an overhead stirrer with a low speed between 10-15 rpm (Hei-TORQUE value 100, Heidolph Instruments, Germany) including paddle stirrer blade specially designed by the INFOGEST network. Table 6.1 summarizes the parameters used in the gastric digestion experiments.

To simulate the fasting state, a basal volume of SGF is transported into the reactor (10% of total gastric secretions). After the introduction of bolus, both the SGF and the pepsin solution started to be injected at a flow rate of 0.27 mL/min and 0.015 mL/min, respectively. The pH of chyme was monitored throughout the entire gastric phase and pH values were registered every 5 minutes. Gastric halftime ($t_{1/2}$) and thus total digestion time is influenced by several factors, including the volume, consistency, and the energy content of the meal (Camilleri, 2006).

Gastric halftime represents the time required by the stomach to empty 50% of the ingested meal (Seok, 2011) and was calculated as described in the paragraph 4.3 (formula no. 1).

Table 6.1. Gastric conditions for the *in vitro* semi-dynamic digestion of bread simulating adult conditions.

Simulated Gastric Fluid (SGF)	SGF volume (mL)	27.45
	HCl (6M) (μL)	200
	0.3 M $CaCl_2(H_2O)_2$ (μL)	19.60
Fasted state/initial conditions	Quantity of food (g)	25.00
	Volume of bolus (mL)	39.21
	Basal SGF volume (mL)	3.92
Gastric conditions (37°C)	T (°C)	37±2
	pH	2-6
	Gastric volume (Food+oral+basal) at t = 0	43.13
	Gastric fluid rate (mL/min)	0.27
	Pepsine solution rate (mL/min)	0.015
	Energy content of meal (kcal)	57.42
	Energy emptying rate (kcal/min)	0.45
	Volume emptying rate (mL/min)	0.34
	$t_{1/2}$ (min)	63.17
	Total digestion time (min)	126.33
Gastric Emptying	Number of emptying steps	5
	Volume to empty (mL)	15.68

The computation of this parameter as well as of the energy and the volume emptying rate is based on the delivery of 2 kcal/min of a food volume of 500 mL based on *in vivo* considerations (Hunt, Smith, & Jiang, 1985). Emptying was performed 5 times by manually taking selected aliquots (approx. 15.68 mL) each 25 minutes from the bottom of the vessel.

The pH of each aliquot was adjusted to 7 with 1M NaOH (to inactivate pepsin and to simulate the environment of the small intestine) and samples were snap-frozen in liquid nitrogen. It

follows that, at the end of the gastric phase we had five samples, one for each emptying time (25 min: Ag; 50 min: Bg; 75 min: Cg; 100 min: Dg; 125 min: Eg) as illustrated in Figure 6.1.
The intestinal phase of digestion was simulated *in vitro* following the INFOGEST static method (Brodkorb *et al.*, 2019). To be specific, approximately 2.5 mL of each digested sample coming from the gastric phase (A_g, B_g, C_g, D_g, E_g) were mixed with 2.5 mL of Simulated Intestinal Fluid (SIF), 10 mM of bile in SIF and pancreatin to achieve a trypsin activity of 100 U/mL (Fig. 6.1). The final volume of each digested sample (A_i, B_i, C_i, D_i, E_i) was approximately of 5 mL. Samples were kept in a shaking incubator at 37°C for 120 min, after that the intestinal phase was stopped by heating at 85°C for 15 min. Samples were stored at − 20°C until analysis.

6.2.6. Scanning Electron Microscopy (SEM) analysis

Bread samples before digestion and after oral (bolus) and intestinal phases (E_i) were lyophilized, dried at the critical point, and coated with gold particles. Microstructure was examined by means of Scanning Electron Microscopy (LEO EVO 40 SEM, Zeiss, Germany) with a 20 kV acceleration voltage and a magnification of ×1500.

6.2.7. Changes in free glucose (FG) and total starch (TS) content during digestion

FG and TS content were analyzed according to the methods described in the previous section (6.2.4). In this case, TS content may reasonably associate to the starch fraction resistant to the digestion process and indicated as TS*. These parameters were calculated for all samples (control, 10LF and 20LF) at each stage of digestion and at selected time points: i) at the end of the oral phase (bolus); ii) during the gastric phase (A_g, B_g, C_g, D_g, E_g); iii) during the intestinal phase
(A_i, B_i, C_i, D_i, E_i). Results were the average of three determinations.

6.2.8. Sodium dodecyl sulfate-polyacrylamide gel electrophoresis

The evaluation of the protein profile has been performed on samples after the oral (bolus), gastric (A_g, B_g, C_g, D_g, E_g) and intestinal phase (A_i, B_i, C_i, D_i, E_i) by means of sodium dodecyl sulfate-polyacrylamide gel electrophoresis (SDS-PAGE) employing a 150 g/L acrylamide separating gel. Samples were normalized according to the protein content (4 mg/mL) and then dissolved in sample buffer (Tris-HCl 0.05 M, pH = 6.8) containing 2% of 2-mercaptoethanol. Electrophoresis

was conducted for 1 h at a constant voltage of 150 V. Subsequently, gels were stained with 0.5 mg/mL Coomassie brilliant blue-R250. The 2-D gels were scanned with a Versa-Doc image system (Bio-Rad).

6.2.9. Statistical analysis

All the parameters were expressed as mean value ± standard deviation. Statistical analysis was performed using SPSS version 19.0 (SSPS Inc., Chicago, IL, USA). One way ANOVA with Duncan's test at a significance level of 0.05 were performed to evaluate differences i) among the undigested bread samples ii) among bread samples under the same digestion stage and iii) for each bread sample throughout the digestion process.

6.3. Results and discussion

6.3.1. Loaf physico-chemical and structural properties

Colorimetric indices (L*, a*, b*, ΔE and Chroma) of control and breads containing 10% (10LF) and 20% (20LF) of LF are presented in Table 6.2.

Table 6.2. Colorimetric indices, moisture content, density and crumb structural parameters of bread samples made with 0% (control), 10% (10LF) and 20% (20LF) of lentil flour (LF). Each value is expressed as mean ± SD.

Parameter	control	10LF	20LF
L* (crumb)	$70.37 \pm 1.7_{b}$	$67.22 \pm 4.6_{b}$	$46.10 \pm 3.1_{a}$
a* (crumb)	$9.68 \pm 0.8_{b}$	$10.75 \pm 0.8_{b}$	$7.52 \pm 0.5_{a}$
b* (crumb)	$39.93 \pm 1.3_{b}$	$40.63 \pm 0.4_{b}$	$29.52 \pm 1.9_{a}$
ΔE (crumb)	$50.67 \pm 1.9_{a}$	$53.39 \pm 2.6_{a}$	$61.95 \pm 2.5_{b}$
Chroma (crumb)	$41.09 \pm 1.4_{b}$	$42.03 \pm 0.2_{b}$	$30.47 \pm 1.8_{a}$
Moisture content (%)	$43.16 \pm 0.23_{a}$	$43.77 \pm 0.64_{a}$	$43.34 \pm 0.78_{a}$
density (g/mL)	$0.275 \pm 0.01_{a}$	$0.289 \pm 0.02_{b}$	$0.294 \pm 0.02_{b}$
avg bubble area (cm^2)	$0.03 \pm 0.0_{a}$	$0.04 \pm 0.0_{a}$	$0.07 \pm 0.0_{b}$
bubble $area_{max}$ (cm^2)	$0.38 \pm 0.02_{a}$	$0.36 \pm 0.06_{a}$	$0.52 \pm 0.08_{b}$
roundness	$1.37 \pm 0.1_{a,b}$	$1.33 \pm 0.0_{a}$	$1.42 \pm 0.0_{b}$
n/Ad	$8.89 \pm 0.9_{b}$	$7.36 \pm 0.9_{b}$	$4.15 \pm 1.2_{a}$
AF (%)	$30.74 \pm 0.6_{b}$	$27.22 \pm 1.8_{a}$	$27.41 \pm 1.2_{a}$

[a-c] Different letters in the same row indicate significant differences ($P < 0.05$).
Crumb structure parameters: n, number of bubbles counted; Ad, area loaf section; AF, gas bubble area fraction.

Results for colorimetric parameters indicate that no significant differences ($P > 0.05$) were found between control and 10LF samples (Table 6.2). In contrast, significant color changes ($P < 0.05$) were observed for 20LF bread samples. Specifically, L*, a* and b* values were significantly lower ($P < 0.05$) for 20LF than for the other bread samples, indicating a darker appearance as well as an increase in crumb greenness and blueness. Besides, 20LF showed the highest ΔE and the lowest Chroma ($P < 0.05$) with respect to control and 10LF.

In Table 6.2, moisture content, density, bubble macrostructure parameters of all bread loaves are also reported. The mean crumb moisture values were similar ($P > 0.05$) for all the samples, ranging from 43.2 to 43.8%.

Bread density significantly increased ($P < 0.05$) when WF was replaced with LF, varying from 0.28 ± 0.01 g/mL for control to 0.29 ± 0.02 g/mL for 10LF and 20LF samples. This means that bread containing LF had a denser and more compact structure compared to the control. It was probably due to the introduction of non-gluten proteins and fibre which may weaken the gluten network, thus negatively affecting gas holding capacity and specific volume of bread as described by Hsieh *et al.* (2017). Furthermore, these findings are in good agreement with Cavella *et al.* (2008) which stated that fibre may destabilize the interface between gas bubbles, thus limiting dough expansion.

The effect of replacement of WF with LF on macrostructural properties of samples was evident in Figure 6.2.

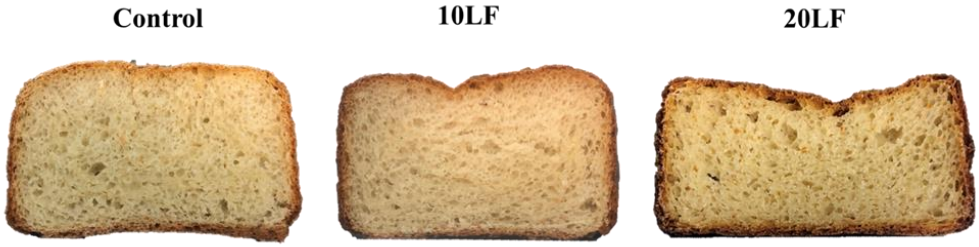

Fig. 6.2. Representative images of bread samples made with 0% (control), 10% (10LF) and 20% (20LF) of lentil flour (LF).

From a structural point of view, bread crumb is a solid foam characterized by a high porosity, also classified as a cellular solid (Keetels, van Vliet, & Walstra, 1996; Raiola *et al.*, 2020). The average bubble area as well as the bubble $area_{max}$ were significantly higher ($P < 0.05$) in 20LF bread, while no significant differences ($P > 0.05$) were found between control and 10LF bread. This probably resulted

from a weak dough structure and thus from the coalescence of individual gas cells (Le Bleis *et al.*, 2015). Furthermore, bubbles in 20LF bread showed the highest roundness ($P < 0.05$), indicating that the bubbles were less circular and therefore more irregular than the other bread samples. This may be due to the higher compactness of 20LF bread which resulted in lightly flattened bubbles.

As regards the n/Ad parameter, where n was the number of bubbles counted and Ad was the loaf section area, it was observed that the smallest number of bubbles per unit area was found in 20LF samples.

VF (gas bubble area fraction) in control bread had a mean value of 30.74 ± 0.58%, which was significantly higher ($P < 0.05$) than samples containing LF (10% and 20%). The reduction of this parameter with increasing of LF concentration suggests that the substitution of WF with LF led to a dilution of the gluten network, negatively affecting its ability to retain the carbon dioxide produced during the fermentation phase.

6.3.2. Protein and starch characterisation

Initial amounts of proteins, TS, FG, RDS, SDS and eGI are reported in Table 6.3.

Table 6.3. Nutritional composition of bread samples made with 0% (control), 10% (10LF) and 20% (20LF) of lentil flour (LF). Each value is expressed as mean ± SD.

Bread samples	Protein (%)	TS (g/100g)	FG (%)	RDS (%)	SDS (%)	eGI (%)
control	$9.69 \pm 0.2_a$	$69.33 \pm 1.5_c$	$3.10 \pm 0.4_a$	$34.71 \pm 1.3_a$	$31.83 \pm 1.9_c$	$100.14 \pm 0.4_a$
10LF	$10.29 \pm 0.5_b$	$63.83 \pm 0.7_b$	$5.36 \pm 0.4_b$	$45.81 \pm 0.1_b$	$16.94 \pm 1.3_b$	$106.16 \pm 0.2_b$
20LF	$12.42 \pm 0.1_c$	$61.75 \pm 0.2_a$	$9.03 \pm 0.3_c$	$48.02 \pm 0.0_c$	$13.61 \pm 0.2_a$	$110.64 \pm 0.2_c$

[a-c] Different letters in the same column indicate significant differences ($P < 0.05$).
TS, total starch; FG, free glucose; RDS, rapidly digestible starch; SDS, slowly digestible starch; eGI, expected Glycemic Index.

As expected, protein content significantly increased ($P < 0.05$) with the increase of LF content, ranging from 9.69 ± 0.2% (control bread) to 12.42 ± 0.1% (20LF bread). This was due to the higher protein content of LF (25.2%) than WF (9.0%).

On the other hand, control bread showed the highest TS (69.33 ± 1.5%) and the lowest FG content (61.75 ± 0.2%), reflecting the composition of relevant raw material. As can be seen from Table 6.3, TS content significantly decreased ($P < 0.05$) while FG significantly increased ($P < 0.05$) as LF concentration rises.

Moreover, the *in vitro* starch digestion was investigated by measuring the released glucose content during starch digestion using an enzymatic method with minor modifications (Romano *et al.*, 2016). Fig. 6.3 reports the hydrolysis curves of the three types of bread under examination.

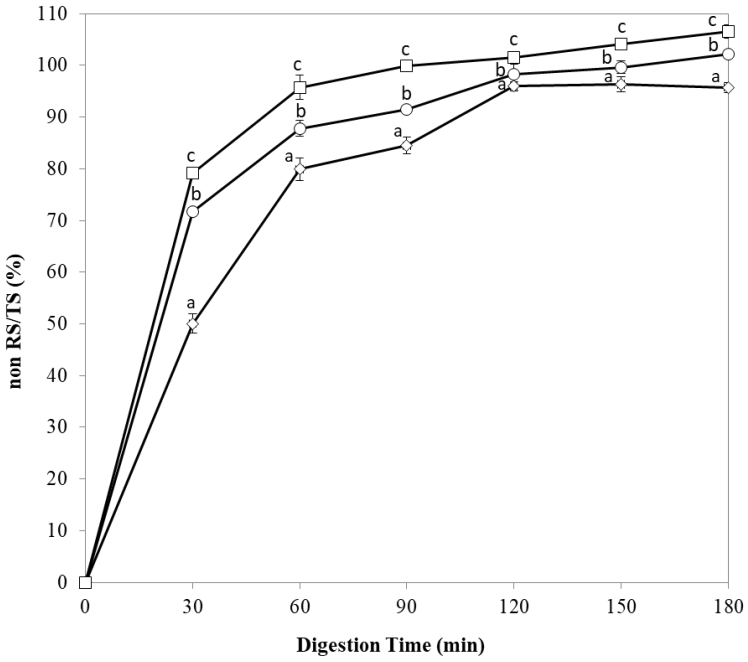

Fig. 6.3. Starch digestibility profiles of bread containing 0% (◊), 10% (○) and 20% (□) of lentil flour. (a-c) indicate statistically significant differences between samples at each digestion time ($P < 0.05$).

Samples showed a different starch hydrolysis kinetics which significantly incremented ($P < 0.05$) with increasing of LF concentration. Overall, it was observed a rapid rise in starch hydrolysis within the first 30 min, and then the percentage of digested starch increased gradually for the additional 150 min. In detail, as reported in Table 6.3, 20LF samples had the highest RDS content and eGI ($P < 0.05$) followed by 10LF and control, respectively. RDS is the starch fraction that is rapidly and totally digested in the gastrointestinal tract and it is associated with fast elevation of postprandial plasma glucose (Gallo, Romano, & Masi, 2020). This parameter was significantly lower ($P < 0.05$) for control and higher for 20LF samples, ranging from 34.71 ± 1.3% and 48.02 ± 0.0%. Unlike SDS, that is the starch fraction which is slowly digested in the gastrointestinal tract, significantly decreased ($P < 0.05$) with the increase of LF content, ranging from 13.61 ± 0.2% for 20LF and 31.83 ± 1.9% for the control. These results were quite unexpected, since the addition of legume flour in cereal-based products usually leads to a reduction in the eGI (Romano *et al.*, 2021; Fujiwara *et al.*, 2017). The

increase in starch hydrolysis with increase of LF content could be related to a concentration effect due to bran removal by sieving (Li, Zhang, & Dhital, 2019). In fact, it has been demonstrated that cell integrity and the degree of refining, significantly affect flour composition (ash, protein, and starch content), nutrients bioaccessibility and thus the functional properties of legumes flours (Boukid *et al.*, 2019). Specifically, some in *vitro* studies showed that finely milled flours led to a higher starch hydrolysis than coarse flours (Bhattarai *et al.*, 2016). Moreover, according to Fardet *et al.* (2006), the presence of a strong gluten network around the starch granules may protect them from digestion, hindering amylase to easily access the granule and leading to slow starch hydrolysis. This is supported by some studies (Jenkins *et al.*, 1987; Packer, Dornhorst, & Frost, 2000; Berti *et al.*, 2004; Lin *et al.*, 2020) who reported significantly higher glycaemic response for gluten-free bread than the common one. These results are also confirmed by the true association between celiac disease and type 1 diabetes (Leonard, Cureton, & Fasano, 2015). On the contrary, other studies have yielded conflicting results, demonstrating that gluten-free products produce lower glycemic responses than their regular gluten-containing counterparts. According to Scazzina *et al.*, 2015, these findings can be attributed to the novel use of ingredients such as fibre (e.g., psyllium fibre, guar gum and hydroxypropylmethylcellulose) known for delaying gastric emptying thus reducing postprandial glycaemic response.

6.3.3. In *vitro* digestion

6.3.3.1. Semi-dynamic digestion pH curve

Fig. 6.4 shows the pH trends during the *in vitro* gastric digestion trials performed for each bread sample with a progressive medium acidification. To work under standard conditions, the volume of 6 M HCl added to the SGF was previously calculated for the control and was always the same in all the experiments (200 μL) (Table 6.1).

As one can see from Fig. 6.4, the reduction in pH during gastric digestion was more pronounced for the control while it was less marked with the rise of LF concentration. In fact, the pH value reached by the samples at the end of gastric digestion was significantly lower ($P < 0.05$) for the control than the other samples, ranging from 2.25 ± 0.11 for control to 3.47 ± 0.18 for 20LF samples. These findings suggest a higher protein hydrolysis for samples containing the highest amount of LF (20LF), followed by 10LF and control bread, respectively. In fact, the pH increase

can be linked to the free amino acid carboxyl groups from the protein chain released by the pepsin during digestion (Mulet-Cabero *et al.*, 2020). Meanwhile, the higher pH values observed for 10LF and 20LF may reflect i) the protons consumption by the amino groups of the peptides produced (Mat *et al.*, 2018) and ii) the different aminoacidic composition of wheat and lentil proteins. In fact, it is well known that lentil proteins are quite rich in basic amino acid such as lysine and arginine (Foschia *et al.*, 2017; Joshi *et al.*, 2017). On the other hand, an early study found that milling wheat to flour may reduce the concentration of some basic amino acids such as lysine, arginine, and histidine (Shoup, Pomeranz, & Deyoe, 1996).

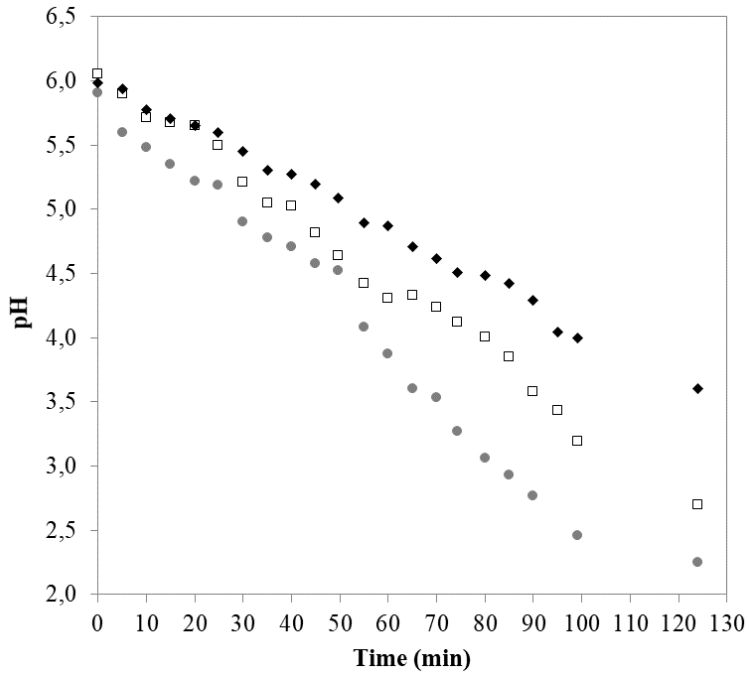

Fig. 6.4. pH trend measured in the digestion vessel during the *in vitro* gastric digestion of bread containing 0% (●), 10% (□) and 20% (♦) of lentil flour.

From the results, we can reasonably conclude that the pH tracing may be a useful method to predict and study the evolution of protein hydrolysis during gastric digestion.

6.3.3.2. Microstructural analysis: Scanning Electron Microscopy (SEM)

Microstructural properties of bread samples have been examined by means of SEM before digestion and after the oral (bolus) and intestinal (E_i) phase of digestion (6.5).

As regards the undigested bread samples (6.5a - c. Panel A), only slight differences have been found between control bread (6.5a), 10LF (6.5b), and 20LF samples (6.5c). In particular, control bread (6.5a) seems to possess the most developed protein network with the smaller number of cavity due to a strong dough structure.

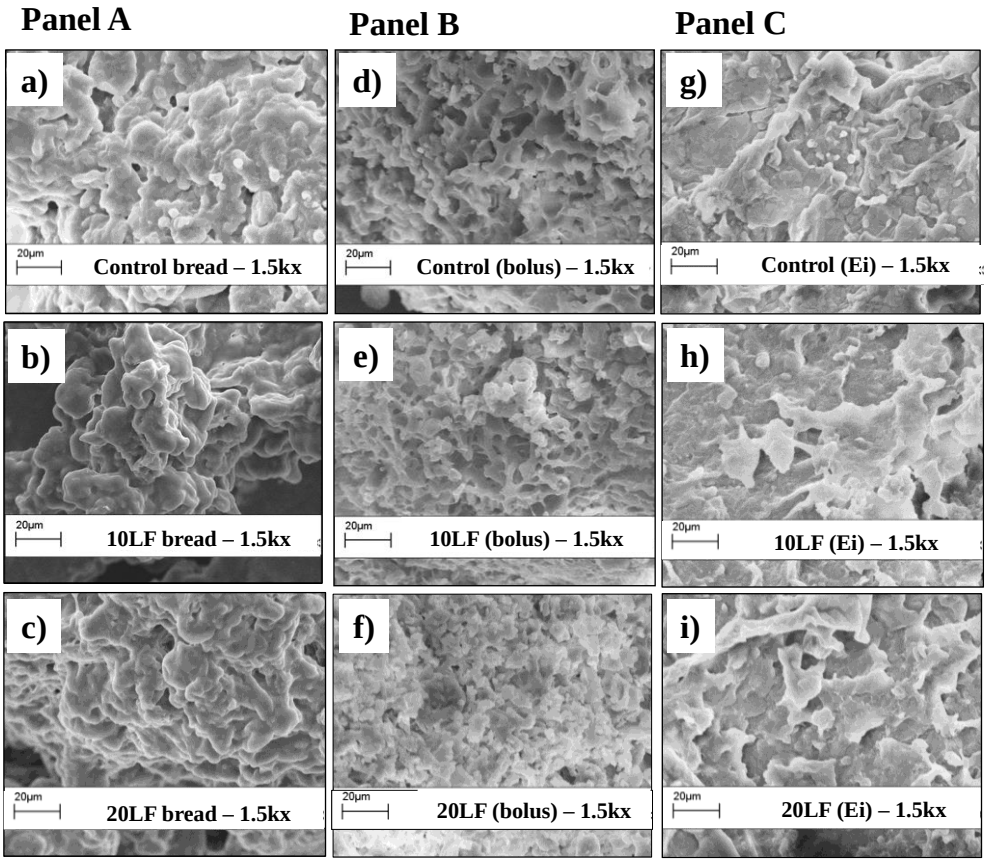

Fig. 6.5. Scanning electron micrographs of control, 10LF and 20LF bread samples before and after oral (bolus) and intestinal (Ei) digestion: **Panel A:** undigested samples: a) control; b) 10LF; c) 20LF. **Panel B:** bolus: d) control; e) 10LF; f) 20LF. **Panel C:** intestinal digests: g) control; h) 10LF; i) 20LF.

The *in vivo* oral digestion had a marked effect on bolus samples (6.5d - f. Panel B), which lost their cohesive structure, showing a porous, sponge-like microstructure. Specifically, control bolus (6.5d) showed a well-developed gluten network with little visible starch granules. On the other hand, the increase in LF concentration resulted in a heterogeneous structure with the presence of more intact and isolated starch granules (6.5e, f). The higher fragmentation with increasing LF content could be explained by the presence of higher amounts of fibre and non-gluten proteins in 20LF bread followed by 10LF and control, respectively. In fact, this induced a

disruption of the gluten network, leading to a weakening of the structure, as previously described by Jourdren *et al.*, 2016.

Finally, no evident differences have been found between the microstructure of control, 10LF and 20LF bread samples taken at the end of the intestinal (E_i) phase (6.5g - i. Panel C) in accordance with the residual starch determination. In fact, as will be discussed in the next paragraph, the starch fraction resistant to the intestinal digestion was extremely low (Fig. 6.6c).

6.3.3.3. Changes in TS and FG content during digestion

The mechanical breakdown of bread matrix during mastication led to a progressive release of starch, thus enhancing its exposure to the digestive enzymes.

Fig. 6.6a, b, c showed the starch fraction resistant to the digestion process (TS*) measured at each digestion stage.

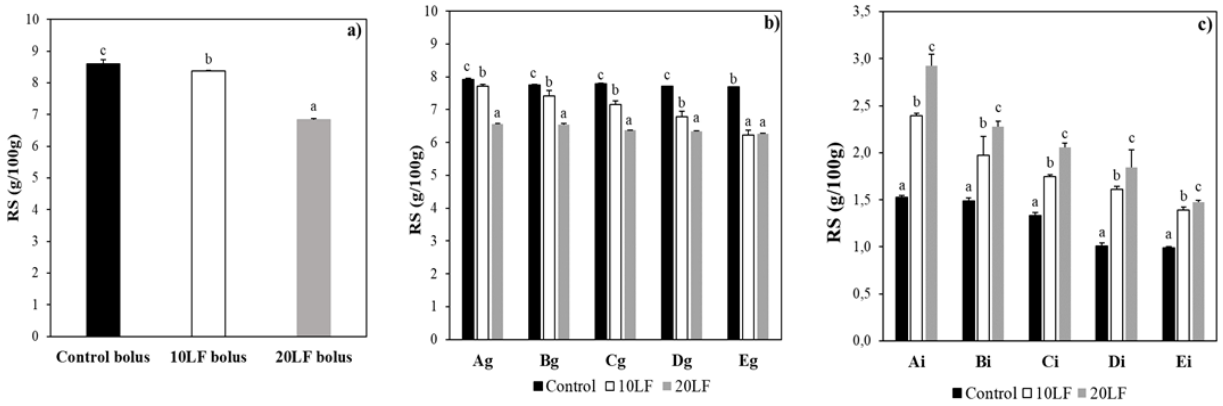

Fig. 6.6. Resistant starch content (g/100g) of bread samples made with 0% (control), 10% (10LF) and 20% (20LF) of lentil flour (LF) during digestion: a) oral (bolus); b) gastric digests (A_g, B_g, C_g, D_g, E_g); c) intestinal digests (A_i, B_i, C_i, D_i, E_i).

[a-c] For each digested sample, means with different letters are significantly different ($P < 0.05$).

Regarding the oral phase (Fig. 6.6a), TS* content decreased significantly ($P < 0.05$) with the increase of LF concentration, ranging from 8.59 ± 0.14% for the control to 6.83 ± 0.04% for 20LF samples. This result can be explained by the initial TS content (Table 6.3) which was higher in the control bread as well as by the bolus structure (6.5d - f) which was more compact for the control, making the starch granules less accessible to salivary α-amylase. The higher starch digestibility with rising LF addition was also confirmed by the release of higher amount of FG in 20LF and 10LF bolus, respectively (Fig. 6a).

As showed in Figure 6.6b, the same trend observed in the oral phase was maintained during the gastric phase of digestion. Overall, for all samples (control, 10LF and 20LF) there was a slow but significant reduction ($P < 0.05$) in the TS* content with increasing of the digestion time, ranging from 7.92 ± 0.04% (A_g) to 7.69 ± 0.01% (E_g) for control, from 7.72 ± 0.04% (A_g) to 6.22 ± 0.15% (E_g) for 10LF and from 6.56 ± 0.01% (A_g) to 6.26 ± 0.03% (E_g) for 20LF. Salivary α-amylase is inactivated in the stomach at low pH and thus its role on starch hydrolysis during gastric digestion is often ignored. By contrast, the present study show that amylase activity also continued at the gastric conditions. Our findings are in accordance with several other studies (Bustos *et al.*, 2017; Bhattarai *et al.*, 2016; Butterworth, Warren, & Ellis, 2011) which also found that the activity of amylase can be protected from gastric inactivation by other food components such as proteins, starch, and oligosaccharides. As showed previously (Fig. 6.4), the reduction in pH during the gastric phase of digestion was less pronounced with the increasing of LF concentration and this could have promoted amylase activity in 10LF and 20LF bread.

Concerning the intestinal phase (Fig. 6.6c), TS* content significantly increased ($P < 0.05$) with raising LF substitution level while, for each bread sample, significantly decreased ($P < 0.05$) with increasing digestion time. In fact, the starch fraction resistant to digestion was higher for 20LF (A_i: 2.93 ± 0.12% - E_i: 1.48 ± 0.02%) followed by 10LF (A_i: 2.39 ± 0.02% – E_i: 1.39 ± 0.03%) and control (A_i: 1.53 ± 0.01% – E_i: 0.99 ± 0.02%).

Maltose and glucose are the main products of the oral starch hydrolysis and are gradually released in the liquid phase of bolus during mastication. In this study, the release of FG has been determined for all samples at each digestion stage (Fig. 6.7a, b, c). Concerning the oral digestion (Fig. 6.7a), the release of FG was stronger ($P < 0.05$) with the increase in LF concentration, ranging from 20.06 ± 0.85% (control) to 28.54 ± 0.3% (20LF).

Our results are consistent with Jourdren *et al.*, (2016) which found a highest release of glucose during the *in vivo* oral digestion of whole wheat bread than common white bread.

Findings for the gastric phase of digestion (Fig. 6.7b) suggest a greater ($P < 0.05$) starch hydrolysis for 20LF samples, followed by 10LF and control bread. In fact, FG content varied from 23.45 ± 0.59% (A_g) to 41.61 ± 0.20% (E_g) for the control, from 28.52 ± 0.53% (A_g) to 38.54 ± 0.32% (E_g) for 10LF and from 33.36 ± 0.81% (A_g) to 42.95 ± 0.25% (E_g) for 20LF.

During the intestinal phase (Fig. 6.7c), the trend was reverse. In detail, FG content significantly decreased ($P < 0.05$) with increasing LF concentration but, for each sample, significantly increased ($P < 0.05$) as digestion time progressed.

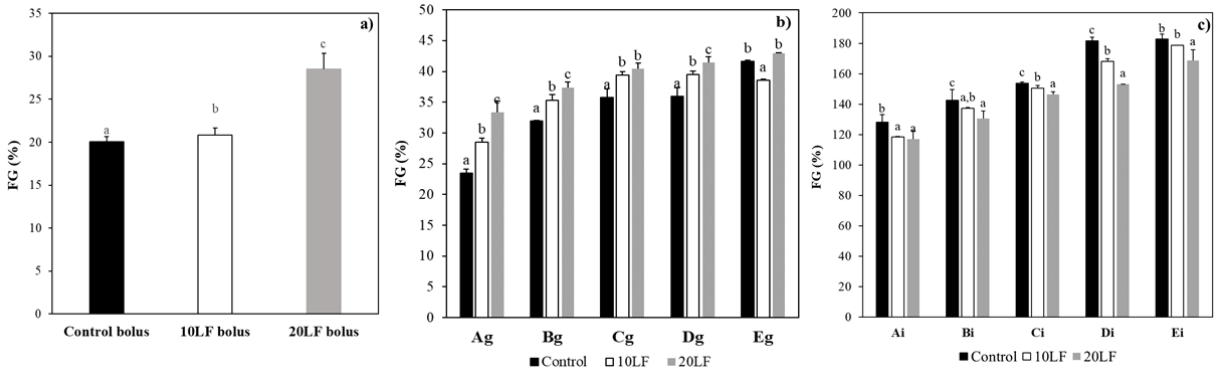

Fig. 6.7. Free glucose content (%) of bread samples made with 0% (control), 10% (10LF) and 20% (20LF) of lentil flour (LF) during digestion: a) oral (bolus); b) gastric digests (A_g, B_g, C_g, D_g, E_g); c) intestinal digests (A_i, B_i, C_i, D_i, E_i).

[a-c] For each digested sample, means with different letters are significantly different ($P < 0.05$).

Specifically, FG varied from 128.26 ± 4.74% (A_i) to 182.66 ± 3.24% (E_i) for the control, from 118.31 ± 0.43% (A_i) to 178.71 ± 0.10% (E_i) for 10LF and from 117.10 ± 5.55% (A_i) to 168.72 ± 7.10% (E_i) for 20LF. These achievements were in good agreement with the determination of TS* content and indicate higher amount of slow digestible starch in control bread than in 10LF and 20LF samples, respectively.

6.3.3.4. Protein profile by SDS-PAGE

The analysis of protein profile during digestion is shown on representative gels (Fig. 6.8a, b). Concerning the oral phase (Fig. 6.8a), SDS-PAGE clearly showed bands corresponding to gluten components (high molecular weight glutenins (HMW-GS) at 65–90 kDa, ω-gliadins at 44–70 kDa, low molecular weight glutenins (LMW-GS) at 30–40 kDa and α-/β-/γ-gliadins at 30–45 kDa, albumins and globulins at 13-17 kDa. Furthermore, changes in the intensity and number of bands are also evident among samples. In lanes 7 and 13 (Fig. 6.8a), bands corresponding to gluten components were accompanied by LF protein bands such as convicilin (70 kDa), legumin fragments (20 kDa) and vicilin component (14 kDa).

In the case of control bread, intact proteins such as HMW-GS and ω-gliadin started to disappear after the first 75 min (line 3) of gastric digestion. The visible intact band at approximately 37

kDa can be attributed to pepsin from porcine gastric mucosa which has a molecular weight of 34.6 kDa. 10LF and 20LF showed bands of intact proteins at all gastric times. Specifically, for 10LF samples high molecular weight proteins (60-90 kDa) started to disappear after the first 75 min (line 10) of digestion while the electrophoretic bands under 15 kDa became more intense since they correspond to the degradation products. SDS-PAGE demonstrates minimal digestion of legume proteins (*e.g.*, legumin fragments at 20 kDa) whose bands were clearly persistent until the end of gastric digestion.

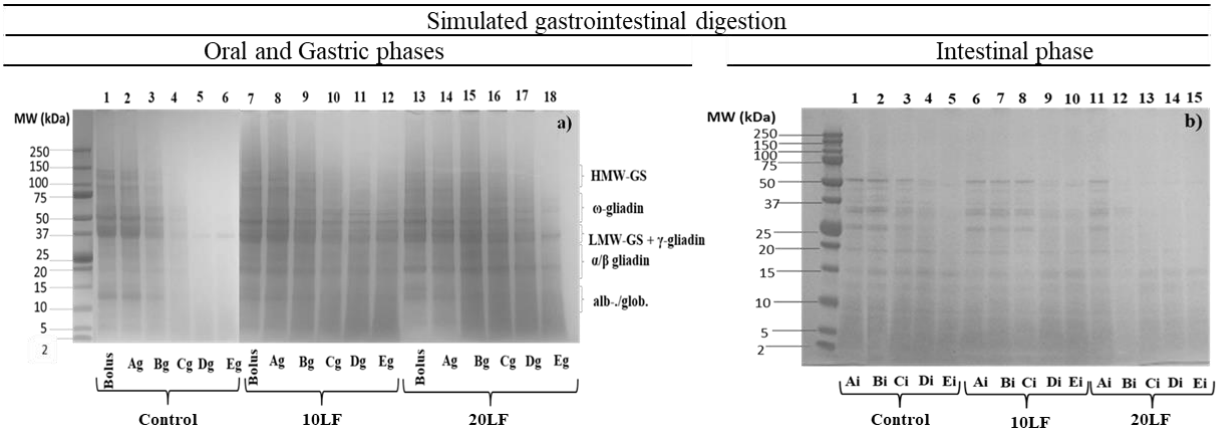

Fig. 6.8. SDS-PAGE protein profile of bread samples made with 0% (control), and with 10% (10LF) and 20% (20LF) of lentil flour (LF) at different stages of a) *in vivo* oral digestion (bolus) and *in vitro* semi-dynamic gastric digestion (A_g, B_g, C_g, D_g, E_g) and b) *in vitro* static intestinal digestion (A_i, B_i, C_i, D_i, E_i). HMW-GS, high molecular weight glutenins; LMW-GS, low molecular weight glutenins.
Lane numbers represent samples from different steps of the digestion process. MW = molecular marker.

Lastly, 20LF samples showed higher resistance to the proteolysis with the presence of intact bands at all time points except the last one (E_g). The reduction in protein digestibility with the increase of LF concentration, can be attributed both to the higher protein content and to the lower pepsin activity caused by a less pronounced pH decrease (Fig. 6.4).

Protein patterns of intestinal digests (A_i, B_i, C_i, D_i, E_i) of all samples by SDS-PAGE are shown in Fig. 6.8b. During the intestinal digestion, gluten was readily hydrolyzed into low molecular weight peptides with few intact protein bands visible. In detail, as can be noted from Fig. 6.8b, bands under 10 kDa seemed to be more pronounced in the control and 10LF samples compared to 20LF. These bands may be attributed to the degradation products (electrophoretic bands under 15 kDa) as well as to the digestive enzymes such as trypsin, chymotrypsin, and lipase (electrophoretic bands between 20 and 50 kDa) in accordance with Santos-Hernández *et al.*,

(2020) and Ogilvie *et al.*, (2020). Probably, SDS-PAGE is not a very useful tool to follow the rate of protein digestion in such complex matrices and thus further analysis performed using more quantitative methods would have been necessary.

Chapter 7

Properties and *in vitro* digestibility of a bread enriched with lentil flour at different leavening times

Abstract

The effects of three leavening times (60, 105 and 150 minutes) on structure and some physico-chemical and nutritional properties of bread enriched with 20% of green lentil flour (LF) were investigated. The LF dough has been characterized by means of farinographic properties and pH values. A positive correlation between crumb macrostructural and mechanical properties has been observed (R^2 = 0.772). Specifically, crumb of bread leavened for the longest time (B150) showed the most compact structure and the highest resistance to the compression while Young's modulus raised linearly as leavening time increased. By contrast, bread samples leavened for shorter times (B60 and B105) showed a more porous structure with more circular bubbles compared to B150, exhibiting lower deformation resistance. These outcomes were also confirmed by microstructural findings.

Different bread macrostructure (B60, B105 and B150) had a significant impact on the *in vitro* starch digestibility, while no differences were noted between samples in terms of protein *in vitro* digestibility. In particular, the expected Glycemic Index (eGI), evaluated by enzymatic methods was significantly lower for B150 probably because of its compact structure which hindered the accessibility of starch granules to the amylase. In fact, eGI showed a linear correlation both with the Young's modulus (R^2 = 0.926) and macrostructural properties (R^2 = 0.902), suggesting that modelling bread structure by acting on leavening time can be a novel approach to develop healthier products.

7.1. Introduction

Bread represents a staple part of the Mediterranean diet (Arora *et al.*, 2021) with a complex structure and a high Glycemic Index (GI) in general. Bread physical structure was identified as one of the most important factors determining the GI, implying that the higher porous structure, the higher the GI (Lin *et al.*, 2020). Crumb structure can be defined as a two-phase soft cellular solid, formed by a solid phase consisting of the cell wall structure and a liquid phase made up of air (Scanlon & Zghal, 2001). Such sponge-like crumb structure (Dahiya *et al.*, 2020) is developed during the phase of mixing, leavening and thermal setting (baking) (Zhou & Hui, 2014). The most macroscopic variation related to the development of leavening in the dough is the increase of its volume (Romano *et al*., 2013; Campagna *et al.*, 2020). In fact, during leavening, carbon dioxide generated inside the dough, allows the product to rise (Romano, 2020), producing a porous structure and reducing dough density. A typical curve of dough volume expansion is characterized by a lag, a growth, a stationary and a collapse phase (Romano *et al.*, 2007). The duration of each phase and volume expansion ratio were strictly dependent on dough viscoelasticity (Rathnayake, Navaratne, & Navaratne, 2018), on the type and the amount of yeast used (Holmes *et al.*, 2020; Romano *et al.* 2007) as well as on the raw materials characteristics (Verdú *et al.*, 2015). In the case of bread making, dough preparation has a significant effect on porous structure and quality of the end product. Besides, the control of processing conditions has been proved to be an effective way in manipulating the structure formation (Besbes *et al.*, 2013; Gao *et al.*, 2017a; 2017b; 2017c) and influencing bread digestion. In the literature, there are several proposed strategies to reduce the GI of high digestible products (Borczak *et al.*, 2018). The most notable of these are: i) the incorporation of different raw materials into white bread; ii) changes in bread physical structure. Most of the attention has been focused on reformulations using low GI ingredients, such as whole wheat flour or legumes flour (Gallo, Romano, & Masi, 2020; Di Stefano *et al.*, 2021).

Typically, bread is made with wheat flour, *S. cerevisiae* yeast strain (Siepmann *et al.*, 2018; Ali *et al.*, 2012), salt and water (Raheem, Liu, & Li, 2019) to obtain doughs that are leavened inside a leavening chamber, where both temperature and relative humidity are regulated. But in recent years food companies are constantly seeking unconventional ingredients such as lentil flour (LF) to meet consumer demand for healthier foods (Boukid *et al.*, 2020; Marchini *et al.*, 2020). LF has been recently used as highly nutrition ingredient in bakery products (bread, cake, crackers),

offering a wide range of functionalities as well as textural and nutritional benefits (Bresciani & Marti, 2019; Monnet *et al.*, 2019; Romano *et al.*, 2021), mostly depending on flour substitution level (Bresciani & Marti, 2019; Monnet *et al.*, 2019). In fact, from a nutritional point of view, the addition of high level (20–30%) of pulse flour may increase protein and dietary fibre content as well as lower bread's GI (Portman *et al.*, 2018; Ficco *et al.*, 2018). In the specific case of LF, the enrichment of focaccia bread with 16% of split green LF proved to reduce its GI both *in vitro* and *in vivo* (Fujiwara, Hall, & Jenkins, 2017). Besides, blending wheat flour with LF up to 24% has been found to produce bread with acceptable loaf volume and the organoleptic features (Turfani *et al.*, 2017).

To the best of the author knowledge, the control of bread structure as one of the options to influence bread digestion has rarely been attempted so far and there are very few studies in the literature that cover the effects of leavening time on the technological and nutritional properties of bread.

Thus, the aim of this work was to investigate the relationships between structure imparted by leavening phase (time) and some properties (physico-chemical, textural, and nutritional) of bread enriched with 20% of LF from green lentils. In this study, three leavening times (60, 105 and 150 min) were selected.

7.2. Materials and methods

7.2.1. Materials

Commercial wheat flour type "00" (WF) (Mulino Caputo, Naples, Italy) and green lentil flour (LF) from Altamura PGI (Terre di Altamura, Bari, Apulia, Italy) were obtained directly from producers. LF was achieved by grinding the whole green seeds (not decorticated) and then sifted to obtain a particle size < 300 μm.

Nutritional composition (% w/w) of flour samples can be reassumed as follows: WF – carbohydrates 70.0, proteins 13.0, fibre 3.0, fat 1.5, salt < 0.02; LF – carbohydrates 54.0, proteins 25.2, fibre 5.0, fat 1.9, salt < 0.01.

Digestive enzymes: thermostable α-amylase and amyloglucosidase were purchased from Megazyme (Megazyme International Ireland). Pepsin from porcine gastric mucosa, pancreatin from porcine pancreas and bile extract were all obtained from Sigma Aldrich (St Louis, MO, USA) in line with those indicated by the INFOGEST protocol.

7.2.2. Dough analyses

7.2.2.1. Farinographic analysis

Farinograph characteristics of the flour blend (80% WF - 20% LF) dough were studied by using a Brabender farinograph (Type AT, Brabender OHG, Duisburg, Germany), fitted with a 50 g mixing bowl. Then, the following parameters were determined: water absorption (WA, percentage of water required to reach a standard dough consistency of 500 Brabender Units), dough development time (DDT, time to achieve peak consistency), stability (DS, time dough consistency remains at the desired consistency) and degree of softening (DOS, difference in height between the centre of the graph at maximum resistance to mixing and the centre of the graph at a point 12 minutes later). Results were the average of three Farinograph tests.

7.2.2.2 pH

pH values of doughs after mixing and leavening phases were measured using a calibrated digital pH meter (XS instruments pH-8, Carpi, Italy). Each average value represents the mean of three independent measurements.

7.2.3. Bread preparation

All the experimental tests have been conducted on bread enriched with 20% of LF. Dough was prepared using the following ingredients: WF (48.61%), green LF (12.15%), water (36.90%), fresh compressed yeast (1.21%) and salt (1.13%). All the ingredients were mixed for 15 min by using a spiral kneader (IM5-230 Grilletta, FA.M.A.G. S.r.l., Monteforte, Italy). Then, dough pieces (600 g) were placed into three aluminum molds (27.5 x 14 x 7 cm) and leavened for three selected leavening times: 60 (optimal leavening time), 105 (time to reach the maximum dough expansion) and 150 min (dough collapse time) in a leavening cabinet at 32°C and 72% RH. The optimal time (60 min) was calculated as 75% of the time required by the dough at 30°C to reach its maximum volume (previously investigated) (Romano *et al.*, 2007). After each leavening phase, doughs were baked in an electric oven (iD 60.60 M, Moretti Forni S.p.A., Mondolfo, Italy) at 170°C for 90 min.

Three lots were produced for each leavening time and three bread loaves were obtained for each lot. The relative bread samples were identified as B60, B105 and B150, respectively.

After 1 h of cooling at room temperature, bread samples were stored in sealed plastic bags for further analyses.

7.2.4. Quality evaluation of bread

Properties of bread leavened for 60, 105 and 150 minutes were determined. Average values of at least three measurements were calculated for each parameter.

7.2.4.1. Crumb microstructural properties

Scanning Electron Microscopy (SEM, LEO EVO 40, Zeiss, Germany) was used to investigate the microstructural changes occurring in bread samples (B60, B105 and B150) by increasing leavening time. Bread samples were lyophilized, dried at the critical point, coated with gold particles, and then observed with a 20 kV acceleration voltage and a x 1500 magnification.

7.2.4.2. Colour parameters

Colorimetric indices (L*, a*, b*, ΔE and Chroma) were determined with an electronic visual analyzer (IRIS visual analyzer, Alpha MOS, Toulouse, France).

7.2.4.3. Moisture content

The moisture content was determined in triplicate for each sample by the AACC method (number 44–15.02, 1999). The results were calculated as percentage (%) of water per sample weight (g/100g).

7.2.4.4. Weight loss

Weight loss (WL) was expressed as percentage of weight lost during leavening and baking per sample weight (%). It was calculated using the following formula:

$$WL\ (\%) = \frac{A - B}{A} \times 100 \qquad (10)$$

where A = initial weight of dough; B = weight of bread after baking.

7.2.4.5. pH

pH was measured using a pH meter as reported in paragraph 7.2.2.2.

7.2.4.6. Crumb structural features

Structural properties of bread crumb were evaluated by digital image analysis as previously reported by Raiola *et al.* (2020). Specifically, loaves were cut into 20 mm thick slices using an electric knife. Approximately four slices were taken from the middle of the loaf. 2D slice images were captured with an Olympus® mod. C-7070Wide ZOOM camera (Olympus, Milan, Italy) and then processed by Image tool software: Image Pro Plus 6.1 for Windows® (Media Cybernetics Inc.).

Structural computed parameters were the following:

- average bubble area (cm^2).
- bubble wall roundness. Roundness calculates circularity of an object and it is equal to 1 when a bubble is a perfect circle (Romano *et al.*, 2013).
- number of bubbles counted (n).
- area of the loaf section (A_d).
- gas bubble area fractions (VF). This parameter was calculated following the formula no. 7 indicated in the paragraph 6.2.3.
- average bubble thickness (mm).

7.2.4.7. Mechanical properties

Mechanical properties of B60, B105 and B150 breads were studied using an Instron Universal Testing Machine (Instron Ltd., mod. 4467, High Wycombe, GB) equipped with a 0.1 kN load cell. Cylindrical crumb samples (diameter = 16 mm, height = 17 mm) were subjected to a compression test and thus deformed to 80% their initial height, at a crosshead speed of 10 mm/min. Original data were converted into stress vs. Hencky Strain, and the elastic modulus (Young's modulus) was calculated from the initial linear region of the curve. Five measurements were performed for each loaf.

7.2.5. Nutritional evaluation of bread

7.2.5.1 In *vitro* starch digestibility

Total Starch (TS), Rapidly Digestible Starch (RDS), Slowly Digestible Starch (SDS), Resistant Starch (RS) and eGI were determined by different enzymatic methods. Each measurement was

carried out on bread sample after being frozen, freeze-dried, minced by a blender, and sieved to obtain a particle size ≤ 500 μm.

TS was measured using an enzymatic assay kit (Total Starch Assay Kit, Megazyme International Ireland) by AOAC (Official Method 996.11) and AACC (Method 76.13) and determined using the formula no. 8 reported in the paragraph 6.2.4.

RDS and SDS contents as well as the eGI were assessed using an enzymatic assay kit (Resistant Starch Assay Kit, Megazyme International Ireland) by AACC method (number 32–40.01, AACC International Approved Methods of Analysis, 2009) with minor modifications reported by Romano *et al.*, (2016). RDS was the percentage of total starch hydrolyzed within 30 min of incubation in a shaking water bath (200 strokes/min, horizontal agitation) at 37°C (Romano *et al.*, 2016). SDS was the percentage of total starch hydrolyzed within 30 and 120 min of incubation under the same condition. The *in vitro* digestion kinetics were calculated in accordance with the procedure established by Goñi, Garcia-Alonso & Saura-Calixto (1997).

7.2.5.2. *In vitro* protein digestibility

Bread samples (B60, B105 and B150) were digested according to the INFOGEST static digestion method (Brodkorb *et al.*, 2019). Specifically, bread crumbs (500 mg) were minced coarsely and diluted (1:1; w:v) with Simulated Salivary Fluid (SSF) containing human salivary α-amylase (final amylase concentration 75 U/mL of oral digesta). The mixture was immediately incubated for 2 min at pH 7. The oral bolus was then mixed 1:1 (v:v) with Simulated Gastric Fluid (SGF) containing pepsin from porcine gastric mucosa (2000 U/mL of gastric digesta). After 120 min of incubation at 37°C and pH 3, the reaction was stopped raising the pH at 7 with 1M NaOH. Lastly, Simulated Intestinal Fluid (SIF) containing pancreatin from porcine pancreas (trypsin activity of 100 U/mL) and porcine bile extract (10 mM in SIF) was added 1:1 (v:v) to the gastric digesta and incubated for 120 min at 37°C. The intestinal phase was stopped by heating at 85°C for 15 min. Intestinal digesta was centrifuged at 5.000 ×g for 20 min to separate soluble and insoluble fractions. Samples were frozen in liquid nitrogen, then stored at −20°C until analysis.

7.2.5.2.1. Sodium dodecyl sulfate-polyacrylamide gel electrophoresis

The evaluation of the protein profile has been performed on the undigested samples and on the intestinal digesta (soluble fraction) by means of sodium dodecyl sulfate-polyacrylamide gel

electrophoresis (SDS-PAGE) employing a 150 g/L acrylamide separating gel. Samples were normalized according to the protein content (4 mg/mL) and then dissolved in sample buffer (Tris-HCl 0.05 M, pH = 6.8) containing 2% of 2-mercaptoethanol. Electrophoresis was conducted for 1 h at a constant voltage of 150 V. Subsequently, gels were stained with 0.5 mg/mL Coomassie brilliant blue-R250. The 2-D gels were scanned with a Versa-Doc image system (Bio-Rad).

7.2.6. Statistical analysis

All the parameters were expressed as mean value ± standard deviation. Differences among samples were determined by applying variance analysis (ANOVA) and post-hoc comparisons (Duncan's test) to significant $P < 0.05$. Correlations between eGI and breads' characteristics (elastic modulus -Young's modulus and gas bubble area fractions -VF) were carried out by correlation matrix using the Pearson product moment correlation distribution to significant $P < 0.05$. All analyses were performed using SPSS software (version 19.0, SPSS Inc., USA).

7.3. Results and discussion

7.3.1. Dough properties

Farinographic properties and pH values of LF dough (80% WF – 20% LF) are listed in Table 7.1.

Table 7.1. Farinographic parameters (WA - Water Absorption; DDT- Dough Development Time; DS - Dough Stability; DOS -Degree of Softening) of the dough and pH of dough at different leavening times (0, 60, 105 and 150 min). Each value is expressed as mean ± SD.

Dough parameter	**Leavening time (min)**	
WA (%)	0	60.25 ± 0.07
DDT (min)	0	5.31 ± 0.06
DS (min)	0	6.54 ± 0.69
DOS (BU)	0	59.50 ± 6.36
pH	**Leavening time (min)**	
	0	$5.71 \pm 0.02_{d}$
	60	$5.60 \pm 0.03_{c}$
	105	$5.55 \pm 0.04_{b}$
	150	$5.48 \pm 0.02_{a}$

[a-d] Different letters of pH values indicate significant differences ($P < 0.05$).

LF dough was characterized by a good aptitude for bread-making proved by high Water Absorption (WA) and by medium values of Dough Development Time (DDT), Dough Stability time (DS) and Degree of Softening (DOS) (Aydoğan *et al.*, 2015). The WA (%) to obtain a consistency of 500 BU (Brabender Unit) was in fact 60.3 ± 0.07%. Similar results have been found by Turfani *et al.*, 2017 (58.1%) which investigated the impact of WF substitution with green LF (at 6, 12 and 24% levels) on dough technological properties. Usually, blending WF with legume flours leads to an increase in WA (Turfani *et al.*, 2017) probably because of their greater amounts of hydrophilic constituents such as polysaccharides and proteins (Kaur & Singh, 2005, Bourré *et al.*, 2019) which form more hydrogen bonding with water than gluten and starch (Turfani *et al.*, 2017).
Dough development time (DDT) and stability (DS) are good indicators of the flour strength and higher values suggest stronger doughs (Wang, Rosell, & Benedito, 2002). As reported in Table 7.1, LF dough has a DDT average value of 5.31 ± 0.06 min, while usually, wheat doughs show a DDT of about 1.5 (Turfani *et al.*, 2017; Raiola *et al.*, 2020). In fact, as argued by Dhinda, Prakash, & Dasappa (2012), the introduction of fibre and non-gluten proteins may delay the hydration and development of gluten, thus lengthening the DDT value. In addition, Kohajdová, Karovičová, & Magala (2013) argued that the incorporation of LF in wheat dough led to a significant decrease in DS, especially when higher levels of flour were added (20-30%). In fact, wheat doughs have DS values of approximately 12 min (Aydoğan *et al.*, 2015) while our LF dough had a DS equal to 6.54 ± 0.69 min. In general, the increase of DDT and the reduction of DS in dough may result from a decrease in gluten content (Shahzadi *et al.*, 2005) which in turns may cause a weakening of the gluten network during mixing. Finally, the DOS which is used to reveal the degree of dough softening during mixing, was equal to 59.50 ± 6.36 BU.
pH values of LF dough after mixing (leavening time = 0 min) and each leavening time are listed in Table 7.1. As expected, immediately after mixing the pH of dough was significantly higher (5.70 ± 0.02) than the leavened ones ($P < 0.05$). Moreover, the pH of dough significantly dropped ($P < 0.05$) with increasing leavening time, ranging from 5.55 ± 0.04 (B60) to 5.48 ± 0.02 (B150) due to the amount of organic acids (e.g., lactic and acetic acids) produced by the yeast cells during leavening. pH is among the most popular properties of foods and is very important during leavening because it can affect protein solubility in the dough aqueous phase, protein conformation, surface activity and foaming properties (Kinsella, 1981; Pauly *et al.*, 2014).

7.3.2. Quality evaluation of bread

7.3.2.1. Crumb microstructural properties

In Figure 7.1 representative pictures (Fig. 7.1a - c) and SEM micrographs (Fig. 7.1d - f) of breads under examination are reported.

All samples showed a well-developed and continuous protein network with entangled starch granules which represents an important pre-condition for good performances during baking (Wang *et al.*, 2021). Additionally, it was clearly visible that starch granules lost they original structure as a result of the complete gelatinization. With increasing leavening time, bread samples exhibited different microstructures. Specifically, B60 samples (Fig. 7.1d) showed an aerated structure with a higher number of cavities compared with the microstructure of the other bread samples (Fig. 7.1e, f). Increasing leavening time until 105 min, caused the formation of a more homogeneous structure with cavities and micropores which were evenly distributed through the protein network (Fig. 7.1e) which showed a web-like structure. Then, at the dough collapse time (150 min) bread showed a more compact microstructure (Fig. 7.1f) with clustered starch granules and gluten proteins which became more tightly connected to the surface of starch. These outcomes are also supported by the significant reduction in moisture content and the increase in weight loss (Table 7.2) found for the most leavened bread (B150), which suggest a remarkable reduction in bread volume.

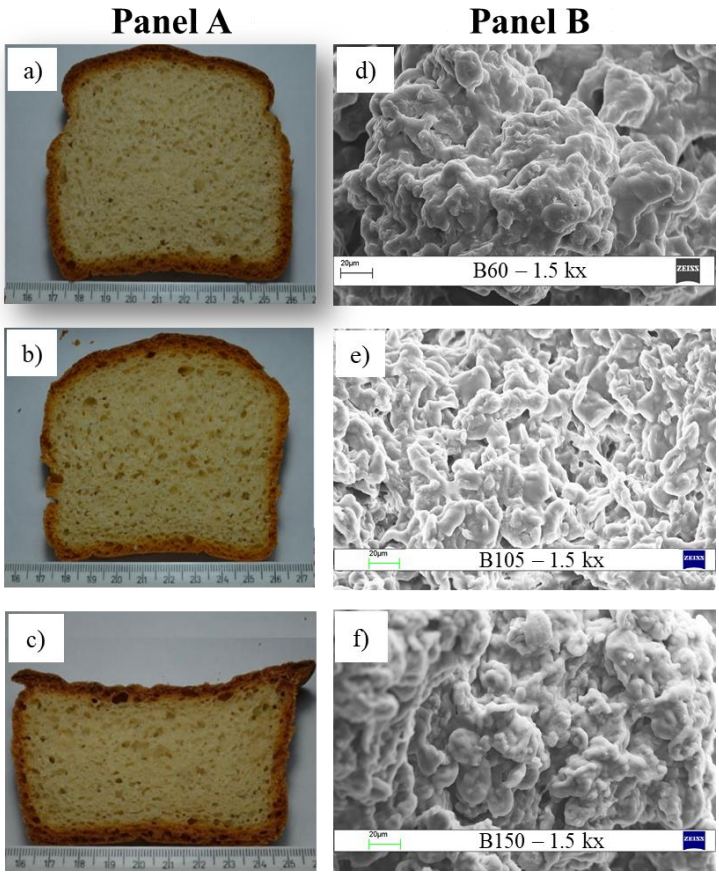

Fig. 7.1. Macrostructure and microstructure of bread samples. Panel A: Representative pictures of bread slices leavened for: a) 60 minutes; b) 105 minutes; c) 150 minutes. Panel B: SEM images of bread crumb leavened for: d) 60 minutes; e) 105 minutes; f) 150 minutes.

7.3.2.2 Physico-chemical characteristics

Physico-chemical and macrostructural properties of bread samples are showed in Table 7.2. Bread leavened for longer time (B150) showed the lowest value of moisture content (41.02 ± 0.5%), and the greatest value ($P < 0.05$) of weight loss (19.08 ± 0.61%) after baking. On the contrary no significant differences ($P > 0.05$) were found between B60 and B105. The extent of moisture and weight loss could be linked to the different dough structures generated during leavening. In fact, prolonging leavening time determines a greater gas production by yeast which in turns could lead to changes in the molecular organization of starch and proteins (Alvarez-Ramirez *et al.*, 2019). It follows that, rising leavening time may enhance dough softness and thus water loss by evaporation during baking. Bread-making involves in fact moisture and weight loss which are mainly due to the water evaporation during baking (Kotoki & Deka, 2010).

Table 7.2. Physico-chemical, colorimetric, and macrostructural parameters of bread leavened for 60, 105 and 150 minutes. Each value is expressed as mean ± SD.

	Leavening time (min)		
Parameter	60	105	150
moisture content (%)	$42.58 \pm 0.4_{c}$	$41.69 \pm 0.7_{b}$	$41.02 \pm 0.5_{a}$
pH	$5.75 \pm 0.06_{a}$	$5.78 \pm 0.01_{a}$	$5.76 \pm 0.03_{a}$
weight loss (%)	$17.06 \pm 0.57_{a}$	$17.45 \pm 1.29_{a}$	$19.08 \pm 0.61_{b}$
L* (crumb)	$63.53 \pm 0.42_{b}$	$64.84 \pm 0.96_{b}$	$61.99 \pm 0.74_{a}$
a* (crumb)	$0.95 \pm 0.41_{a}$	$1.00 \pm 0.43_{a}$	$0.90 \pm 1.23_{a}$
b* (crumb)	$11.95 \pm 0.13_{a}$	$13.90 \pm 0.18_{b}$	$13.89 \pm 0.07_{b}$
ΔE (crumb)	$38.39 \pm 0.41_{a}$	$37.83 \pm 0.83_{a}$	$40.48 \pm 0.69_{b}$
Chroma (SI) (crumb)	$11.98 \pm 0.14_{a}$	$15.23 \pm 0.17_{b}$	$14.42 \pm 0.04_{b}$
bubble area (cm^2)	$0.012 \pm 0.001_{a,b}$	$0.013 \pm 0.002_{b}$	$0.011 \pm 0.002_{a}$
roundness	$1.31 \pm 0.04_{a}$	$1.37 \pm 0.04_{b}$	$1.41 \pm 0.02_{c}$
n/Ad	$17.72 \pm 1.70_{a}$	$22.70 \pm 5.35_{b}$	$22.45 \pm 2.30_{b}$
VF (%)	$27.55 \pm 2.16_{b}$	$28.73 \pm 1.67_{c}$	$25.71 \pm 1.83_{a}$
bubble thickness (mm)	$1.06 \pm 0.12_{b}$	$0.88 \pm 0.17_{a}$	$0.92 \pm 0.08_{a}$
Young's Modulus (kPa)	$11.61 \pm 1.66_{a}$	$17.37 \pm 2.67_{b}$	$45.66 \pm 7.76_{c}$

[a-c] Different letters in the same row indicate significant differences ($P < 0.05$).
Crumb structure parameters: n, number of bubbles counted; Ad, area loaf section; VF, gas bubble area fraction.

Concerning the pH (Table 7.2), baking seemed to erase the difference between bread samples ($P > 0.05$) which did not differ for this parameter. Moreover, for all samples baking caused an increase in pH values, going from 5.60 ± 0.03 to 5.75 ± 0.06 for B60, from 5.55 ± 0.04 to 5.78 ± 0.01 for B105 and from 5.48 ± 0.02 to 5.76 ± 0.03 for B150.

Concerning colorimetric indices (Table 7.2), B150 samples showed the lowest lightness and the highest ΔE ($P < 0.05$). Moreover, a rise in leavening time (105 and 150 min) led to a significant increase ($P < 0.05$) in yellowness (b*) and Chroma. Lastly, there were no significant differences ($P > 0.05$) among the three samples in terms of a* value.

7.3.2.3. Crumb structural features

Representative pictures of bread samples (B60, B105 and B150) are showed in Fig. 7.1 while morphological parameters of bread crumb are listed in Table 7.2.

The average bubble area was significantly higher ($P < 0.05$) in B105 bread (0.013 ± 0.002 cm^2), and lower ($P < 0.05$) in B150 (0.011 ± 0.002 cm^2), while B60 showed intermediate values (0.012 ± 0.001 cm^2).

Roundness significantly increased ($P < 0.05$) with increasing leavening time. In fact, B60 bread showed the lowest average value (1.31 ± 0.04) suggesting more circular bubbles, whereas B150 the highest (1.41 ± 0.02), indicating that the bubbles were more irregular than the other bread samples. This may be due to the higher compactness of B150 bread (Fig. 7.1c) which resulted in lightly flattened bubbles. Area and roundness results were quite expected since 60 min was identified as the optimum leavening time, 105 min as the time needed to reach the maximum dough expansion and 150 min as the time of dough collapse.

Concerning the n/Ad parameter, where n was the number of bubbles counted, it was observed that the smallest number of bubbles per unit area ($P < 0.05$) was found in B60 samples (17.72 ± 1.70) while no significant differences ($P > 0.05$) were found between B105 and B150 bread.

Regarding instead VF (gas bubble area fraction), B105 samples had the highest mean value while B150 the lowest ($P < 0.05$) as they were the most porous and compact bread samples, respectively. In addition, B60 samples showed the highest ($P < 0.05$) bubble thickness (1.06 ± 0.12 mm) suggesting a greater distance between the gas bubbles. Conversely, the lower bubble thickness of B105 and B150 could be linked to the larger gas bubbles found in B105 as well as to the higher compactness of B150 that clearly reduced the distance between the alveolus.

Therefore, it could be concluded that the increase in leavening time induced a marked dough expansion until 105 min, resulting in a highly porous bread crumb. This may be linked to the greater gas generation and bubbles enlargement. Then, dough structure starts to collapse resulting, after 150 min, in a compact crumb with flattened bubbles.

7.3.2.4. Mechanical properties

Representative stress–Hencky strain curves for the bread crumbs (B60, B105 and B150) are reported in Figure 7.2. As described by Gibson & Ashby (1997), each curve displayed the typical phases of a cellular solid: i) linear elasticity, ii) plateau and iii) densification. At low strain, bread crumbs showed a linear elastic behaviour which is mainly linked to the cell wall bending as well as to the cell face stretching. After that, cells start to collapse, hence the stress remain roughly

constant reaching a plateau. Lastly, during the densification phase, stress values grow rapidly in response to the compression of the cell wall material (Gibson & Ashby, 1997).

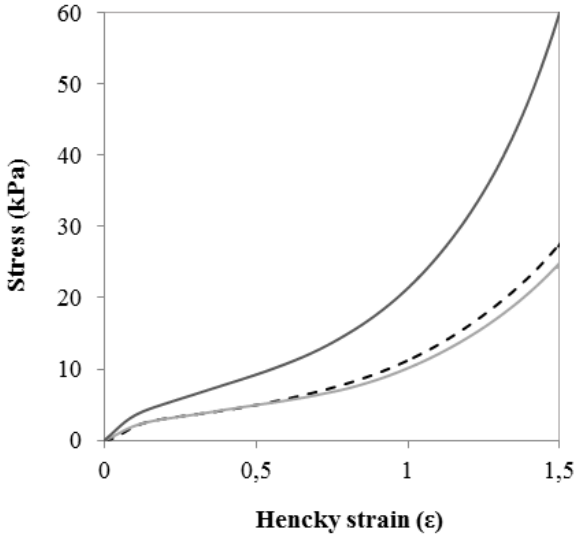

Fig. 7.2. Stress–strain curves of bread leavened for: (- -) 60 minutes; (—) 105 minutes; (**—**) 150 minutes.

As can be seen from Figure 7.2, the stress-strain curves for B60 and B105 samples followed a similar path, while B150 differed significantly in the linear elasticity, plateau, and densification zone. Basically, B150 exhibited higher resistance across the studied deformation range, suggesting that the magnitude of stress was greater as bread compactness increased. Furthermore, it is important to note that B150 bread had the lowest moisture content (41.02 ± 0.5 %) compared to the other samples. Our results are in good agreement with earlier studies which stated that crumbs with low moisture may have a harder texture than the ones rich in moisture (Baik & Chinachoti, 2003).

As shown in Table 7.2, the Young's modulus increased significantly ($P < 0.05$) with rising leavening time. In fact, its average value was lower for B60 (11.61 ± 1.66 kPa) and higher for B150 (45.66 ± 7.76 kPa). According to Wang, Austin & Bell (2011), the Young's modulus of crumb samples increased linearly as bread compactness increase and exponentially with increase in the number of air bubbles. In fact, B105 and B150 breads had the highest n/Ad (Table 7.2). In our case, too, mechanical findings were positively related to the crumb morphological properties since we noted a good correlation between Young's modulus and the VF ($R^2 = 0.772$).

7.3.3. Nutritional bread characterization

7.3.3.1. *In vitro* starch digestibility

The effects of different leavened structures on TS content, starch nutritional fractions (RDS, SDS, and RS) and expected Glycemic Index (eGI) of breads have been investigated. Nutritional results are reported in Table 7.3. Bread samples showed a similar TS content ($P > 0.05$).

The *in vitro* starch digestibility was analyzed enzymatically, determining the amount of released glucose during starch digestion. Figure 7.3 reports the hydrolysis curves of bread samples under examination compared with those performed by white bread used as reference food.

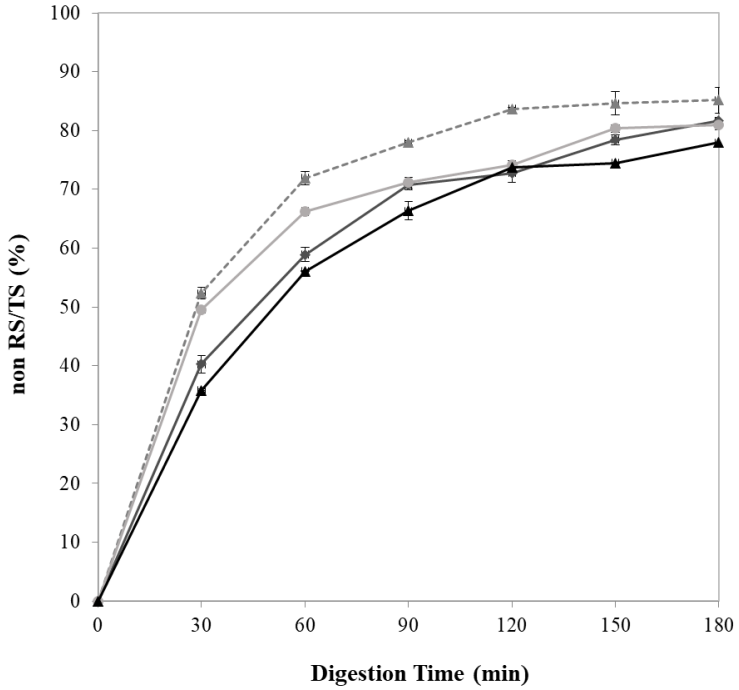

Fig. 7.3. Starch digestibility profiles of reference bread (▲) and LF breads leavened for 60 (♦), 105 (●) and 150 minutes (▲).

The hydrolysis curves showed the same trend, with a rapid rise in starch hydrolysis within the first 60 min followed by a gradual rise during the additional 120 min.

As reported in Table 7.3, B105 breads had the highest ($P < 0.05$) eGI (89.77 ± 0.21%) followed by B60 (87.60 ± 0.34%) and B150 (80.42 ± 0.48%), respectively.

Table 7.3. Total starch content (TS), starch nutritional fractions (RDS, rapidly digestible starch, SDS, slowly digestible starch, and RS, resistant starch) and expected Glycemic Index (eGI) of bread at different leavening time (60, 105 and 150 minutes). Each value is expressed as means ± S.D.

Nutritional properties	**Leavening time (min)**		
	60	**105**	**150**
TS (%)	$68.17 \pm 0.62_a$	$69.35 \pm 0.20_a$	$68.42 \pm 0.97_a$
RDS (%)	$27.44 \pm 0.69_b$	$33.22 \pm 1.40_c$	$24.42 \pm 0.12_a$
SDS (%)	$22.19 \pm 0.06_b$	$18.17 \pm 1.81_a$	$25.92 \pm 0.18_c$
RS (%)	$18.53 \pm 0.75_a$	$17.95 \pm 0.41_a$	$17.91 \pm 0.30_a$
eGI (%)	$87.60 \pm 0.34_b$	$89.77 \pm 0.21_c$	$80.42 \pm 0.48_a$

[a-c] Different letters in the same row indicate significant differences ($P < 0.05$).

A similar trend was observed for RDS since it represents the starch fraction that is rapidly and totally digested in the gastrointestinal tract, leading to a fast elevation of postprandial plasma glucose (Gallo, Romano, & Masi, 2020). This parameter was significantly lower ($P < 0.05$) for B150 and higher for B105 samples, ranging from 24.42 ± 0.12 % and 33.22 ± 1.40 %. Conversely, SDS that is the starch fraction which is more slowly digested in the gastrointestinal tract, reached the highest value ($P < 0.05$) for B150 samples (25.92 ± 0.18 %) and the lowest for B105 (18.17 ± 1.81%). Samples did not differ in terms of RS ($P > 0.05$).

Our results suggested that, the different bread structure due to leavening time influenced the *in vitro* starch digestibility, resulting in increased RDS and eGI in B105 and reduced RDS and eGI in B150, while B60 showed intermediate values. To confirm this, positive correlations between the eGI and the VF ($R^2 = 0.902$) as well as among the eGI and the Young modulus ($R^2 = 0.926$) were noticed. Our results are in good agreement with several studies (Lin *et al.*, 2020; Fardet *et al.*, 2006; Eelderink *et al.*, 2015) which found an interesting correlation between bread physical structure and its GI. Specifically, according to Fardet *et al.* (2006) the production of bread with a compact structure or high density, could be a good strategy for reducing the GI. To confirm this, Lin *et al.* (2020) stated that the use of fine whole wheat flour for bread production led to a highly porous texture which led to a greater *in vitro* starch digestibility than common wheat bread. This suggested that the bread physical structure can also be a major factor in determining the glycemic response than the raw materials. Low GI foods is desirable not only for consumers with diabetes, but also for consumers in general, since it prevents the incidence of chronic metabolic diseases (Brand-Miller *et al.*, 2009).

7.3.3.2. *In vitro* protein digestibility

The SDS-PAGE protein profiles of bread samples before digestion (B60, B105 and B150) and after the simulated gastrointestinal intestinal digestion (B60i, B105i and B150i) are shown in Fig. 7.4.

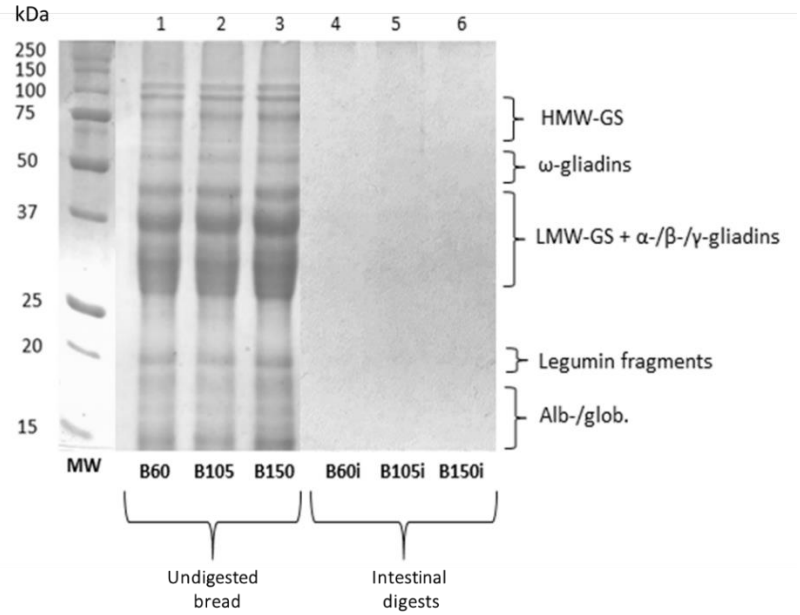

Fig. 7.4. SDS-PAGE protein profile of bread before being digested (B60, B105 and B150) and after intestinal digestion ($B60_i$, $B105_i$ and $B150_i$).
Left column denotes molecular marker (kDa).
Lane numbers represent different samples. MW = molecular marker.

The pattern of the undigested samples showed the typical protein components of common wheat (Triticum aestivum) flour, which can be grouped into high molecular weight glutenins (HMW-GS, 65−90 kDa), ω-gliadins (44−55 kDa), low molecular weight glutenins (LMW-GS, 30−40 kDa), and α/β- and γ-gliadins (30−45 kDa). Bands of albumins, globulins (13-17 kDa) and legumin fragments (20 kDa) were also identified, as previously described by Santos-Hernández *et al.*, (2020). The protein bands of bread samples leavened for different times (B60, B105 and B150) showed different intensities (lines 1 - 3).

In particular, B60 samples exhibited the weakest protein bands, followed by the ones of B105 and B150. During mixing, gluten proteins (gliadins and glutenins) interact with each other forming a three-dimensional network that entraps the starch granules. According to Zhang, Mu, & Sun (2018), the intensity of gluten bands may depend on the strength of starch–gluten interactions. In particular, the lower intensity of the gluten fraction bands, the stronger

interactions between gluten and starch (Zhang *et al.*, 2018). Our findings may be ascribed to a weakening of the gluten network with the increase of leavening time and hence with the rise of CO2 production which causes bubbles enlargement (Alvarez-Ramirez *et al.*, 2019) as also evidenced by the mechanical findings (Fig. 2 and Table 2). Since the protein patterns of the intestinal digests (lines 4 - 6) did not show protein bands, the α amino nitrogen amount (mg) of leavened bread samples before and after the simulated gastrointestinal digestion has been evaluated (Figure 7.5).

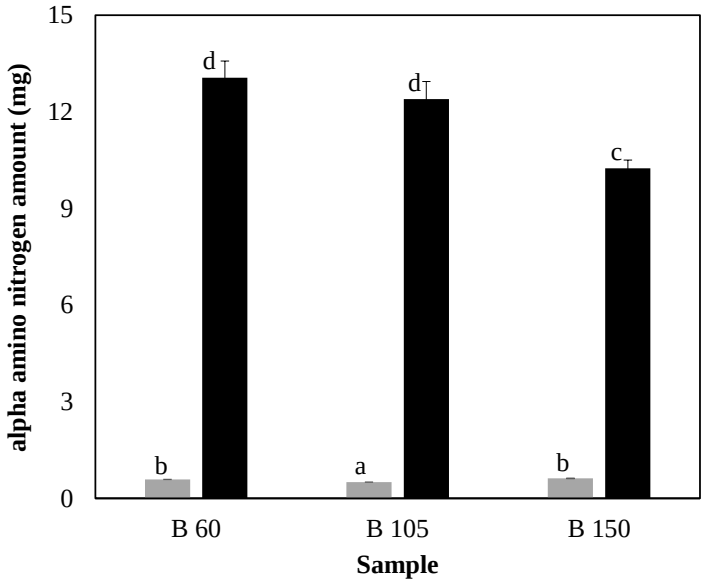

Fig. 7.5. α amino nitrogen release (mg) for the different leavening times before and after simulated Oral-Gastric-Duodenal digestion.

From this analysis, it appears that the amount of released amino acids at the end of digestion was the lowest ($P < 0.05$) for B150 sample while no significant differences were found between B60 and B105 samples. as shown in Fig. 7.5. Therefore, we can conclude that the leavening time influenced the strength of starch–gluten interactions and the optimal protein digestion corresponded to the 60 and 105 minutes of leavening.

Conclusions and perspectives

Conclusions and perspectives

During digestion, food undergoes to physico-chemical transformations which can be technically difficult and costly to study. However, the development of *in vitro* digestion models increasingly accurate allow to improve our knowledge about the fate of foods during digestion but also to design foods targeted for specific health functionalities.

Food structure may strongly affect the bioaccessibility and thus the digestibility of the nutrients they contain. Thus, understanding how food structure can influence kinetics of nutrients release and hydrolysis by the digestive enzymes, may provide more-effective ways to keep a healthy diet.

The primary aim of this PhD thesis was to develop a new dynamic *in vitro* digestion apparatus able to provide a better simulation of both the physical and chemical conditions encountered in the gastrointestinal tract. Therefore, a huge part of this PhD project has been dedicated to the setting up of the CAISIAL digestive system (DICA) (4^{th} Chapter). To date, every single part of this multi-compartmental apparatus can be controlled via software giving the possibility to dynamically monitor and regulate relevant physiological parameters. Hence, DICA could be used to simulate the digestive system of different target populations, breaking new ground in the development of tailored foods.

The DICA shows several strengths, including:

1. The reactor capacity (500 - 1000 mL) that allows to analyse large amounts of test meal.
2. The central part of each reactor is made of transparent material, allowing visual observations throughout the digestion process.
3. The possibility to perform tests in real time because the length of each digestion phase can be adjusted considering data obtained from *in vivo* studies.
4. The gradual and controlled addition of digestive fluids and enzymatic solutions depending on the characteristics of the food tested (volume, composition, energy content).
5. The opportunity to set number and duration of each peristalsis, providing a better understanding of the complex mechanism driving food breakdown during digestion.
6. The simulation of the gastric emptying thanks to the presence of a proportional valve downstream the stomach which reproduce the sieving effect of pylorus.
7. The possibility to constantly monitor and then control temperature and pH values.

This system also has some weaknesses, like:

1. It considers only the oral, gastric, and duodenal phase of digestion.
2. There are no *in vivo* satiety signals controlling the rate of digestion.
3. The absorption of the bioaccessible fraction is not simulated.
4. The system has not yet been validated.

Clearly, the next step will be the validation of the system against specific nutrients and model food.

The secondary aim of this PhD thesis, spread over three study cases, was to investigate how food structure can affect nutrients bioaccessibility and digestibility by means of both static and semi-dynamic *in vitro* digestion models. For this purpose, pasta and bread have been used as model foods and the potentiality of lentil flour (LF) as functional ingredient in these products as been extensively evaluated.

In fact, as stated in the 3th Chapter, LF has been recently used as highly nutrition ingredient for a wide range of food products, offering a wide range of functionalities as well as textural benefits. Unit operations used to pre-process and /or process LF can greatly impact on its nutritional, physicochemical, and functional properties. *In vitro* digestibility studies have shown that protein and/or starch of LF can be improved depending on the type of process used. LF has also excellent functional properties, improving food texture, shelf life, cooking quality and overall consumer acceptance of foods, at extent related to the specific food application and to the level of LF concentration. Furthermore, LF can be use by alone or blended with wheat or other cereals to obtain a more balanced nutritional profile of bakery products (with or without gluten). The outcome is that a combination of formulation and processing strategies can be very effective in achieving the objective of improving the use of LF in novel foods, matching consumers' expectations (implicit and explicit).

The first study case (5th Chapter) aimed to investigate the effects of formulation on the microstructure, cooking quality, water absorption and mobility during cooking and nutritional properties of commercial Italian pasta. For this purpose, three type of spaghetti Barilla n.5 made of durum wheat semolina (S), whole durum wheat semolina (WS) and red lentil spaghetti were used. Three main points emerged from this study. First, the presence of high amount of fibre and non-gluten proteins significantly affects the microstructure of both the uncooked and cooked samples. As regard the latter, fibre interferes with gluten-starch matrix in WS samples, while the

higher protein content of LS samples resulted in a strong protein matrix which limited starch gelatinization.

Second, the presence of fibre and non-gluten proteins affects cooking quality, water absorption and water mobility at a molecular level. In this respect, WS and LS showed an increase in water absorption and a decrease in transversal relaxation times of protons compared to S samples. It was due to the interaction of water molecules with fibre, starch, and proteins for WS samples and to the presence of a highly reticulated protein matrix for LS samples. In this context, the choice to analyse the raw CPMG decay curves, turned out to be a successful strategy to study the change in molecular water mobility in pasta as function of the cooking time as well as of its formulation.

Third, *in vitro* starch digestibility method revealed that the presence of fibre had a negative impact on pasta nutritional properties, causing an undesirable increase in the RDS and eGI values of WS compared with the S and in particular LS which featured the lowest starch digestibility. All together, these results may help to better understand to what extent raw materials influence pasta microstructure and nutritional properties. In some respects, these findings were quite unexpected because the consumption of whole grain products is generally linked to reduced risks of various health diseases including the type II diabetes. On the other hand, the reduction in starch digestibility reported in the literature linked to the use of lentil flour for pasta-making has been confirmed.

In the second study case (6th Chapter) the positive impact of bread enrichment with LF (10% and 20%) on its nutritional properties have been reported (e.g., increase in high-quality proteins and decrease in starch content). Specifically, during the oral and gastric phase of digestion, the addition of increasing amounts of LF led to a decrease in the total starch residue (TS*) and a simultaneous increase in FG content, while the trend was reverse during the intestinal digestion. These findings were in good agreement with structural findings and the determination of RDS content which followed this order 20LF > 10LF > control. On the contrary, protein profile by SDS-PAGE suggested a decrease in proteins digestibility of LF bread enrichment due to minimal gastric digestion of gluten and legume proteins whose bands were clearly persistent until the end of gastric digestion. Besides, during the intestinal digestion, samples showed an extensive gluten hydrolysis and thus an increase in low molecular weight peptides. Starch and proteins bioaccessibility was strictly related to the structural features of bread samples. The use of the semi-dynamic model allowed for a proper simulation of both physical and chemical conditions

encountered in the GIT since it considers crucial kinetic aspects associated with the gastric phase of digestion. Thus, it proved to be a very useful tool for evaluating bread disintegration during digestion as well as to investigate the kinetics of nutrients hydrolysis.

Lastly, the third study case (7th Chapter) provided interesting information on how and to what extent leavening time can affect the structure and other properties of bread enriched with 20% of LF. Bread quality attributes and *in vitro* starch digestibility were significantly influenced by the structure resulting from different leavening times (60, 105 and 150 min). Firstly, the rise in leavening time greatly impacted on bread physico-chemical properties determining an increase in the weight loss during baking and reducing bread lightness. Crumb macrostructural properties were also affected by leavening time, showing a growing porosity until 105 min of and the highest compactness for bread leavened until the collapse time (150 min). Regarding instead the mechanical behavior of breads crumb, the Young's modulus increased linearly with rising leavening time, also displaying a good correlation (R^2 = 0.772) with the VF. *In vitro* starch digestion tests highlighted an interesting correlation between crumb macrostructural/mechanical features and nutritional properties. Specifically, the more compact crumb structure (< VF) of B150 samples led to lower RDS and eGI followed by samples with the shortest leavening time (B60). Besides, protein profiles of intestinal digesta investigated by SDS-PAGE suggested that leavening time did not impact on the *in vitro* protein digestibility. In conclusion, this study case allowed to fill the gap in the literature on the possible effects of leavening time on bread structural and nutritional properties. Leavening time turned out to be a key factor for modelling bread structures enhancing both the *in vitro* starch and protein digestibility in well-developed loaves (B105). However, further studies would be necessary to find the right balance between consumers acceptance in terms of bread quality (texture, appearance) and its health benefits.

The present PhD project opens new paths for the *in vitro* digestion modelling providing also interesting insights about the role of food formulation and processing in defining its structure.

LF has proved to be a valuable ingredient for pasta- and bread-making, enhancing the nutritional profile of the products concerned. In all the study cases, both the use of LF (alone or in combination with wheat flour) and food processing (such as pasta cooking and dough leavening) caused substantial structural changes which in turns inevitably affected the sample behavior during the simulated gastrointestinal digestion. In this context, the combination of different techniques such as analytic methods, 2D image analysis, SEM, NMR, and *in vitro* digestion tests

provided useful information about the interaction between food constituents and their role in the food matrix formation, the rate of nutrients release during digestion and their accessibility to the digestive enzymes, also facilitating the interpretation and the explanation of the data obtained. These knowledges could be valuable to develop food structures with specific functionalities, giving the scientific community useful tools for controlling (promoting/hindering) nutrients bioaccessibility and digestibility according to the needs. Overall, despite the inability to reproduce certain *in vivo* digestion events, the use of static and semi-dynamic digestion models, alone or in combination, provided quite good results. In fact, human digestion is a dynamic and very complex process which is very difficult to simulate in laboratory. In this context, even if the DICA is at a preliminary stage of development and more work is still required, it exhibits great potential for driving scientific breakthroughs in the field of nutrition, food technology, pharmaceutical and more.

Published papers

1. Romano, A., Gallo, V., Ferranti, P., & Masi, P. (2021). Lentil flour: nutritional and technological properties, *in vitro* digestibility and perspectives for use in the food industry. *Current Opinion in Food Science*, 40, 157-167. https://doi.org/10.1016/j.cofs.2021.04.003

2. Santos-Hernández, M., Alfieri, F., Gallo, V., Miralles, B., Masi, P., Romano, A., Ferranti, P., & Recio, I. (2020). Compared digestibility of plant protein isolates by using the INFOGEST digestion protocol. Food Research International, 137, 109708.

https://doi.org/10.1016/j.foodres.2020.109708

3. Gallo, V., Romano, A., & Masi, P. (2020). Does the presence of fibres affect the microstructure and *in vitro* starch digestibility of commercial Italian pasta? *Food Structure*, 24, 100139. https://doi.org/10.1016/j.foostr.2020.100139

Submitted papers

1. Gallo, V., Romano, A., Miralles, B., Ferranti, P., Santos-Hernández, M., Masi, P., & Recio, I. (2021). Properties of breads with flour from typical green lentils during simulated gastrointestinal digestion. *LWT*.

2. Gallo, V., Romano, A., Ferranti, P., & Masi, P. (2021). Properties and *in vitro* digestibility of a bread enriched with lentil flour at different leavening times. *Food Hydrocolloids*.

3. Romano, A., Gallo, V., Ferranti, P., & Masi, P., 2021. New ingredients and alternatives to durum wheat semolina for a high-quality dried pasta. *Current Opinion in Food Science*.

List of References

AACC International (2010). Approved Methods. 11th ed. (online). AACC International, St., Paul, MN.

AACC International Approved Methods of Analysis (1999) Method 44-15.02. Moisture–Air-Oven Methods. St. Paul, MN, USA.

AACC International Approved Methods of Analysis (2009). Method 32-40.01. St. Paul, MN, USA.

Abrahamse, E., Minekus, M., van Aken, G. A., van de Heijning, B., Knol, J., Bartke, N., Oozeer, R., van der Beek E. M., & Ludwig, T. (2012). Development of the digestive system-experimental challenges and approaches of infant lipid digestion. *Food Digestion*, 3, 63-77. https://doi.org/10.1007/s13228-012-0025-x

Alan Mackie (2019): The Digestive Tract: A Complex System. In O. Gouseti, G. M. Bornhorst, S. Bakalis, & A. Mackie (Eds.), Interdisciplinary Approaches to Food Digestion (pp. 11-28). Springer. https://doi.org/10.1007/978-3-030-03901-1

Ali, A., Shehzad, A., Khan, M., Shabbir, M., & Amjid, M. (2012). Yeast, its types and role in fermentation during bread making process – A review. *Pakistan Journal of Food Sciences*, 22(3), 171–179.

Alminger, M., Aura, A. M., Bohn, T. C., Dufour, S. N. E. L., Gomes, A., Karakaya, S., & Santos, C. N. (2014). In vitro models for studying secondary plant metabolite digestion and bioaccessibility. *Comprehensive Reviews in Food Science and Food Safety*, 13, 413–436. https://doi.org/10.1111/1541-4337.12081

Aravind, N., Sissons, M. J., Egan, N. E., & Fellows, C. M. (2012). Effect of insoluble dietary fibre addition on technological, sensory, and structural properties of durum wheat spaghetti. *Food Chemistry*, 130(2), 299–309. https://doi.org/10.1016/j.foodchem.2011.07.042

Argel, N. S., Ranalli, N., Califano, A. N., & Andrés, S. C. (2020). Influence of partial pork meat replacement by pulse flour on physicochemical and sensory characteristics of low-fat burgers. *Journal of the Science of Food and Agriculture*, 100, 3932–3941. https://doi.org/10.1002/jsfa.10436

Armand, M., Hamosh, M., Mehta, N. R., Angelus, P. A., Philpott, J. R., Henderson, T. R., Dwyer, N. K., Lairon, D., & Hamosh, P. (1996). Effect of human milk or formula on gastric function and fat digestion in the premature Infant. *Pediatric Research*, 40, 429-437. https://doi.org/10.1203/00006450-199609000-00011

Arora, K., Ameur, H., Polo, A., Di Cagno, R., Rizzello, C. G., & Gobbetti, M. (2021). Thirty years of knowledge on sourdough fermentation: A systematic review. *Trends in Food Science and Technology*, 108, 71–83. https://doi.org/10.1016/j.tifs.2020.12.008

Aydoğan, S., Şahin, M., Göçmen Akçacik, A., Hamzaoğlu, S., & Taner, S. (2015). Relationships between Farinograph Parameters and Bread Volume, Physicochemical Traits in Bread Wheat Flours. *Journal of Bahri Dagdas Crop Research*, 3(1), 14-18.

Aydogdu, A., Yildiz, E., Aydogdu, Y., Sumnu, G., Sahin, S., & Ayhan, Z. (2019). Enhancing oxidative stability of walnuts by using gallic acid loaded lentil flour based electrospun nanofibers as active packaging material. *Food Hydrocolloids*, 95, 245–255. https://doi.org/10.1016/j.foodhyd.2019.04.020

Baik, M., & Chinachoti, P. (2003). Water Self-Diffusion Coefficient and Staling of White Bread as Affected by Glycerol. *Food Chemistry*, 80(6), 740–744. https://doi.org/10.1094/CCHEM.2003.80.6.740

Baugreet, S., Gomez, C., Auty, M. A. E., Kerry, J. P., Hamill, R. M., & Brodkorb, A. (2019). In vitro digestion of protein-enriched restructured beef steaks with pea protein isolate, rice protein and lentil flour following sous vide processing. *Innovative Food Science & Emerging Technologies*, 54, 152–161. https://doi.org/10.1016/j.ifset.2019.04.005

Baugreet, S., Kerry, J. P., Allen, P., Gallagher, E., & Hamill, R. M. (2018). Physicochemical characteristics of protein-enriched restructured beef steaks with phosphates, transglutaminase, and elasticised package forming. *Journal of Food Quality*, 1-11. https://doi.org/10.1155/2018/4737602

Benmeziane, F., Raigar, R. K., Ayat, N. E. H., Aoufi, D., Djermoune-Arkoub, L., & Chala, A. (2021). Lentil (Lens culinaris) flour addition to yogurt: Impact on physicochemical, microbiological and sensory attributes during refrigeration storage and microstructure changes. *LWT - Food Science and Technology*, 140, 110793. https://doi.org/10.1016/j.lwt.2020.110793

Bernin, D., Steglich, T., Röding, M., Moldin, A., Topgaard, D., & Langton, M. (2014). Multi-scale characterization of pasta during cooking using microscopy and real-time magnetic resonance imaging. *Food Research International*, 66, 132–139. https://doi.org/10.1016/j.foodres.2014.09.007

Berrazaga, I., Bourlieu-Lacanal, C., Laleg, K., Jardin, J., Briard-Bion, V., Dupont, D., Walrand, S., & Micard, V. (2020). Effect of protein aggregation in wheat-legume mixed pasta diets on their in vitro digestion kinetics in comparison to “rapid” and “slow” animal proteins. *PLoS One*, 15, 1–29. https://doi.org/10.1371/journal.pone.0232425

Berti, C., Riso, P., Monti, L. D., & Porrini, M. (2004). In vitro starch digestibility and in vivo glucose response of gluten-free foods and their gluten counterparts. *European Journal of Nutrition*, 43(4), 198–204. https://doi.org/10.1007/s00394-004-0459-1

Besbes, E., Jury, V., Monteau, J.Y. & Le Bail, A. (2013). Characterizing the cellular structure of bread crumb and crust as affected by heating rate using X-ray microtomography. *Journal of Food Engineering*, 115, 415–423. https://doi.org/10.1016/j.jfoodeng.2012.10.005

Bhattarai, R. R., Dhital, S., & Gidley, M. J. (2016). Interactions among macronutrients in wheat flour determine their enzymic susceptibility. *Food Hydrocolloids*, 61, 415–425. https://doi.org/10.1016/j.foodhyd.2016.05.026

Bock, J. E., Connelly, R. K., & Damodaran, S. (2013). Impact of bran addition on water properties and gluten secondary structure in wheat flour doughs studied by attenuated total reflectance Fourier transform infrared spectroscopy. *Cereal Chemistry*, 90(4), 377–386. https://doi.org/10.1094/CCHEM-01-13-0008-FI

Bonomi, F., D’Egidio, M. G., Iametti, S., Marengo, M., Marti, A., Pagani, M. A., & Ragg, E. M. (2012). Structure-quality relationship in commercial pasta: A molecular glimpse. *Food Chemistry*, 135, 348–355. https://doi.org/10.1016/j.foodchem.2012.05.026

Borczak, B., Sikora, M., Sikora, E., Dobosz, A., & Kapusta-duch, J. (2018). Glycaemic index of wheat bread. *Starch Bioengineering*, 70, 1700022. https://doi.org/10.1002/star.201700022

Bornhorst, G. M., & Singh, P. R. (2014). Gastric digestion in vivo and in vitro: how the structural aspects of food influence the digestion process. *Annual Review of Food Science and Technology*, 5, 111-132. https://doi.org/10.1146/annurev-food-030713-092346

Bosmans, G. M., Lagrain, B., Deleu, L. J., Fierens, E., Hills, B. P., & Delcour, J. A. (2012). Assignments of proton populations in dough and bread using NMR relaxometry of starch, gluten, and flour model systems. *Journal of Agricultural and Food Chemistry*, 60, 5461–5470. https://doi.org/10.1021/jf3008508

Bouhlal, O., Mona, T., Nadia, B., Benali, A., Visioni, A., & Benba, J. (2019). Wheat-lentil fortified flours: health benefits, phsicochemical, nutritional and technological properties.

Journal of Materials and Environmental Science, 10, 1098–1106. https://doi.org/10(11):1098-1106

Boukid, F., Gentilucci, V., Vittadini, E., De Montis, A., Rosta, R., Bosi, S., Dinelli, G., & Carini, E. (2020). Rediscovering bread quality of "old" Italian wheat (Triticum aestivum L. ssp. aestivum.) through an integrated approach: Physicochemical evaluation and consumers' perception. *LWT - Food Science and Technology*, 122, 109043. https://doi.org/10.1016/j.lwt.2020.109043

Boukid, F., Vittadini, E., Lusuardi, F., Ganino, T., Carini, E., Morreale, F., & Pellegrini, N. (2019). Does cell wall integrity in legumes flours modulate physiochemical quality and in vitro starch hydrolysis of gluten-free bread? *Journal of Functional Foods*, 59, 110–118. https://doi.org/10.1016/j.jff.2019.05.034

Boukid, F., Zannini, E., Carini, E., & Vittadini, E. (2019). Pulses for bread fortification: A necessity or a choice? *Trends in Food Science & Technology*, 88, 416–428. https://doi.org/10.1016/j.tifs.2019.04.007

Bourlieu, C., Menard, O., Bouzerzour, K., Mandalari, G., Macierzanka, A., Mackie, A. R., & Dupont, D. (2014). Specificity of infant digestive conditions: Some clues for developing relevant in vitro models. *Critical Reviews in Food Science and Nutrition*, 54, 1427-1457. https://doi.org/10.1080/10408398.2011.640757

Bourré, L., Frohlich, P., Young, G., Borsuk, Y., Sopiwnyk, E., Sarkar, A., Nickerson, M. T., Ai, Y., Dyck, A., & Malcolmson, L. (2019). Influence of particle size on flour and baking properties of yellow pea, navy bean, and red lentil flours. *Cereal Chemistry*, 96, 655–667. https://doi.org/10.1002/cche.10161

Brand-Miller, J., McMillan-Price, J., Steinbeck, K., & Caterson, I. (2009). Dietary glycemic index: Health implications. *Journal of the American College of Nutrition*, 28, 446–449. https://doi.org/10.1080/07315724.2009.10718110

Brand-Miller, J.C., Stockmann, K., Atkinson, F., Petocz, P., & Denyerx, G. (2009). Glycemic index, postprandial glycemia, and the shape of the curve in healthy subjects: analysis of a database of more than 1000 foods. *The American Journal of Clinical Nutrition*, 89(1), 97-105. https://doi.org/10.3945/ajcn.2008.26354

Bresciani, A., & Marti, A. (2019). Using Pulses in Baked Products: Lights, Shadows, and Potential Solutions. *Foods*, 8, 451. https://doi.org/10.3390/foods8100451

Brodkorb, A., Egger, L., Alminger, M., Alvito, P., Assunção, R., Ballance, S., Bohn, T., Bourlieu-Lacanal, C., Boutrou, R., Carrière, F., Clemente, A., Corredig, M., Dupont, D., Dufour, C., Edwards, C., Golding, M., Karakaya, S., Kirkhus, B., Le Feunteun, S., Lesmes, U., Macierzanka, A., Mackie, A. R., Martins, C., Marze, S., McClements, D. J., Ménard, O., Minekus, M., Portmann, R., Santos, C. N., Souchon, I., Singh, R. P., Vegarud, G. E., Wickham, M. S. J., Weitschies, W., & Recio, I. (2019). INFOGEST static in vitro simulation of gastrointestinal food digestion. *Nature Protocols*, 14(4), 991–1014. https://doi.org/10.1038/s41596-018-0119-1

Bustos, M. C., Perez, G. T., & Leon, A. E. (2015). Structure and quality of pasta enriched with functional ingredients. *RSC Advances*, 5(39), 30780–30792. https://doi.org/10.1039/C4RA11857J

Bustos, M. C., Vignola, M. B., Pérez, G. T., León, A. E. (2017). In vitro digestion kinetics and bioaccessibility of starch in cereal food products. *Journal of Cereal Science*, 77, 243–250. https://doi.org/10.1016/j.jcs.2017.08.018

Butterworth, P. J., Warren, F. J., & Ellis, P. R. (2011). Human α-amylase and starch digestion: An interesting marriage. *Clinical Nutrition-Applications of Alpha-glucans*, 63(7), 395–405. https://doi.org/10.1002/star.201000150

Cafieri, S., Mastromatteo, M., Chillo, S., & Del Nobile, M. A. (2010). Modeling the mechanical properties of pasta cooked at different times. *Journal of Food Engineering*, 100(2), 336–342. https://doi.org/10.1016/j.jfoodeng.2010.04.019

Camilleri, M. (2006). Integrated Upper Gastrointestinal Response to Food Intake. *Gastroenterology*, 131(2), 640–658. https://doi.org/10.1053/j.gastro.2006.03.023

Camillieri, M., & Prather, C. M. (1994). Axial forces during gastric emptying in health and models of disease. *Digestive Diseases and Sciences*, 39, 14S-17S. https://doi.org/10.1007/BF02300361

Campagna, R., Romano, A., Raiola, A., Masi, P., Toraldo, G., & Cavella S. (2020). Effects of UVC treatment on re- milled semolina dough and data - driven analysis of leavening process. *Food and Bioproducts Processing*, 119, 31-37. https://doi.org/10.1016/j.fbp.2019.10.009

Carcea, M. (2020). Nutritional Value of Grain-Based Foods. *Foods*, 9, 504. https://doi.org/10.3390/foods9040504

Carcea, M., Turfani, V., Narducci, V., Durazzo, A., Finamore, A., Roselli, M., & Rami, R. (2019). Bread for the aging population: The effect of a functional wheat-lentil bread on the immune function of aged mice. *Foods*, 8, 510. https://doi.org/10.3390/foods8100510

Carini, E., Curti, E., Littardi, P., Luzzini, M., & Vittadini, E. (2013). Water dynamics of ready to eat shelf stable pasta meals during storage. *Innovative Food Science & Emerging Technologies*, 17, 163–168. https://doi.org/10.1016/j.ifset.2012.09.010

Carini, E., Curti, E., Minucciani, M., Antoniazzi, F., & Vittadini, E. (2014). Pasta. In R. D. P. F. Guine, & P. M. dos Reis Correia (Eds.). Engineering aspects of cereal and cereal based products (pp. 211–238). Boca Raton: CRC Press.

Cavella, S., Romano, A., Giancone, T., & Masi, P. (2008). The Influence of Dietary Fibres on Bubble Development During Bread Making. In G. M. Campbell, M. G. Scanlon, & D. L. Pyle (Eds.), Bubbles in Food 2: Novelty, Health and Luxury. AACC International, Inc. https://doi.org/10.1016/B978-1-891127-59-5.50035-3

Chaudhary, A., & Tremorin, D. (2020). Nutritional and environmental sustainability of lentil reformulated beef burger. *Sustainability*, 12, 1–18. https://doi.org/10.3390/su12176712

Chávez-Murillo, C. E., Veyna-Torres, J. I., Cavazos-Tamez, L. M., de la Rosa-Millán, J., & Serna Saldívar, S. O. (2018). Physicochemical characteristics, ATR-FTIR molecular interactions and in vitro starch and protein digestion of thermally-treated whole pulse flours. *Food Research International*, 105, 371–383. https://doi.org/10.1016/j.foodres.2017.11.029

Chelladurai, V., & Erkinbaev, C. (2020): Lentils. In A. Manickavasagan, & P. Thirunathan (Eds.), Pulses: Processing and product development (pp. 129-144). Springer. https://doi.org/10.1007/978-3-030-41376-7

Ciudad-Mulero, M., Fernández-Ruiz, V., Cuadrado, C., Arribas, C., Pedrosa, M. M., Berrios, J. J., Pan, J., & Morales, P. (2020). Novel gluten-free formulations from lentil flours and nutritional yeast: Evaluation of extrusion effect on phytochemicals and non-nutritional factors. *Food Chemistry*, 315, 126175.

Clune, S., Crossin, E., & Verghese, K. (2017). Systematic review of greenhouse gas emissions for different fresh food categories. *Journal of Cleaner Production*, 140, 766-78. https://doi.org/10.1016/j.jclepro.2016.04.082

Cummings, D. E., & Overduin, J. (2007). Gastrointestinal regulation of food intake. *Journal of Clinical Investigation*, 117, 13–23.

Cunin, C., Handschin, S., Walther, P., & Escher, E. (1995). Structural changes of starch during cooking of durum wheat pasta. *LWT - Food Science and Technology*, 28, 323–328. https://doi.org/10.1016/S0023-6438(95)94552-0

Dahiya, S., Bajaj, B. K., Kumar, A., Tiwari, S. K., & Singh, B. (2020). A review on biotechnological potential of multifarious enzymes in bread making. *Process Biochemistry*, 99, 290–306. https://doi.org/10.1016/j.procbio.2020.09.002

de Noni, I., & Pagani, M. A. (2010). Cooking properties and heat damage of dried pasta as influenced by raw material characteristics and processing conditions. *Critical Reviews in Food Science and Nutrition*, 50(5), 465–472. https://doi.org/10.1080/10408390802437154

Dhinda, F., A, J. L., Prakash, J., & Dasappa, I. (2012). Effect of Ingredients on Rheological, Nutritional and Quality Characteristics of High Protein, High Fibre and Low Carbohydrate Bread. *Food and Bioprocess Technology*, 5, 2998–3006. https://doi.org/10.1007/s11947-011-0752-y

Di Cairano, M., Condelli, N., Caruso, M. C., Marti, A., Cela, N., & Galgano, F. (2020). Functional properties and predicted glycemic index of gluten free cereal, pseudocereal and legume flours. *LWT - Food Science and Technology*, 133, 109860. https://doi.org/10.1016/j.lwt.2020.109860

Di Stefano, V., Pagliaro, A., Del Nobile, M. A., Conte, A., & Melilli, M. G. (2021). Lentil fortified spaghetti: Technological properties and nutritional characterization. *Foods*, 10(1), 4. https://doi.org/10.3390/foods10010004

Diantom, A., Curti, E., Carini, E., Boukid, F., Mattarozzi, M., Vodovotz, Y., Careri, M., & Vittadini, E. (2019). A multi-scale approach for pasta quality features assessment. *LWT - Food Science and Technology*, 101, 285–292. https://doi.org/10.1016/j.lwt.2018.11.004

Drulyte, D., & Orlien, V. (2019). The Effect of Processing on Digestion foods. *Foods*, 8, 1–9. https://doi.org/10.3390/foods8060224

Dupont, D., & Mackie, A. R. (2015). Static and Dynamic in Vitro Digestion Models to Study Proteins Stability in the Gastrointestinal Tract. *Drug Discovery Today: Disease Models*, 17-18, 23-27. https://doi.org/10.1016/j.ddmod.2016.06.002

Dupont, D., Mandalari, G., Molle, D., Jardin, J., Leonil, J., Faulks, R. M., Wickham, M. S. J., Clare Mills, E. N., & Mackie, A. R. (2010a). Comparative resistance of food proteins to

adult and infant in vitro digestion models. *Molecular Nutrition & Food Research*, 54, 767-780. https://doi.org/10.1002/mnfr.200900142

Dupont, D., Mandalari, G., Molle, D., Jardin, J., Rolet-Repecaud, O., Duboz, G., Léonil, J., Mills, C. E. N., & Mackie, A. R. (2010b). Food processing increases casein resistance to simulated infant digestion. *Molecular nutrition & food research*, 54, 1677-1689. https://doi.org/10.1002/mnfr.200900142

Edginton, A. N., & Fotaki, N. (2010). Oral drug absorption in pediatric populations. In Dressman, J. B., Reppas, C. (Eds.), Oral drug absorption: Prediction and assessment (pp. 108-126.). New York: Informa Healthcare.

Eelderink, C., Noort, M. W. J., Sozer, N., Koehorst, M., Holst, J. J., Deacon, C. F., Rehfeld, J. F., Poutanen, K., Vonk, R. J., Oudhuis, L., & Priebe, M. G. (2015). The structure of wheat bread influences the postprandial metabolic response in healthy men. *Food & Function*, 10. https://doi.org/10.1039/c5fo00354g

Englyst, H. N., Kingman, S. M., & Cummings, J. H. (1992). Classification and measurement of nutritionally important starch fractions. *European Journal of Clinical Nutrition*, 46, S33-50. https://doi.org/10.1016/S0271-5317(97)00010-9

European Union. (2017). Official Journal of European Union L 337/15 (December 2017), COMMISSION IMPLEMENTING REGULATION (EU) 2017/2362.

Fardet, A., Leenhardt, F., Lioger, D., Scalbert, A., & Rémésy, C. (2006). Parameters controlling the glycaemic response to breads. *Nutrition Research Reviews*, 19, 18–25. https://doi.org/10.1079/NRR2006118

Faris, M. A. I. E., Mohammad, M. G., & Soliman, S. (2020). Lentils (Lens culinaris L.): A candidate chemopreventive and antitumor functional food. In Y. Kabir (Eds.), Functional Foods in Cancer Prevention and Therapy (pp. 99-120). Academic Press.

Ferrua, M. J., & Singh, R. P. (2015). Human Gastric Simulator (Riddet Model). In K. Verhoeckx, P. D. Cotter, I. López-Expósito, C. Kleiveland, T. Lea, A. Mackie, T. Requena, D. Swiatecka, & H. Wichers (Eds.), The Impact of Food Bio-Actives on Gut Health: In Vitro and Ex Vivo Models (pp. 61-71). Springer Cham Heidelberg New York Dordrecht London. https://doi.org/10.1007/978-3-319-16104-4

Ficco, D. B. M., Muccilli, S., Padalino, L., Giannone, V., Lecce, L., Giovanniello, V., Del Nobile, M. A., De Vita, P., & Spina, A. (2018). Durum wheat breads 'high in fibre' and with

reduced in vitro glycaemic response obtained by partial semolina replacement with minor cereals and pulses. *Journal of Food Science and Technology*, 55, 4458–4467. https://doi.org/10.1007/s13197-018-3374-9

Finkina, E. I., Melnikova, D. N., Bogdanov, I. V., Matveevskaya, N. S., Ignatova, A. A., Toropygin, I. Y., & Ovchinnikova, T. V. (2020). Impact of different lipid ligands on the stability and ige-binding capacity of the lentil allergen len c 3. *Biomolecules*, 10, 1–15. https://doi.org/10.3390/biom10121668

Foschia, M., Horstmann, S. W., Arendt, E. K., & Zannini, E. (2017). Legumes as Functional Ingredients in Gluten-Free Bakery and Pasta Products. *Annual Review of Food Science and Technology*, 8, 4.1–4.22. https://doi.org/10.1146/annurev-food-030216-030045

Foschia, M., Peressini, D., Sensidoni, A., Brennan, M. A., & Brennan, C. S. (2013). The effects of dietary fibre addition on the quality of common cereal products. *Journal of Cereal Science*, 58, 216–227. https://doi.org/10.1016/j.jcs.2013.05.010

Fuad, T., & Prabhasankar, P. (2010). Role of ingredients in pasta product quality: A review on recent developments. *Critical Reviews in Food Science and Nutrition*, 50(8), 787–798. https://doi.org/10.1080/10408390903001693

Fujiwara, N., Hall, C., & Jenkins A. L. (2017). Development of Low Glycemic Index (GI) Foods by Incorporating Pulse Ingredients into Cereal-Based Products: Use of In Vitro Screening and In Vivo Methodologies. *Cereal Chemistry*, 94(1), 110–116. https://doi.org/10.1094/CCHEM-04-16-0119-FI

Gallo, V., Romano, A., & Masi, P. (2020). Does the presence of fibres affect the microstructure and in vitro starch digestibility of commercial Italian pasta? *Food Structure*, 24(April), 100139. https://doi.org/10.1016/j.foostr.2020.100139

Gao, J., Koh, A.H.S., Tay, S.L. & Zhou, W. (2017a). Dough and bread made from high- and low-protein flours by vacuum mixing: Part 1: Gluten network formation. *Journal of Cereal Science*, 74, 288–295. https://doi.org/10.1016/j.jcs.2017.03.008

Gao, J., Ong, J.J.-X., Henry, J. & Zhou, W. (2017b). Physical breakdown of bread and its impact on texture perception: a dynamic perspective. *Food Quality and Preference*, 60, 96–104. https://doi.org/10.1016/j.foodqual.2017.03.014

Gao, J., Tay, S.L., Koh, A.H.S. & Zhou, W. (2017c). Dough and bread made from high- and low-protein flours by vacuum mixing: Part 2. Yeast activity, dough proofing and bread quality.

Journal of Cereal Science, 77, 275–283. https://doi.org/10.1016/j.jcs.2017.08.015

Gibson, L. J., & Ashby, M. F. (1997). In C. A. Harper (Ed.). Cellular solids: Structure and properties (2nd ed.). New York, USA 0975: Mcgraw-Hill.

Gómez, M., Oliete, B., Pando, V., Ronda, F., & Caballero, P. A. (2008). Effect of fermentation conditions on bread staling kinetics. *European Food Research and Technology*, 226(6), 1379-1387. https://doi.org/10.1007/s00217-007-0668-y

Gonçalves, M. C., & Cardarelli, H. R. (2019). Changes in water mobility and protein stabilization of Mozzarella cheese made under different stretching temperatures. *LWT - Food Science and Technology*, 104, 16-23. https://doi.org/10.1016/j.lwt.2019.01.022

Göncü, A., & Çelik, İ. (2020). Investigation of some properties of gluten-free tarhanas produced by red, green and yellow lentil whole flour. *Journal of Food Science and Technology*, 40, 574–581. http://orcid.org/0000-0002-9676-1503

Goñi, I., Garcia-Alonso, A., & Saura-Calixto, F. (1997). A starch hydrolysis procedure to estimate glycemic index. *Nutrition Research*, 17(3), 427–437. https://doi.org/10.1016/S0271-5317(97)00010-9

Graf, D., Monk, J. M., Wu, W., Wellings, H. R., Robinson, L. E., & Power, K. A. (2020). Red lentil supplementation reduces the severity of dextran sodium sulfate-induced colitis in C57BL/6 male mice. *Journal of Functional Foods*, 64, 103625. https://doi.org/10.1016/j.jff.2019.103625

Granfeldt, Y., & Björck, I. (1991). Glycemic response to starch in pasta: A study of mechanisms of limited enzyme availability. *Journal of Cereal Science*, 14, 47–61. https://doi.org/10.1016/S0733-5210(09)80017-9

Guerra, A., Etienne-Mesmin, L., Livrelli, V., Denis, S., Blanquet-Diot, S., & Alric, M. (2012). Relevance and challenges in modeling human gastric and small intestinal digestion. *Trends in Biotechnology*, 30, 591-600. https://doi.org/10.1016/j.tibtech.2012.08.001

Henderson, T. R., Hamosh, M., Armand, M., Mehta, N. R., & Hamosh, P. (1998). Gastric proteolysis in the preterm Infant: Protein digestion is limited and is not affected by diet, human milk or formula. *Pediatric Research*, 43, 101-101. https://doi.org/10.1007/978-1-4615-1371-1_50

Hernandez-Aguilar, C., Dominguez-Pacheco, A., Palma Tenango, M., Valderrama-Bravo, C., Soto Hernández, M., Cruz-Orea, A., & Ordonez-Miranda, J. (2020). Lentil sprouts: a

nutraceutical alternative for the elaboration of bread. *Journal of Food Science and Technology*, 57(5), 1817–1829. https://doi.org/10.1007/s13197-019-04215-5

Holmes, J. T., Jaberansari, Z., Collins, W., Latour, M. L., Modulevsky, D. J., & Pelling, A. E. (2020). Homemade bread: Repurposing an ancient technology for low cost in vitro tissue engineering. *BioRxiv*, 1–15. https://doi.org/10.1101/2020.11.13.353698

Hsieh, P. H., Weng, Y. M., Yu, Z. R., & Wang, B. J. (2017). Substitution of wheat flour with wholegrain flours affects physical properties, sensory acceptance, and starch digestion of Chinese steam bread (Mantou). *LWT - Food Science and Technology*, 86, 571–576. https://doi.org/10.1016/j.lwt.2017.08.051

Hunt, J. N., Smith, J. L., & Jiang, C. L. (1985). Effect of meal volume and energy density on the gastric emptying of carbohydrates. *Gastroenterology*, 89(6), 1326–1330. https://doi.org/10.1016/0016-5085(85)90650-X

Hur, S. J., Limb, B. O., Deckerc, E. A., & McClements, J. D. (2011). *In vitro* human digestion models for food applications. *Food Chemistry*, 125, 1–12. https://doi.org/10.1016/j.foodchem.2010.08.036

Jenkins, D. J. A., Thorne, M. J., Wolever, T. M. S., Jenkins A. L., Rao, A. V., & Thompson, L. U. (1987). The effect of starch-protein interaction in wheat on the glycemic response and rate of in vitro digestion. *American Journal of Clinical Nutrition*, 45(5), 946–951. https://doi.org/10.1093/ajcn/45.5.946

Jenkins, D. J. A., Wolever, T. M. S., Taylor, R. H., Barker, H. M., Fielden, H., Baldwin, J. M., Bowling, A. C., Newman, H. C., Jenkins, A. L., & Goff, D. V. (1981). Glycemic index of foods: A physiological basis for carbohydrate exchange. *The American Journal of Clinical Nutrition*, 34, 362–366. https://doi.org/10.1093/ajcn/34.3.362

Joshi, M., Timilsena, Y., & Adhikari, B. (2017). Global production, processing and utilization of lentil: A review. *Journal of Integrative Agriculture*, 16(12), 2898–2913. https://doi.org/10.1016/S2095-3119(17)61793-3

Jourdren, S., Panouillé, M., Saint-Eve, A., Déléris, I., Forest, D., Lejeune, P., & Souchon, I. (2016). Breakdown pathways during oral processing of different bread: Impact of crumb and crust structures. *Food and Function*, 7(3), 1446–1457. https://doi.org/10.1039/c5fo01286d

Kamba, M., Seta, Y., Kusai, A., & Nishimura, K. (2001). Evaluation of the mechanical destructive force in the stomach of dog. *International Journal of Pharmaceutics*, 228: 209-17. https://doi.org/10.1016/s0378-5173(01)00844-4

Kamba, M., Seta, Y., Kusai, A., Ikeda, M., & Nishimura, K. (2000). A unique dosage form to evaluate the mechanical destructive force in the gastrointestinal tract. *International Journal of Pharmaceutics*, 208, 61-70. https://doi.org/10.1016/s0378-5173(00)00552-4

Kathirvel, P., Yamazaki, Y., Zhu, W., & Luhovyy, B. L. (2019). Glucose release from lentil flours digested in vitro: The role of particle size. *Cereal Chemistry*, 96, 1126–1136. https://doi.org/10.1002/cche.10223

Kaur, M., & Singh, N. (2005). Studies on functional, thermal and pasting properties of flours from different chickpea (Cicer arietinum L.) cultivars. *Food Chemistry*, 91, 403–411. https://doi.org/10.1016/j.foodchem.2004.06.015

Keetels, C. J. A. M., van Vliet, T., & Walstra, P. (1996). Gelation and retrogradation of concentrated starch systems: 2. Retrogradation. *Food Hydrocolloids*, 10(3), 355–362. https://doi.org/10.1016/S0268-005X(96)80012-9

Khazaei, H., Subedi, M., Nickerson, M., Martínez-Villaluenga, C., Frias, J., & Vandenberg, A. (2019). Seed Protein of Lentils: Current Status, Progress, and Food Applications. *Foods*, 8, 391. https://doi.org/10.3390/foods8090391

Kinsella, J. E. (1981). Functional properties of proteins: possible relationships between structure and function in foams. *Food Chemistry*, 7, 273-288. https://doi.org/10.1016/0308-8146(81)90033-9

Kohajdová, Z., Karovičová, J., & Magala, M. (2013). Effect of lentil and bean flours on rheological and baking properties of wheat dough. *Chemical Papers*, 67(4), 398–407. https://doi.org/10.2478/s11696-012-0295-3

Kong, F., & Singh, R. P. (2008). Disintegration of solid foods in human stomach. *Journal of Food Science*, 73, R67-R80. https://doi.org/10.1111/j.1750-3841.2008.00766.x

Kong, F., & Singh, R. P. (2010). A Human Gastric Simulator (HGS) to Study Food Digestion in Human Stomach. *Journal of Food Science*, 75, E627-E635. https://doi.org/10.1111/j.1750-3841.2010.01856.x

Kotoki, D., & Deka, S. C. (2010). Baking loss of bread with special emphasis on increasing water holding capacity. *Journal of Food Science and Technology*, 47(February), 128–131. https://doi.org/10.1007/s13197-010-0008-2

Kumar, S., & Pandey, G. (2020). Biofortification of pulses and legumes to enhance nutrition. *Heliyon*, 6, e03682. https://doi.org/10.1016/j.heliyon.2020.e03682

Le Bleis, F., Chaunier, L., Chiron, H., Valle, G. Della, & Saulnier, L. (2015). Rheological properties of wheat flour dough and French bread enriched with wheat bran. Journal of Cereal Science, 65, 167–174. https://doi.org/10.1016/j.jcs.2015.06.014

Lea, T. (2015). Caco-2 Cell Line. In K. Verhoeckx, P. D. Cotter, I. López-Expósito, C. Kleiveland, T. Lea, A. Mackie, T. Requena, D. Swiatecka, & H. Wichers (Eds.), The Impact of Food Bio-Actives on Gut Health: In Vitro and Ex Vivo Models (pp. 103-111). Springer Cham Heidelberg New York Dordrecht London. https://doi.org/10.1007/978-3-319-16104-4

Lebenthal, E., Lee, P., & Heitlinger, L. A. (1983). Impact of development of the gastrointestinal tract on infant feeding. *The Journal of pediatrics*, 102, 1-9. https://doi.org/10.1016/s0022-3476(83)80276-5

Leonard, M. M., Cureton, P. A., & Fasano, A. (2015). Managing coeliac disease in patients with diabetes. *Diabetes, Obesity and Metabolism*, 17(1), 3–8. https://doi.org/10.1111/dom.12310

Li, P., Zhang, B., & Dhital, S. (2019). Starch digestion in intact pulse cells depends on the processing induced permeability of cell walls. *Carbohydrate Polymers*, 225, 115204. https://doi.org/10.1016/j.carbpol.2019.115204

Lin, S., Gao, J., Jin, X., Wang, Y., Dong, Z., Ying, J., & Zhou, W. (2020). Whole-wheat flour particle size influences dough properties, bread structure and in vitro starch digestibility. *Food & Function*, 11, 3610–3620. https://doi.org/10.1039/c9fo02587a

Liu, Q., Donner, E., Yin, Y., Huang, R. L., & Fan, M. Z. (2006). The physicochemical properties and *in vitro* digestibility of selected cereals, tubers and legumes grown in China. *Food Chemistry*, 99(3), 470–477. https://doi.org/10.1016/j.foodchem.2005.08.008

Liu, S., Yin, H., Pickard, M., & Ai, Y. (2020). Influence of infrared heating on the functional properties of processed lentil flours: A study focusing on tempering period and seed size. *Food Research International*, 136, 109568. https://doi.org/10.1016/j.foodres.2020.109568

Lu, Z. H., Donner, E., Tsao, R., Ramdath, D. D., & Liu, Q. (2018). Physicochemical and digestion characteristics of flour and starch from eight Canadian red and green lentils.

International Journal of Food Science & Technology, 53, 735– 746. https://doi.org/10.1111/ijfs.13649

Lucas-González, R., Viuda-Martos, M., Pérez-Alvarez, J. A., & Fernández-López, J. (2018). In vitro digestion models suitable for foods: Opportunities for new fields of application and challenges. *Food Research International*, 107, 423-436. https://doi.org/10.1016/j.foodres.2018.02.055

Luo, S., Chan, E., Masatcioglu, M. T., Erkinbaev, C., Paliwal, J., & Koksel, F. (2020). Effects of extrusion conditions and nitrogen injection on physical, mechanical, and microstructural properties of red lentil puffed snacks. *Food and Bioproducts Processing*, 121, 143–153. https://doi.org/10.1016/j.fbp.2020.02.002

Macfarlane, G. T., Cummings, J. H., Macfarlane, S., & Gibson, G. R. (1989). Influence of retention time on degradation of pancreatic-enzymes by human colonic bacteria grown in a 3-stage continuous culture system. *Journal of Applied Bacteriology*, 67, 521–527. https://doi.org/10.1111/j.1365-2672.1989.tb02524.x

MacWilliam, S., Parker, D., Marinangeli, C. P., & Trémorin, D. (2018). A meta-analysis approach to examining the greenhouse gas implications of including dry peas (*Pisum sativum L.*) and lentils (*Lens culinaris M.*) in crop rotations in western Canada. *Agricultural Systems*, 166, 101-110. https://doi.org/10.1016/j.agsy.2018.07.016

Manthey, F., & Schorno, A. (2002). Physical and cooking quality of spaghetti made from whole wheat durum. *Cereal Chemistry*, 79(4), 504–510. https://doi.org/10.1094/CCHEM.2002.79.4.504

Marchini, M., Carini, E., Cataldi, N., Boukid, F., Blandino, M., Ganino, T., Vittadini, E., & Pellegrini, N. (2021). The use of red lentil flour in bakery products: How do particle size and substitution level affect rheological properties of wheat bread dough? *LWT - Food Science and Technology*, 136, 110299. https://doi.org/10.1016/j.lwt.2020.

Mariotti, F., Tomé, D., & Mirand, P. P. (2008). Converting nitrogen into protein - Beyond 6.25 and Jones' factors. *Critical Reviews in Food Science and Nutrition*, 48(2), 177–184. https://doi.org/10.1080/10408390701279749

Mat, D. J. L., Cattenoz, T., Souchon, I., Michon, C., & Le, S. (2018). Monitoring protein hydrolysis by pepsin using pH-stat: In vitro gastric digestions in static and dynamic pH conditions. *Food Chemistry*, 239, 268–275. https://doi.org/10.1016/j.foodchem.2017.06.115

Matamoros, S., Gras-Leguen, C., Le Vacon, F., Potel, G., & de La Cochetiere, M. F. (2013). Development of intestinal microbiota in infants and its impact on health. *Trends in microbiology*, 21, 167-173. https://doi.org/10.1016/j.tim.2012.12.001

Mattila, P. H., Pihlava, J. M., Hellström, J., Nurmi, M., Eurola, M., Mäkinen, S., Jalava, T., & Pihlanto, A. (2018). Contents of phytochemicals and antinutritional factors in commercial protein-rich plant products. *Food Quality and Safety*, 2(4), 213–219. https://doi.org/10.1093/fqsafe/fyy021

Ménard, O., Picque, D., & Dupont, D. (2015). The DIDGI® System. In K. Verhoeckx, P. D. Cotter, I. López-Expósito, C. Kleiveland, T. Lea, A. Mackie, T. Requena, D. Swiatecka, & H. Wichers (Eds.), The Impact of Food Bio-Actives on Gut Health: In Vitro and Ex Vivo Models (pp. 73-81). Springer Cham Heidelberg New York Dordrecht London. https://doi.org/10.1007/978-3-319-16104-4

Minekus, M. (2015). The TNO Gastro-Intestinal Model (TIM). In K. Verhoeckx, P. D. Cotter, I. López-Expósito, C. Kleiveland, T. Lea, A. Mackie, T. Requena, D. Swiatecka, & H. Wichers (Eds.), The Impact of Food Bio-Actives on Gut Health: In Vitro and Ex Vivo Models (pp. 37-46). Springer Cham Heidelberg New York Dordrecht London. https://doi.org/10.1007/978-3-319-16104-4

Minekus, M., Alminger, M., Alvito, P., Balance, S., Bohn, T., Bourlieu, C., Carrière, F., Boutrou, R., Corredig, M., Dupont, D., Dufour, C., Egger, L., Golding, M., Karakaya, S., Kirkhus, B., Le Feunteun, S., Lesmes, U., Macierzanka, A., Mackie, A., Marze, S., McClements, D. J., Ménard, O., Recio, I., Santos, C. N., Singh, R. P., Vegarud, G. E., Wickham, M. S., Weitschies, W., & Brodkorb, A. (2014). A standardised static in vitro digestion method suitable for food - an international consensus. *Food & Function*, 5(6), 1113–1124. https://doi.org/10.1039/c3fo60702j

Monnet, A. F., Laleg, K., Michon, C., & Micard, V. (2019). Legume enriched cereal products: A generic approach derived from material science to predict their structuring by the process and their final properties. *Trends in Food Science & Technology*, 86, 131–143. https://doi.org/10.1016/j.tifs.2019.02.027

Mulet-Cabero, A. I., Egger, L., Portmann, R., Ménard, O., Marze, S., Minekus, M., Le Feunteun, S., Sarkar, A., Grundy, M. M. L., Carrière, F., Golding, M., Dupont, D., Recio, I., Brodkorb, A., & Mackie, A. (2020). A standardised semi-dynamic: in vitro digestion method suitable

for food-an international consensus. *Food and Function*, 11(2), 1702–1720. https://doi.org/10.1039/C9FO01293A

Nilusha, R. A. T., Jayasinghe, J. M. J. K., Perera, O. D. A. N., & Perera, P. I. P. (2019). Development of pasta products with nonconventional ingredients and their effect on selected quality characteristics: A brief overview. *International Journal of Food Science*, (1), 1–10. https://doi.org/10.1155/2019/6750726

Nosworthy, M. G., Medina, G., Franczyk, A. J., Neufeld, J., Appah, P., Utioh, A., Frohlich, P., & House, J. D. (2018). Effect of processing on the in vitro and in vivo protein quality of red and green lentils (Lens culinaris). *Food Chemistry*, 240, 588–593. https://doi.org/10.1016/j.foodchem.2017.07.129

Ogilvie, O., Roberts, S., Sutton, K., Domigan, L., Larsen, N., Gerrard, J., & Demarais, N. (2020). Proteomic modelling of gluten digestion from a physiologically relevant food system: A focus on the digestion of immunogenic peptides from wheat implicated in celiac disease. *Food Chemistry*, 333, 127466. https://doi.org/10.1016/j.foodchem.2020.127466

Packer, S. C., Dornhorst, A., & Frost, G. S. (2000). The glycaemic index of a range of gluten-free foods. *Diabetic Medicine*, 17(9), 657–660. https://doi.org/10.1046/j.1464-5491.2000.00356.x

Papandreou, C., Becerra-Tomás, N., Bulló, M., Martínez-González, M. Á., Corella, D., Estruch, R., Ros, E., Arós, F., Schroder, H., Fitó, M., Serra-Majem, L., Lapetra, J., Fiol, M., Ruiz-Canela, M., Sorli, J. V., & Salas-Salvadó, J. (2019). Legume consumption and risk of all-cause, cardiovascular, and cancer mortality in the PREDIMED study. *Clinical Nutrition*, 38, 348–356. https://doi.org/10.1016/j.clnu.2017.12.019

Pauly, A., Pareyt, B., Fierens, E., & Delcour, J. A. (2014). Fermentation affects the composition and foaming properties of the aqueous phase of dough from soft wheat flour. *Food Hydrocolloids*, 37, 221-228. https://doi.org/10.1016/j.foodhyd.2013.11.008.

Pedersen, A. M., Bardow, A., Jensen, S. B., & Nauntofte, B. (2002). Saliva and gastrointestinal functions of taste, mastication, swallowing and digestion. *Oral Diseases*, 8, 117–129. https://doi.org/10.1034/j.1601-0825.2002.02851.x

Petitot, M., Abecassis, J., & Micard, V. (2009). Structuring of pasta components during processing: Impact on starch and protein digestibility and allergenicity. *Trends in Food Science & Technology*, 20(11-12), 521–532. https://doi.org/10.1016/j.tifs.2009.06.005

Petitot, M., Boyer, L., Minier, C., & Micard, V. (2010) Fortification of pasta with split pea and faba beans flours: pasta processing and quality evaluation. *Food Research International*, 43, 634–641. https://doi.org/10.1016/j.foodres.2009.07.020

Polat, H., Dursun Capar, T., Inanir, C., Ekici, L., & Yalcin, H. (2020). Formulation of functional crackers enriched with germinated lentil extract: A Response Surface Methodology Box-Behnken Design. *LWT - Food Science and Technology*, 123, 109065. https://doi.org/10.1016/j.lwt.2020.109065

Portman, D., Blanchard, C., Maharjan, P., McDonald, L. S., Mawson, J., Naiker, M., & Panozzo, J. F. (2018). Blending studies using wheat and lentil cotyledon flour—Effects on rheology and bread quality. *Cereal Chemistry*, 95, 849–860. https://doi.org/10.1002/cche.10103

Ragaee, S., Guzar, I., Dhull, N., & Seetharaman, K. (2011). Effects of fiber addition on antioxidant capacity and nutritional quality of wheat bread. *LWT - Food Science and Technology*, 44(10), 2147–2153. https://doi.org/10.1016/j.lwt.2011.06.016

Raheem, D., Liu, A., & Li, C. (2019). Textural and sensory characteristics of oven baked and steamed bread. *Emirates Journal of Food and Agriculture*, 31(8), 580–586. https://doi.org/10.9755/ejfa.2019.v31.i8.1986

Raiola, A., Romano, A., Shanakhat, H., Masi, P., & Cavella, S. (2020). Impact of heat treatments on technological performance of re-milled semolina dough and bread. *LWT - Food Science and Technology*, 117, 108607. https://doi.org/10.1016/j.lwt.2019.108607

Rathnayake, H. A., Navaratne, S. B., & Navaratne, C. M. (2018). Porous Crumb Structure of Leavened Baked Products. *International Journal of Food Science*, 1-15. https://doi.org/10.1155/2018/8187318

Remond, D., Shahar, D. R., Gille, D., Pinto, P., Kachal, J., Peyron, M. A., Dos Santos, C. N., Walther, B., Bordoni, A., Dupont, D., Tomás-Cobos, L., & Vergères, G. (2015). Understanding the gastrointestinal tract of the elderly to develop dietary solutions that prevent malnutrition. *Oncotarget*, 6, 13858-13898. https://doi.org/10.18632/oncotarget.4030

Resmini, P., & Pagani, M. A. (1983). Ultrastructure Studies of Pasta: A Review. *Food Microstructure*, 2, 1-12.

Revilla, I., Lastras, C., González-Martín, M. I., Vivar-Quintana, A. M., Morales-Corts, R., Gómez-Sánchez, M. A., & Pérez-Sánchez, R. (2019). Predicting the physicochemical properties and geographical ORIGIN of lentils using near infrared spectroscopy.

The Journal of Food Composition and Analysis, 77, 84–90. https://doi.org/10.1016/j.jfca.2019.01.012

Romano, A., Cavella, S., Toraldo, G., & Masi, P. (2013). 2D structural imaging study of bubble evolution during leavening. *Food Research International*, 50(1), 324–329. https://doi.org/10.1016/j.foodres.2012.10.040

Romano, A., D'Amelia, V., Gallo, V., Palomba, S., Carputo, D., & Masi, P. (2018). Relationships between composition, microstructure and cooking performances of six potato varieties. *Food Research International*, 114, 10–19. https://doi.org/10.1016/j.foodres.2018.07.033

Romano, A., Gallo, V., Ferranti, P., & Masi, P. (2021). Lentil flour: nutritional and technological properties, in vitro digestibility and perspectives for use in the food industry. *Current Opinion in Food Science*, 40, 157-167. https://doi.org/10.1016/j.cofs.2021.04.003

Romano, A., Giosafatto, C. V. L., Di Pierro, P., Romano, R., Masi, P., & Mariniello, L. (2016). Impact of transglutaminase treatment on properties and in vitro digestibility of white bean (Phaseolus vulgaris L.) flour. *Food Research International*, 88, 239–246. https://doi.org/10.1016/j.foodres.2016.02.014

Romano, A., Giosafatto, V., Al-Asmar, A., Masi, P., Romano, R., & Mariniello, L. (2019). Structure and *in vitro* digestibility of grass pea (Lathyrus sativus L.) flour following transglutaminase treatment. *European Food Research and Technology*, 245, 1899–1905. https://doi.org/10.1007/s00217-019-03305-0

Romano, A., Mackie, A., Farina, F., Aponte, M., Sarghini, F., & Masi, P. (2016). Characterisation, *in vitro* digestibility and expected glycemic index of commercial starches as uncooked ingredients. *Journal of Food Science and Technology*, 53(12), 4126–4134. https://doi.org/10.1007/s13197-016-2375-9

Romano, A., Toraldo, G., Cavella, S., & Masi, P. (2007). Description of leavening of bread dough with mathematical modelling. *Journal of Food Engineering*, 83(2), 142–148. https://doi.org/10.1016/j.jfoodeng.2007.02.014

Sackesen, C., Erman, B., Gimenez, G., Grishina, G., Yilmaz, O., Yavuz, S. T., Sahiner, U. M., Buyuktiryaki, B., Yilmaz, E. A., Cavkaytar, O., & Sampson, H. A. (2020). IgE and IgG4 binding to lentil epitopes in children with red and green lentil allergy. *Pediatric Allergy and Immunology*, 31, 158–166. https://doi.org/10.1111/pai.13136

Salles, N. (2007). Basic mechanisms of the aging gastrointestinal tract. *Digestive Diseases*, 25, 112-117. https://doi.org/10.1159/000099474

Santos-Hernández, M., Alfieri, F., Gallo, V., Miralles, B., Masi, P., Romano, A., Ferranti, P., & Recio, I. (2020). Compared digestibility of plant protein isolates by using the INFOGEST digestion protocol. *Food Research International*, 137, 109708. https://doi.org/10.1016/j.foodres.2020.109708

Sarghini, F., Romano, A., & Masi, P. (2016). Experimental analysis and numerical simulation of pasta dough extrusion process. *Journal of Food Engineering*, 176, 56–70. https://doi.org/10.1016/j.jfoodeng.2015.09.029

Saricaoglu, F. T. (2020). Application of high-pressure homogenization (HPH) to modify functional, structural and rheological properties of lentil (Lens culinaris) proteins. *International Journal of Biological Macromolecules*, 144, 760–769. https://doi.org/10.1016/j.ijbiomac.2019.11.034

Sarles, J., Moreau, H., & Verger, R. (1992). Human gastric lipase: Ontogeny and variations in children. *Acta Paediatrica*, 81, 511-513. https://doi.org/10.1111/j.1651-2227.1992.tb12284.x

Scanlon, M. G., & Zghal, M. C. (2001). Bread properties and crumb structure. *Food Research International*, 34, 841–864. https://doi.org/10.1016/S0963-9969(01)00109-0

Scazzina, F., Dall'Asta, M., Pellegrini, N., & Brighenti, F. (2015). Glycaemic index of some commercial gluten-free foods. *European Journal of Nutrition*, 54(6), 1021–1026. https://doi.org/10.1007/s00394-014-0783-z

Schulze, K. (2006). Imaging and modeling of digestion in the stomach and the duodenum. *Neurogastroenterology & Motility*, 18, 172–83. https://doi.org/10.1111/j.1365-2982.2006.00759.x

Schwizer, W., Steingoetter, A., & Fox, M. (2006). Magnetic resonance imaging for the assessment of gastrointestinal function. *Journal of Gastroenterology*, 41(11), 1245 – 60. https://doi.org/10.1080/00365520600827188

Seok, J. W. (2011). How to Interpret Gastric emptying scintigraphy. *Journal of Neurogastroenterology and Motility*, 17(2), 189–191. https://doi.org/10.5056/jnm.2011.17.2.189

Serial, M. R., Blanco Canalis, M. S., Carpinella, M., Valentinuzzi, M. C., León, A. E., Ribotta, P. D., & Acosta, R. H. (2016). Influence of the incorporation of fibre in biscuit dough on

proton mobility characterized by time domain NMR. *Food Chemistry*, 192, 950–957. https://doi.org/10.1016/j.foodchem.2015.07.101

Shaheen, N., Halima, O., Akhter, K. T., Nuzhat, N., Rao, R. S. P., Wilson, R. S., & Ahsan, N. (2019). Proteomic characterization of low molecular weight allergens and putative allergen proteins in lentil (Lens culinaris) cultivars of Bangladesh. *Food Chemistry*, 297, 124936. https://doi.org/10.1016/j.foodchem.2019.06.003

Shahzadi, N., Butt, M. S., Rehman, S., & Sharif, M. K. (2005). Rheological and Baking Performance of Composite Flours. *International Journal of Agriculture & Biology*, 7(1), 100–104. https://doi.org/10.1002/fsn3.321

Shani-Levi, C., Alvito, P., Andrés, A., Assunção, R., Barberá, R., Blanquet-Diot, S., Bourlieu, C., Brodkorb, A., Cilla, A., Deglaire, A., Denis, S., Dupont, D., Heredia, A., Karakaya, S., Giosafatto, C. V. L., Mariniello, L., Martins, C., Ménard, O., Nehir, El S., Vegarud, G. E., Ulleberg, E., & Lesmes, U. (2017). Extending in vitro digestion models to specific human populations: Perspectives, practical tools, and bio-relevant information. *Trends in Food Science & Technology*, 60, 52-63. https://doi.org/10.1016/j.tifs.2016.10.017

Shoup, F. K., Pomeranz, Y., & Deyoe, C. W. (1996). Amino Acid Composition of Wheat Varieties and Flours Varying Widely in Bread-Making Potentialities. *Journal of Food Science*, 31(1), 94 - 101. https://doi.org/10.1111/j.1365-2621.1966.tb15420.x

Siepmann, F. B., Ripari, V., Waszczynskyj, N., & Spier, M. R. (2018). Overview of Sourdough Technology: from Production to Marketing. *Food and Bioprocess Technology*, 11(2), 242–270. https://doi.org/10.1007/s11947-017-1968-2

Siva, N., Thavarajah, P., & Thavarajah, D. (2018). The impact of processing and cooking on prebiotic carbohydrates in lentil. *Journal of Food Composition and Analysis*, 70, 72–77. https://doi.org/10.1016/j.jfca.2018.04.006

Sozer, N., & Kaya, A. (2008). The effect of cooking water composition on textural and cooking properties of spaghetti. *International Journal of Food Properties*, 11(2), 351–362. https://doi.org/10.1080/10942910701409260

Steglich, T., Bernin, D., Röding, M., Nydén, M., Moldin, A., & Topgaard, D. (2014). Microstructure and water distribution of commercial pasta studied by microscopy and 3D magnetic resonance imaging. *Food Research International*, 62, 644–652. https://doi.org/10.1016/j.foodres.2014.04.004

Tam, N., Oguz, S., Aydogdu, A., Sumnu, G., & Sahin, S. (2017). Influence of solution properties and pH on the fabrication of electrospun lentil flour/HPMC blend nanofibers. *Food Research International*, 102, 616-624. https://doi.org/10.1016/j.foodres.2017.09.049

Teterycz, D., Sobota, A., Zarzycki, P., & Latoch, A. (2020). Legume flour as a natural colouring component in pasta production. *Journal of Food Science and Technology*, 57, 301–309. https://doi.org/10.1007/s13197-019-04061-5

Thuenemann, E. C., Mandalari, G., Rich, G. T., & Faulks, R. M. (2015). Dynamic Gastric Model (DGM). In K. Verhoeckx, P. D. Cotter, I. López-Expósito, C. Kleiveland, T. Lea, A. Mackie, T. Requena, D. Swiatecka, & H. Wichers (Eds.), The Impact of Food Bio-Actives on Gut Health: In Vitro and Ex Vivo Models (pp. 47-59). Springer Cham Heidelberg New York Dordrecht London. https://doi.org/10.1007/978-3-319-16104-4

Trevisan, S., Pasini, G., & Simonato, B. (2019). An overview of expected glycaemic response of one ingredient commercial gluten free pasta. *LWT - Food Science and Technology*, 109, 13–16. https://doi.org/10.1016/j.lwt.2019.04.013

Turco, I., Bacchetti, T., Morresi, C., Padalino, L., & Ferretti, G. (2019). Polyphenols and the glycaemic index of legume pasta. *Food & Function*, 10, 5931–5938. https://doi.org/10.1039/c9fo00696f

Turfani, V., Narducci, V., Durazzo, A., Galli, V., & Carcea, M. (2017). Technological, nutritional and functional properties of wheat bread enriched with lentil or carob flours. *LWT - Food Science and Technology*, 78, 361–366. https://doi.org/10.1016/j.lwt.2016.12.030

ul Haq, F., Sameen, A., u Zaman, Q., Mushtaq, B. S., Hussain, M. B., Javed, A., Plygun, S., Korneeva, O., Shariati, M. A. (2019). Development and evalutation of yogurt supplemented with lentil flour. *Journal of Microbiology, Biotechnology and Food Sciences*, 8(4), 1005–1009. https://doi.org/10.15414/jmbfs.2019.8.4.1005-1009

Van de Wiele, T., Van den Abbeele, P., Ossieur, W., Possemiers, S., & Marzorati, M. (2015). The Simulator of the Human Intestinal Microbial Ecosystem (SHIME®). In K. Verhoeckx, P. D. Cotter, I. López-Expósito, C. Kleiveland, T. Lea, A. Mackie, T. Requena, D. Swiatecka, & H. Wichers (Eds.), The Impact of Food Bio-Actives on Gut Health: In Vitro and Ex Vivo Models (pp. 305-317). Springer Cham Heidelberg New York Dordrecht London. https://doi.org/10.1007/978-3-319-16104-4

Vassallo, M. J., Camilleri, M., Prather, C. M., Hanson, R. B., & Thomforde, G. M. (1992).

Measurement of axial forces during emptying from the human stomach. *American Journal of Physiology-Gastrointestinal and Liver Physiology*, 263, G230–G239. https://doi.org/10.1152/ajpgi.1992.263.2.G230

Venema, K. (2015). The TNO In Vitro Model of the Colon (TIM-2). In K. Verhoeckx, P. D. Cotter, I. López-Expósito, C. Kleiveland, T. Lea, A. Mackie, T. Requena, D. Swiatecka, & H. Wichers (Eds.), The Impact of Food Bio-Actives on Gut Health: In Vitro and Ex Vivo Models (pp. 293-304). Springer Cham Heidelberg New York Dordrecht London. https://doi.org/10.1007/978-3-319-16104-4

Verhoeckx, K., & Cotter, P. D. (2015). General Introduction. In K. Verhoeckx, P. D. Cotter, I. López-Expósito, C. Kleiveland, T. Lea, A. Mackie, T. Requena, D. Swiatecka, & H. Wichers (Eds.), The Impact of Food Bio-Actives on Gut Health: In Vitro and Ex Vivo Models (pp. 7-13). Springer Cham Heidelberg New York Dordrecht London. https://doi.org/10.1007/978-3-319-16104-4

Vignola, M. B., Bustos, M. C., & Pérez, G. T. (2018). *In vitro* dialyzability of essential minerals from white and whole grain pasta. *Food Chemistry*, 265, 128–134. https://doi.org/10.1016/j.foodchem.2018.05.012

Villas-Boas, F., Yamauti, Y., Moretti, M. M. S., & Franco, C. M. L. (2019). Influence of molecular structure on the susceptibility of starch to α-amylase. *Carbohydrate Research*, 479, 23–30. https://doi.org/10.1016/j.carres.2019.05.001

Wen, Y., Niu, M., Zhang, B., Zhao, S., & Xiong, S. (2017). Structural characteristics and functional properties of rice bran dietary fiber modified by enzymatic and enzyme micronization treatments. *LWT - Food Science and Technology*, 75, 344–351. https://doi.org/10.1016/j.lwt.2016.09.012

Wickham, M., Faulks, R., & Mills, C. (2009). In vitro digestion methods for assessing the effect of food structure on allergen breakdown. *Molecular Nutrition and Food Research*, 53(8), 952–958. https://doi.org/10.1002/mnfr.200800193

Witczak, T., & Gałkowska, D. (2021). Sorption and thermal characteristics of ancient grain pasta of various compositions. *LWT - Food Science and Technology*, 137, 110433. https://doi.org/10.1016/j.lwt.2020.110433

Withney, E., & Rolfes, S. R. (2008). Understanding nutrition (11th ed.) Belmont: Thomas Wadsworth.

Wojtowicz, A., & Moscicki, L. (2014). Influence of legume type and addition level on quality characteristics, texture and microstructure of enriched precooked pasta. *LWT - Food Science and Technology*, 59, 1175-1185. https://doi.org/10.1016/j.lwt.2014.06.010

Woolnough, J. W., Bird, A. R., Monro, J. A., & Brennan, C. S. (2010). The effect of a brief Salivary α-Amylase exposure during chewing on subsequent in vitro starch digestion curve profiles. *International Journal of Molecular Sciences*, 11(8), 2780-2790. https://doi.org/10.3390/ijms11082780